A Statistics-Based Method for Estimating the Soil Water Retention Curve and Unsaturated Shear Strength in Engineering Practice

George R. French

A Thesis presented for the degree of

Master of Science by Research

Department of Engineering
University of Durham
England

May 2021

Dedicated to

My fiancée Simone Leeson and our baby girl Fleur French

A Statistics-Based Method for Estimating the Soil Water Retention Curve and Unsaturated Shear Strength in Engineering Practice.

George R. French

Submitted for the degree of Master of Science by Research
May 2021

Abstract

Unsaturated soil mechanics is rarely applied by geotechnical engineers working within the construction industry. This could be due to a poor understanding of the subject area, a lack of suitable unsaturated testing data, or a lack of suitable procedures and tools required to apply the theory in practice. The aim of this research is to show how the soil water retention curve (SWRC) and unsaturated shear strength of a soil can be estimated using standard site investigation data and then applied to geotechnical engineering problems in practice. This includes the development of a SWRC prediction procedure using 102 soil datasets from the UNSODA database. Statistical analysis is undertaken to compare the prediction of the SWRC using the Arya and Paris (1981) model (AP), Modified Kovács Model (Aubertin et al., 2003) (MK) and the Perera et al. (2005) model (PM) with the measured drying SWRC from the database. The 5^{th} and 95^{th} percentiles of the error between the predicted and measured suction (suction error) are calculated to assess the performance of each method for different soil types and later used as confidence limits for soils not included in the dataset. Analysis shows that all three SWRC predictive methods can reasonably predict the SWRC of sands, but due to a lack of plasticity data in the database, only the Arya and Paris (1981) can be used to estimate the SWRC of cohesive soils. The SWRC estimation procedure is validated using two soil samples from the literature, a sandy clay soil and a sand soil. A method to estimate the increase in shear strength due to soil suction is presented using each predicted SWRC, along with the the upper and lower confidence limits of the SWRC, for a typical geotechnical engineering

slope stability problem. The use of this research is demonstrated via a two-dimensional PLAXIS finite element model showing how the factor of safety (FoS) of the slope increases as a result of using the SWRC to estimate changes in shear strength using the Fredlund et al. (1996) and Vanapalli et al. (1996) equations. By taking soil suction into account, the FoS of the slope can be significantly increased, with an improvement of 0.24 over the simulation that ignored suction when using the SWRC estimated using the AP model. By using the predicted SWRC upper and lower confidence limits, it is shown that the estimated increase in shear strength is not highly sensitive to the choice of values of soil suction.

Declaration

The work in this thesis is based on research carried out at the OGI Groundwater Specialists Ltd, Durham, England, and at the Department of Engineering, Durham University, England. No part of this thesis has been submitted elsewhere for any other degree or qualification and it is all my own work unless referenced to the contrary in the text.

Acknowledgements

First and foremost, I have to thank my research supervisors, Dr William Coombs and Dr Paul Hughes. Without their assistance and dedicated involvement in every step throughout the process, this thesis would have never been accomplished. I would like to thank you very much for your support and understanding over these past two and half years.

I would also like to thank and show gratitude towards Dr Stephen Thomas of OGI Groundwater Specialists Ltd, my employer, funder and supervisor of this research project. Dr Stephen Thomas came up with the initial research question and then provided direction and support throughout the project. Thanks to Stephen, my time working at OGI has provided me with a strong skill set which has greatly aided me throughout the course of this project.

Getting through my dissertation required more than academic support, and I have my family to thank for listening to and, at times, having to tolerate me over the past two years. I cannot begin to express my gratitude and appreciation to my fiancée Simone Leeson who has given me the time to work on my thesis throughout her pregnancy and once our beautiful baby daughter, Fleur, was born. I must also thank Fleur for being such a joyous and loving baby who has lifted my spirits during the writing of this thesis. I also have my parents to thank for their continued support throughout my educational journey.

Contents

List of Figures

List of Tables

List of Abbreviations

AEV	Air-Entry Value
AP	Arya and Paris (1981) Model
BIONICS	Biological and Engineering Impacts of Climate Change on Slopes
HYPRES	Hydraulic Properties of European Soils
LCL	Lower Confidence Limit
LL	Liquid Limit
MK	Modified Kovács Model (Aubertin et al., 2003)
PF	Particle Fraction
PI	Plasticity Index
PM	Perera Model (Perera et al., 2005)
PS	Particle Size
PSD	Particle Size Distribution
RMSLE	Root Mean Squared Logarithmic Error
SSM	Saturated Soil Mechanics
SVSOILS	Soil Vision Soils
SWCC	Soil Water Characteristic Curve
SWMC	Soil Water Moisture Curve
SWRC	Soil Water Retention Curve
UCL	Upper Confidence Limit
UNSODA	Unsaturated Soil Hydraulic Database
USDA-SCS	United States Department of Agriculture Soil Classification System
USM	Unsaturated Soil Mechanics
VWC	Volumetric Water Content

List of Symbols

σ	Total stress
σ'	Effective stress
u_w	Pore water pressure
u_a	Pore air pressure
ψ	Total suction
$\hat{\psi}$	Predicted suction
π	Osmotic suction
τ	Shear stress on failure plane at failure
ϕ'	Angle of internal friction
c'	Effective cohesion
ψ_e	Suction error
ψ_{e_5}	5^{th} percentile of suction error
ψ_{e50}	Mean or 50^{th} percentile of suction error
ψ_{e95}	95^{th} percentile of suction error
θ	Volumetric water content
θ_s	Saturated volumetric water content
θ_r	Residual volumetric water content
Θ_n	Normalised water content
S	Degree of saturation
S_r	Residual degree of saturation
ψ_{aev}	Air-entry value of soil
$\hat{p}$	Average skeleton mean stress
$\hat{p}$	Mean total stress
χ	Bishop's effective stress
$P_p(d)$	Percentage by mass of particles passing a particular particle size

a_{gr}	Parameter designating the inflection point on the grain-size distribution curve
n_{gr}	Parameter related to the steepest slope on the grain-size distribution curve
m_{gr}	Parameter related to the shape of the grain-size curve in the fine-grained region
d_r	Parameter related to the residual particle size
d	Diameter of any particle size under consideration
d_m	Diameter of the minimum allowable size particle in the grain-size curve
a_f	Fitting parameter related to the air-entry of the SWRC
n_f	Fitting parameter related to the gradient of the SWRC
m_f	Fitting parameter related to residual water content conditions of the SWRC
$C(\psi)$	Correction factor which is a function of suction corresponding to residual water content
ψ_r	Soil suction corresponding to the residual water content
R^2	Coefficient of determination
n	Number of intervals
W_i	Solid mass within interval for Arya and Paris (1981) model
V_{v_i}	Pore volume associated with the solid mass in the i^{th} particle-size interval
γ_w	Weight density of water
ρ_p	Particle density
e	Void ratio
ρ_d	Dry density
ϕ	Porosity
G_s	Specific gravity
θ_{v_i}	Volumetric water content represented by a pore volume
V_b	Sample bulk density
$\theta^*_{v_i}$	Average volumetric water content for the midpoint of the particle-size interval
R_i	Mean particle radius
r_i	Mean pore radius
n_i	Number of spherical particles
α	Empirical constant fitting parameter for the Arya and Paris (1981) model
ψ_i	Soil water potential
g	Acceleration due to gravity
S_c	Degree of saturation associated with the capillary component
S_a	Degree of saturation associated with the adhesive component

h_{c0}	Equivalent capillary height equivalent to the pore diameter and solid surface area
m	Pore-size coefficient
a_c	Adhesion coefficient
ψ_n	Normalisation parameter to maintain consistency in the units for the MK model
ψ_0	Suction head equal to 10^7cm of water corresponding to a dry soil condition
ψ_r	Residual suction head (cm)
D_{10}	Diameter corresponding to 10% passing on the particle size distribution curve
D_{20}	Diameter corresponding to 20% passing on the particle size distribution curve
D_{30}	Diameter corresponding to 30% passing on the particle size distribution curve
D_{60}	Diameter corresponding to 60% passing on the particle size distribution curve
D_{90}	Diameter corresponding to 90% passing on the particle size distribution curve
P_{200}	Percentage passing the No. 200 sieve (opening 0.075mm)
C_u	Coefficient of uniformity equal to D_{60}/D_{10}
ρ_s	Density of the soil particles
w_L	Liquid limit
k	Empirical fitting parameter

Chapter 1

Introduction

It is common practice within the UK construction industry for temporary battered slopes to be built by contractors at high slope angles without any reinforcement. Slopes may be built above ground level, or form part of a temporary excavation and are often constructed without a formal design by a geotechnical engineer. If a geotechnical engineer was later appointed to assess the stability of the slope for long term drained conditions, it is likely that the slope design would fail the Eurocode 7 design standard (BSI, 2004), and would require some form of reinforcement such as soil nails, anchors or geotextile mesh to ensure the slope design is compliant with Eurocode. This could come at a considerable cost to the contractor and is often avoided where possible. As a result the contractor takes on the risk and assumes the slope will remain stable for its design life. A likely reason why a slope design may fail to comply with Eurocode 7, whilst remaining stable in practice, is because the conservative saturated soil mechanics approach is used for the slope stability analysis, and the effects of soil suction (negative pore water pressure) on the soil's shear strength are ignored. This was demonstrated in practice by Ching et al. (1984), who showed that for an existing slope in Hong Kong, when the soil suction was ignored, the slope was shown to be theoretically unstable with a factor of safety of less than 1. When soil suction was taken into consideration, the factor of safety was shown to be greater than 1 and the slope was theoretically considered stable (as it was in reality).

Often groundwater control measures are required when the water table is too high for safe working conditions or construction below the water table is required. The water

table can be lowered and the pore water pressures reduced by using groundwater control techniques such as dewatering wells and stone key drains (Powers et al., 2007). The typical approach for battered excavations is to utilise dewatering wells located behind the crest of the slope with stone key drains designed to intercept any incoming groundwater through the slope face, as shown by the schematic in Figure 1.1. The stone key drains can be located at the toe of the slope or at any material layer interfaces where groundwater seepage and ground loss is an issue. Thomas et al. (2020) demonstrated how these techniques can be applied in practice on a construction project where a large excavation was required to enable the construction of an underground storm water tank in Oldham, Greater Manchester. It is well known by site personnel and geotechnical engineers that lowering of the groundwater table as a result of dewatering increases the strength of the soils which results in an increase in the stability of the slopes (Latief and Zainal, 2019; Thomas et al., 2020). However the theory of unsaturated soil mechanics, which governs this phenomenon, is not well understood by geotechnical engineers working within industry and is therefore not regularly applied in practice. The end result is that slope reinforcement designs can be over-conservative and over-engineered resulting in large and potentially unnecessary costs for the end client.

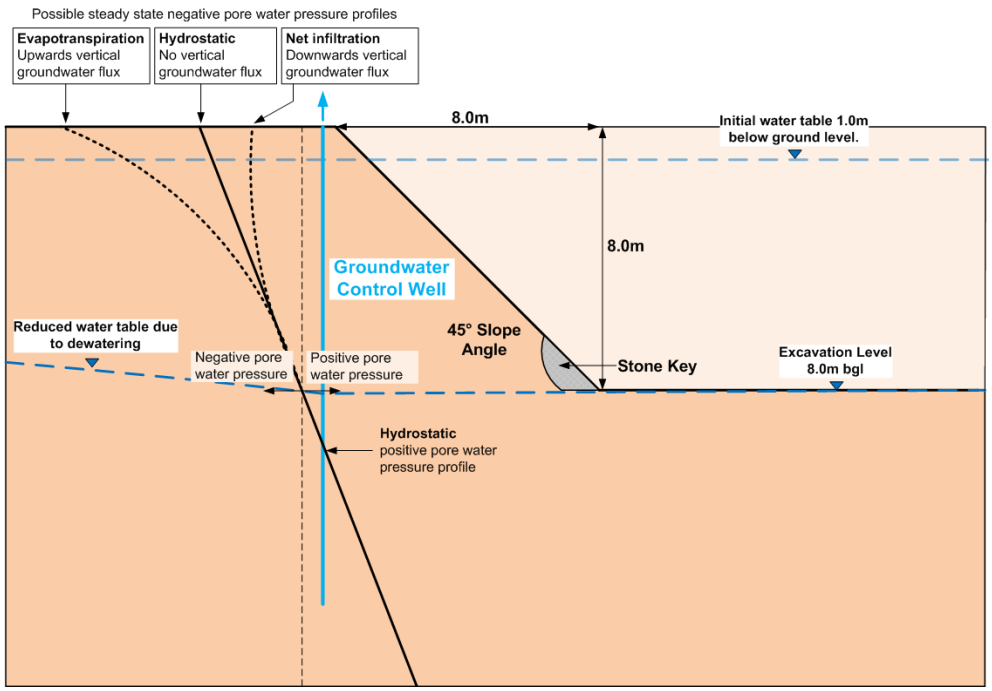

Figure 1.1: Typical problem where groundwater control techniques are required to enable construction of an excavation below the water table.

Considering unsaturated soil mechanics is not regularly applied in the construction industry, the academic community has driven the subject area forward over the last century, with the text by Fredlund et al. (2012) providing a comprehensive review. A key aim of the research is to provide a practical way to use the theory linking water content, soil suction and shear strength to engineering practice. The soil water retention curve (SWRC), discovered first by Buckingham (1907), describes the relationship between water content and soil suction. Several empirical equations have been defined in the literature to enable a continuous curve to be fit to measured soil water retention data (Brooks and Corey, 1964; van Genuchten, 1980; Fredlund and Xing, 1994). A continuous SWRC given by an equation enables the SWRC to be used in computer models such as the finite element method (one example being PLAXIS 2D (Bentley Systems, 2020)) to simulate complex unsaturated soil behaviour. Measuring the SWRC of a soil however requires expensive and time consuming laboratory experiments, as demonstrated by Toll et al. (2016), and is therefore rarely included in site investigation studies for construction projects. As a result many studies have been undertaken to predict the SWRC using standard laboratory test results, including particle size distribution tests, Atterberg limit tests, dry density measurements and void ratio measurements (see the works of Arya and Paris (1981); Aubertin et al. (2003); Fredlund et al. (2002); Perera et al. (2005). The SWRC is key to understanding the relationship between soil suction and shear strength. Unsaturated triaxial shear strength tests can be undertaken to determine the unsaturated shear strength of a soil at given confining pressures and soil suctions, as demonstrated by Mendes and Toll (2016). However, unsaturated shear strength tests are similar to SWRC tests in that they are time consuming and costly and are rarely undertaken during site investigation works for construction projects. As a result, papers have been published which present equations for predicting the unsaturated shear strength using the SWRC (Fredlund et al., 1996; Vanapalli et al., 1996; Oberg and Sallfors, 1997; Toll and Ong, 2003; Khalili and Khabbaz, 1998).

By briefly reviewing some of the key literature available on the subject area, it becomes apparent why unsaturated soil mechanics is not regularly used by geotechnical engineers in practice. Firstly the theory is complex and not part of the core skill set of a typical geotechnical engineer. Extensive learning would be required by a geotechnical engineer to be confident enough to apply the concepts to a slope design during a construction

project. Secondly the required testing results are rarely available in site investigation reports (i.e. SWRC and unsaturated shear strength tests) and the expense of undertaking these tests is rarely justifiable within the available budget of the project. Thirdly there is a lack of freely available guidance, procedures and tools with which a geotechnical engineer can use to apply these concepts in practice. The aim of the research is to provide some solutions to these recurring problems by presenting for the first time a procedure and set of tools that can be used to predict the SWRC followed by the unsaturated shear strength of a soil using only standard laboratory test results. In addition, the procedure aims to show the possible error in the SWRC prediction and therefore the resulting error in the shear strength prediction. The aim is to make unsaturated soil mechanics far more accessible for geotechnical engineers working in industry who strive to learn and then apply these concepts to real construction projects. The application of the procedure is then demonstrated for a typical construction project problem where the groundwater table is lowered around the perimeter of a battered excavation with the objective of increasing the stability of the slopes. The following research objectives have been set out to achieve the research project aims presented above:

- To present the most relevant literature that describes the mechanics and theories of unsaturated soil behaviour, with a focus on understanding how the water content, soil suction and shear strength are related and how these relationships can be predicted using standard laboratory test data. This information is presented in the Literature Review in Chapter 2.
- To develop a procedure that can be used by geotechnical engineers in practice to estimate the SWRC of a soil using standard site investigation test data, such as a particle size distribution, Atterberg limit test data and dry density, and then quantify the possible error in the SWRC prediction. The development of this procedure, along with the statistical analysis undertaken to develop the likely range in error of the SWRC prediction, is given in Chapter 3. The validation of the procedure using two soil samples from the literature is presented in Chapter 4, along with guidance and recommendations for how this procedure can be applied by a geotechnical engineer in practice.
- To develop a procedure that can be used by geotechnical engineers in practice to estimate the increase in shear strength of a soil using a predicted SWRC from the

previous step. The procedure will aim to quantify the possible error in shear strength due to the possible error in the SWRC prediction. The development of this procedure is presented in Chapter 5, along with guidance of how this can be applied to a typical geotechnical engineering problem using the finite element software package PLAXIS 2D.

With the objectives of the research clearly laid out above, the following chapter goes on to present an in depth review of the literature based around the link between water content, soil suction and shear strength and how they can be applied in engineering practice.

Chapter 2

Literature Review

This chapter presents a literature review of the topics that relate water content and shear strength to soil suction, and how this is applied in practice. The key objective of this Thesis chapter is to gain and present an understanding how the strength of soils increase as the groundwater table is lowered. Therefore a firm understanding of the unsaturated soil mechanics theories that govern these processes is absolutely vital. This chapter first looks at some of the differences between saturated and unsaturated soil mechanics, and how a term for unsaturated effective stress has been sought after by researchers to describe unsaturated soil behaviour. The behaviour of unsaturated soils is directly influenced by soil suction, which means it is fundamental to understanding how shear strength changes for unsaturated soils. The soil water retention curve (SWRC) is reviewed in detail as it describes how soil suction changes with water content. Topics reviewed include SWRC measurement techniques, how to fit a best-fit curve to the measured data, and how a SWRC of a soil can be estimated using standard laboratory test data (such as particle size distributions). The shear strength of unsaturated soils is then reviewed. The proposed theory for the extended Mohr-Coulomb equation by Fredlund et al. (1978) is presented, along with several other variations of this equation for estimating the shear strength of an unsaturated soils using the SWRC. Some experimental mechanical shear strength testing results are considered to assess the performance of the reviewed shear strength equations. Finally some case studies are presented which present how these concepts can be applied in practice to assess the stability of slopes where suction has an influence on the shear strength of the soil.

2.1 Stress State Variables and Effective Stress

Soil mechanics has successfully applied continuum mechanics to saturated soils (Terzaghi, 1943) and is regularly used in practice to describe the response of a soil to external forces (Thomas et al., 2020). Saturated soils contain two phases, solid particles which form the matrix of the soil, and water which fills the pore spaces. Saturated soil mechanics (SSM) is therefore based on the requirement that the soil remains fully saturated at all times. Unsaturated soil mechanics (USM) is complicated by the addition of a third phase, air. In USM, the water content of the soil reduces from saturated conditions as pore-water pressures become negative (i.e. suction increases). This is described by the term degree of saturation, S which is the ratio of the volume of water to the volume of voids in a soil sample.

Stress state variables are used to describe the state of equilibrium of a system. When one or more stress state variables are changed, the system will change in response to establish the new equilibrium state (Leong, 2016). Under saturated conditions, the stress state variables include total stress σ, effective stress, σ' and pore water pressure, u_w, which are related by the equation originally proposed by Terzaghi (1925)

$$\sigma' = \sigma - u_w \tag{2.1.1}$$

Effective stress has proven fundamental to the development of SSM over the last century (Terzaghi, 1943; Bishop and Blight, 1963). It is no surprise then that the discovery of an equation for unsaturated effective stress has been a key focus of the geotechnical academic community. Presented in Table 2.1 are equations for effective stress by Croney et al. (1958); Bishop (1959); Aitchison (1961); Jennings (1961); Richards (1966) and Jommi (2000). Of these equations, the most commonly discussed and cited in literature is the equation proposed by Bishop (1959). The equation by Croney et al. (1958) is equivalent to the equation by Bishop (1959) if pore-air pressure is taken as atmospheric pressure. The equations by Aitchison (1961); Jennings (1961) are similar in form to the Bishop (1959) equation, with slight variations in the pore pressure parameters. The equation by Richards (1966) builds on the Bishop (1959) equation by splitting the pore pressure term into two suction components, matric suction (difference between pore air and pore-water pressure) and osmotic suction (suction due to dissolved salt). Rather than use effective stress, Jommi (2000) argued for the use of an average skeleton mean stress, $\hat{p}$ which aligns

well with saturated critical state soil mechanics models which use the $q - p$ space.

The use of the Bishop (1959) equation in USM has proven controversial (Leong, 2016). This is because the Bishop (1959) equation does not fundamentally describe a stress state of an unsaturated soil, as demonstrated in practice by Morgenstern (1979). It was shown that the parameter, χ, when determined for volume change behaviour was different than when determined for shear strength behaviour. It was originally thought that χ was a function of saturation, and therefore bounded by 0 and 1, however it was shown by experimentation to go beyond these bounds. Therefore the Bishop (1959) equation for effective stress cannot be used as a stress state variable, but rather a constitutive equation that links stress state variables. This means that the stress state variables for unsaturated soils must be a combination of the stress variables total stress, σ, pore water pressure, u_w and pore air pressure, u_a. Table 2.2 shows the possible combination of stress state variables which can be used to formulate constitutive relations and elasto-plastic soil models for unsaturated soils. The two stress state variables most commonly used to develop equations for unsaturated shear strength include net total stress, $(\sigma - u_a)$ and matric suction, $(u_a - u_w)$ (Fredlund et al., 2012).

In the geotechnical academic community it is considered best practice to use two stress state variables, net total stress and soil suction, when forming constitutive equations and soil models for unsaturated soils (Fredlund et al., 2012). This is in place of using an equivalent effective stress equation as proposed by Bishop (1959). The next section of the literature review will discuss how soil suction and soil water content are linked in the form of the soil water retention curve (SWRC).

2.2 Soil Water Retention Curves

A soil water retention curve (SWRC) describes how soil suction is a function of water content. SWRCs are commonly referred to in literature as the soil-water characteristic curves (SWCC) (Fredlund et al., 2012) or soil-moisture characteristic curves (SMCC) (Arya and Paris, 1981). An example of a SWRC for sand, silt and clay soils is shown in Figure 2.1. Our early understanding of SWRC behaviour came from research of the soil sciences in fields such as soil physics and agronomy in the late 19^{th} and early 20^{th}

Reference	Effective Stress Equation	Notations
Croney et al. (1958)	$\sigma' = \sigma - \beta' u_w$	σ' = effective stress σ = normal stress β' = bonding factor effective in contributing to the shear strength of a soil u_w = pore water pressure
Bishop (1959)	$\sigma' = (\sigma - u_a) + \chi(u_a - u_w)$	u_a = the pore air pressure χ = the Bishop effective stress parameter related to the degree of saturation of a soil
Aitchison (1961)	$\sigma' = \sigma + \psi p$	p = pore water deficiency ψ = a parameter with values ranging from 0 to 1
Jennings (1961)	$\sigma' = \sigma - \beta' \mid u_w \mid$	β = a statistical factor of the same type as the contact area
Richards (1966)	$\sigma' = \sigma - u_a + \chi_m(h_m + u_a)$ $+\chi_s(h_s + u_a)$	χ_m = effective stress parameter for matric suction h_m = matric suction (cm) χ_s = effective stress parameter for osmotic suction h_s = osmotic suction (cm of water)
Jommi (2000)	$\hat{p} = (p - u_a) + S_r(u_a - u_w)$	$\hat{p}$ = average skeleton mean stress p = mean stress S_r = the degree of saturation

Table 2.1: Equations for effective stress of unsaturated soils

Reference Pressure/Stress	Stress State Variables
Pore Air Pressure, u_a	$(\sigma - u_a)$ and $(u_a - u_w)$
Pore Water Pressure, u_w	$(\sigma - u_w)$ and $(u_a - u_w)$
Total Stress, σ	$(\sigma - u_a)$ and $(\sigma - u_w)$

Table 2.2: Combination of Stress State Variables for Unsaturated Soils

century. Buckingham (1907) undertook pioneering work in the field of soil physics and was credited for introducing the concepts of "capillary potential" and "capillary conductivity". The capillary potential contains two components, "matric suction" $(\sigma - u_a)$, and "osmotic suction", π. Osmotic suction is attributed to the presence of dissolved salt in the pore water and cannot be measured directly, but can be inferred from measurements of total and matric suction (Leong et al., 2003a). The sum of the matric suction and osmotic suction is termed total suction, ψ (Krahn and Fredlund, 1972). The term soil suction is commonly used in place of either total suction or matric suction, and is the term that will be used in this Thesis to describe either.

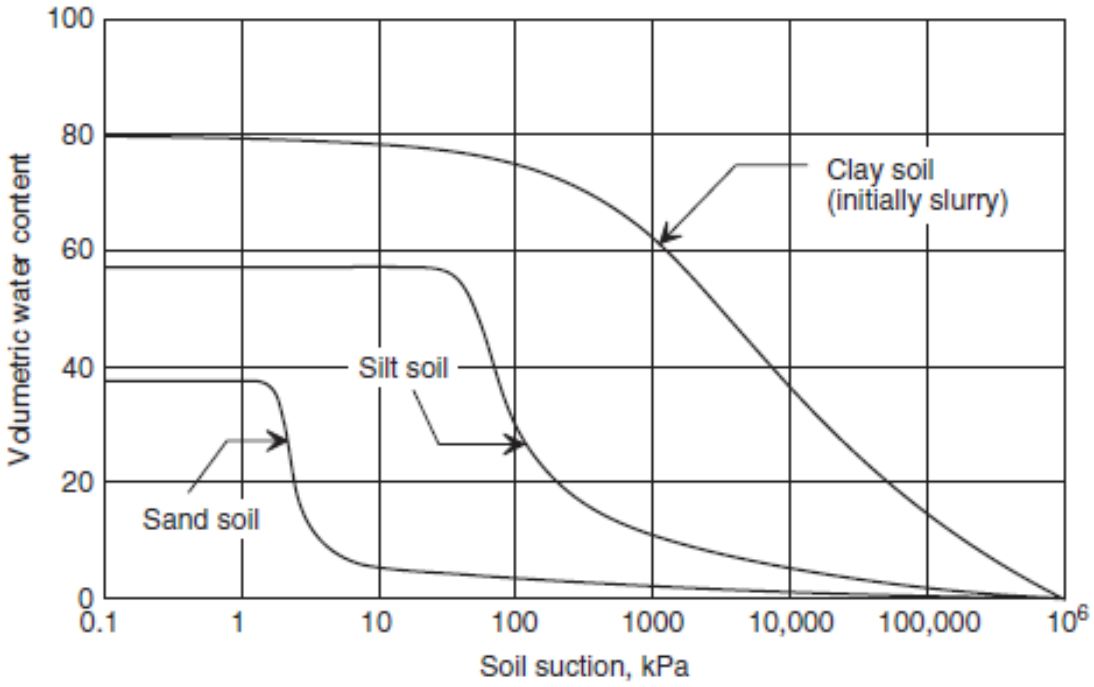

Figure 2.1: Example of SWRC for sand, silt and clay soils (Fredlund et al., 2012).

2.2.1 Description of the SWRC

A SWRC defines soil suction for a given water content. It is standard practice to plot soil suction on a logarithmic scale and water content on a linear scale. This is appropriate due to scale of the variation in the two quantities. Figure 2.2 shows a typical SWRC measured in the laboratory over the suction range 0.1 kPa to 1.0 GPa. Figure 2.2, reproduced from Fredlund et al. (2012) highlights the three zones of desaturation. These desaturation zones are termed the "boundary effect zone", the "transition zone" and the "residual zone". The boundary effect zone is also known as the "capillary zone" when referenced to field conditions, and represents soil above the water table which has a saturation between approximately 90-100%. Water is drawn above the water table due to "capillary action", which is driven by intermolecular forces between the water and soil particles. The height of the capillary zone is dependant on the pore size distribution of the soil. Typically the height increases with decreasing pore size, such that fine grained soils such as clays can have a capillary zone in the order of 10m, whereas in sandy soils the capillary zone may be in the order of 1m).

The point between the boundary effect zone and the transition zone is termed the "air-entry value". It represents the suction that is required to cause desaturation of the largest pores (Vanapalli et al., 1999). The air-entry value is determined by extending the constant slope of a SWRC to intersect the suction axis at the point where the soil is fully saturated, as shown in Figure 2.2). In the transition stage, as the suction increases the soil dries rapidly, reducing the connectivity of the water in the voids resulting in a reduction in the hydraulic conductivity of the soil. Eventually, as suction increases further, only small changes in the water content occur. This is known as the residual zone. The residual state of saturation can be considered the point at which the liquid phase becomes discontinuous, at which point it is very difficult to remove water from the soil. This condition is often not clearly defined from laboratory testing, as high suctions are often not measurable using standard testing apparatus, as will be explored in the following section.

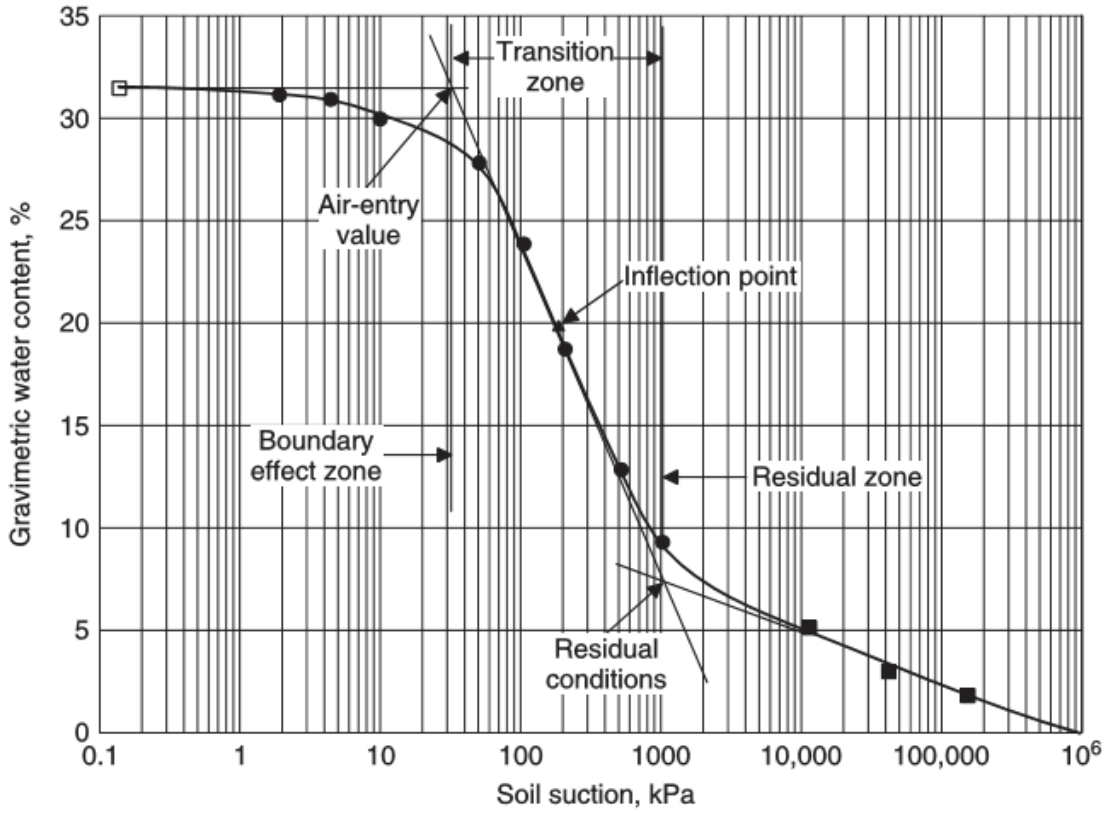

Figure 2.2: Typical SWRC showing zones of desaturation. Reproduced from Fredlund et al. (2012).

2.2.2 Measurement of Suction and Water Content

To determine a SWRC of a soil, suction and water content must be measured simultaneously using specialised instrumentation. The methods for measuring suction can be classified as either direct or indirect methods. Devices that measure suction directly do so by measuring the negative pore water pressure, the most common of which is the tensiometer (Stannard, 1992). Indirect methods measure a variable other than negative pore water pressure, such as an elevated air pressure in the case of pressure plate devices (Vanapalli et al., 2008). Other indirect methods include the filter paper method (Bulut, 1996) and the chilled mirror method which measures relative humidity (Leong et al., 2003b). These devices require calibration of the measuring device to ensure correct calculations of suction. The measured suction range, along with the advantages and disadvantages of each method are summarised in Table 2.3. Other methods include thermal conductivity sensors (Jin et al., 2017), electrical resistivity methods (Hen-Jones et al., 2017), psychrometers (Cardoso

et al., 2007) and pore fluid squeezers which are used to measure osmotic suction (Peroni and Tarantino, 2006). The pressure plate device and tensiometer are discussed in greater detail below. These methods are most commonly used to measure suctions in the low suction range (1-2000kPa) accurately, which is the area of most interest in geotechnical engineering, and more specifically groundwater control operations, where suctions greater than 1000kPa would be unlikely.

A pressure plate device is one of the traditional methods used to measure a SWRC in a laboratory. The pressure plate device uses a technique called null-type axis-translation, originally proposed by Hilf (1956), to apply matric suction to soil specimens. This technique translates the origin of reference for pore-water pressure from atmospheric pressure to a final increased air pressure (Vanapalli et al., 2008). This method requires the pore-water pressure to be controlled using a ceramic disk with fine pores. The soil is placed on top of the ceramic disk, which then creates an interface which separates air and water phases. The soil specimen and ceramic disc are contained within a pressurised steel chamber, which is depicted in a schematic detailing the features of a basic pressure plate device in Figure 2.3. As air pressure within the chamber is increased, drainage of water is allowed through the pores of the ceramic disk. Once equilibrium is attained, the water content can be determined by weighing the specimen. This method is limited by the maximum air pressure which can be imposed in the pressure chamber, plus the air entry value of the ceramic disc. This means that the pressure plate device is often limited to suctions in the region of 1500 kPa.

Conventional tensiometers can be used to measure negative pore-water pressures between suctions of 0 kPa to 90 kPa (Stannard, 1992), and usually consist of a plastic tube which contains a high-air entry porous ceramic cup connected to a pressure measuring device. The tube and cup are filled with deaired water and the ceramic cup must be in good contact with the surrounding soil. The water in the tensiometer will have the same pressure as the pore water once equilibrium is achieved between the soil and measuring system (Fredlund et al., 2012). In the past 30 years, high-capacity tensiometers have been developed, the first of which was developed by Ridley and Burland (1993) which could measure negative pressures to -1500kPa. Since then a number of high-capacity tensiometers have been used in the field and laboratory successfully (Oliveira and Marinho, 2008; Toll et al., 2016). A high suction tensiometer has been developed at Durham University which can directly

Device	Suction Component	Suction Range (kPa)	Advantages	Disadvantages
Standard tensiometer	Matric suction	0 to 90	Quick to run tests. Suitable if only low suctions are necessary. (Stannard, 1992)	Limited suction range. (Stannard, 1992)
High-capacity tensiometer	Matric suction	0 to 2000	Drying is imposed naturally where negative pore water pressure is created. Tests quicker than pressure plate devices. (Lourenço, 2008)	Range of measurement is a function of the air-entry value of the ceramic disc. Cavitation at high suctions can lead to erroneous results. (Marinho et al., 2008)
Pressure plate (axis-translation)	Matric suction	0 to 1500	Cavitation at high values of suction does not occur because pore water pressure does not become negative. (Vanapalli et al., 2008)	Range of measurement is a function of the air-entry value of the ceramic disc. Tests can take a long time to complete, especially if soils are fine grained. (Lourenço, 2008)
Filter paper	Total suction	Entire range	Inexpensive and simple. Measures full suction range. (Bulut, 1996)	May be less accurate at low suctions due to sensitivity of filter paper (Bulut, 1996)
Chilled mirror	Total suction	Entire range	Test times range from two minutes to one hour. (Leong et al., 2003b)	Overestimates suction over full suction range. Error increases as suction increases. (Leong et al., 2003b)

Table 2.3: Summary of devices used to measure soil suction.

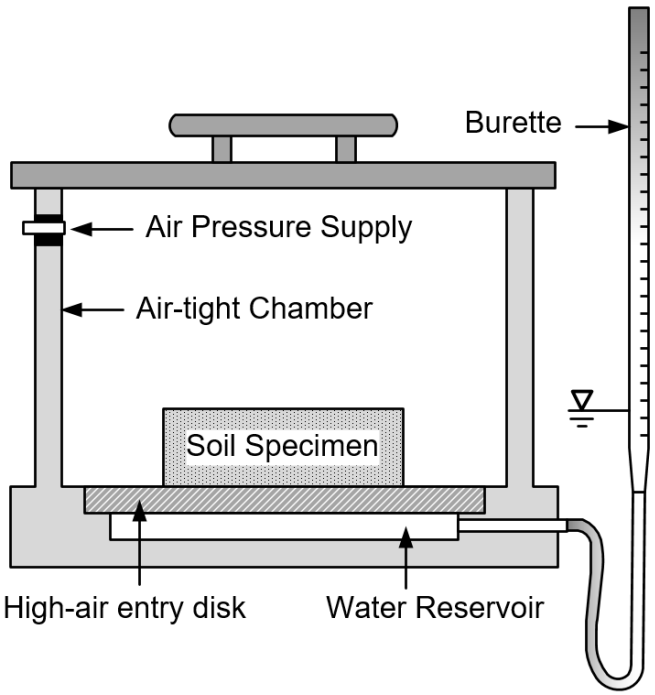

Figure 2.3: Typical laboratory pressure plate cell for measuring the soil water retention curve of soil specimens.

measure suctions as high as 2000 kPa (Toll et al., 2013, 2015). The apparatus, shown in Figure 2.4, allows continuous measurements of water content, suction and volume change. The frame is placed on an electronic balance to determine the change in weight, and hence water content (Lourenço et al., 2011). Four displacement transducer were installed through the outside beams of the frame to measure radial displacement of the specimen, and two more were placed through the upper beam to measure axial displacement. The high suction tensiometer was fitted through a hole in the support plate.

The main advantage of using high-capacity tensiometers is that drying is imposed naturally, where negative pore water pressures are created, as opposed to pressure plate devices where atmospheric pressure is elevated inside a chamber. However, as a consequence of this, internal pores inside the porous disk can desaturate by cavitation when the pore pressure becomes highly negative leading to erroneous results (Marinho et al., 2008). It is also considerably quicker to determine a SWRC of a soil using a tensiometer than a pressure plate device. Lourenço (2008) reports that tests to determine a SWRC of a glacial till soil sample using a pressure plate device took 7 weeks, whereas using a high-capacity

Figure 2.4: Durham SWRC high-capacity tensiometer equipment. Reproduced from Toll et al. (2015).

tensiometer on the same material took less than 7 days.

A study by Toll et al. (2015) compared measured SWRCs using different laboratory apparatus. These included the Durham high capacity tensiometer, pressure plate device, filter paper and chilled mirror. The results from each method showed reasonable agreement. The chilled mirror and filter paper methods show good agreement at high suctions (1,000 to 10,000kPa) wheras at low suctions (less than 2,000kPa) the pressure plate data plots at lower suctions than the tensiometer data. This difference is explained by different volumetric responses, specifically the pressure plate device shows different shrinkage paths indicating less volume change.

Figure 2.5 shows an example of two SWRCs for a silty sand soil. There are individual curves for desorption (drying) and adsorption (wetting). Laboratory experiments of repeated drying and wetting cycles show that soil water retention behaviour is hysteretic in nature (Toll et al., 2016; Mualem, 1974). Repeated cycles of wetting and drying, caused by seasonal fluctuations in weather cycles, has been shown to cause irrecoverable changes to the micro-structure of the soil, leading to a weakening of the soil (Hen-Jones et al., 2017; Stirling et al., 2020). This could potentially lead to unstable slopes used for infrastructure,

and is a growing concern as climate change drives more extreme weather patterns across the globe (Tang et al., 2018).

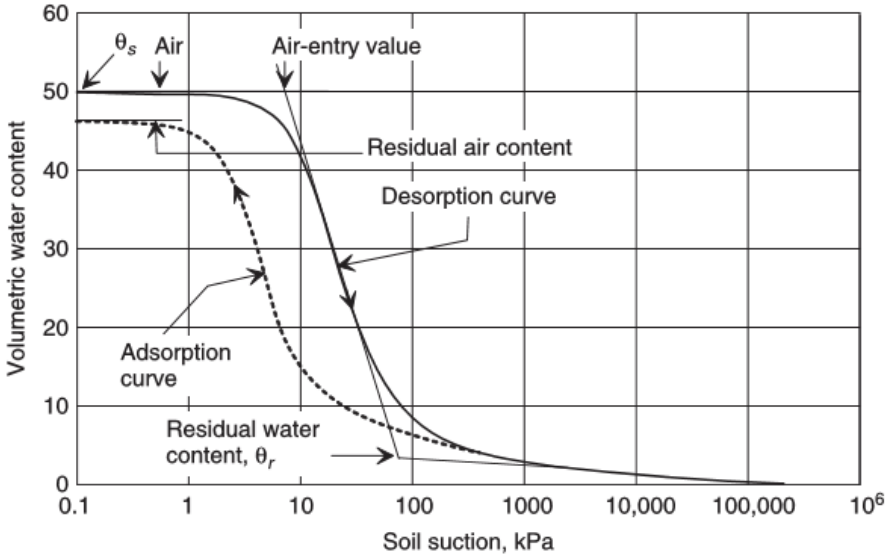

Figure 2.5: Typical SWRC for a silty soil showing adsorption and desorption curves (Fredlund et al., 2012).

Undertaking a SWRC test can be time consuming and expensive, which means they are not commonly undertaken in the UK construction industry. As a result a number of soil databases containing unsaturated soil datasets have been collated and released by the scientific community. Three notable databases include the UNsaturated SOil Hydraulic DAtsabase (UNSODA) (Nemes et al., 2001), the database of HYdraulic PRoperties of European Soils (HYPRES) (Wösten et al., 1999), which is part of the larger European Soil Database and the SVSOILS database from Soil Vision (Bentley Systems, 2020). The UNSODA database was developed in the agricultural discipline, and contains over 790 soil samples from around the world. The database is freely available to download, meaning it has been used in numerous academic studies since it was introduced in 1996 (Nemes et al., 2001; Ostovari et al., 2015; Schaap and Leij, 1998; Chai and Khaimook, 2020). The HYPRES database was formed from a joint initiative of 20 European institutions. It contains information on a total of 5521 soil samples, however the database is not freely available to download as no agreement has been reached with the participating institutions regarding their distribution. The SVSOILS database is a commercial software product which contains data on more than 6,200 soil-water characteristic curves and provides numerous theoretical methods for estimating the SWRC or unsaturated hydraulic

conductivity curve. As the database is a commercial product, it is not freely available, meaning it tends to be used in commercial projects rather than in academia.

With soil water retention data measured using any one of the methods outlined in this section, or extracted from a soils database, it is often necessary to fit a curve to the measured data points. This has the benefit of giving the likely suction water content relationship over the full suction range, and can be used in computer models of unsaturated soil behaviour. The following section reviews several empirical equations for the shape of the SWRC proposed in literature.

2.2.3 Empirical Curve-Fit Equations for the SWRC

A number of closed-form empirical solutions have been proposed in literature to provide a best-fit curve to measured soil water retention data (Gardner, 1958; Brooks and Corey, 1964; van Genuchten, 1980; Fredlund and Xing, 1994; Pham and Fredlund, 2008). These equations, summarised in Table 2.4, can be classified as two or three parameter equations, meaning they have 2 or 3 curve fitting parameters. Each equation has a curve fitting parameter that relates to the air-entry value of the soil and the slope of the curve in the transition zone. Additional parameters allow the low-suction range near the air-entry value to have an independent shape to the high suction range near residual conditions, and provides greater flexibility when fitting the curve to measured data.

Gardner (1958) originally proposed an empirical two parameter equation used to describe the unsaturated permeability function. The curve generated by this equation takes the same form as the SWRC equation and was therefore subsequently used to fit a curve to measured SWRC data. Brooks and Corey (1964) proposed a two-parameter equation which represents the desaturation of the soil when soil suction is greater than the air-entry value. Therefore this model requires a fixed point for the air-entry value. This leads to a sharp discontinuity in the slope near the air-entry value (AEV). The equation can provide a good solution to soils that have a sharp change in gradient at the AEV, such as larger pore size soils such as sands. However, this slope discontinuity is not suitable for soils with smoother curves such as clays and silts. The discontinuity in the gradient of the slope can also cause issues when simulating unsaturated soil behaviour using numerical

Reference	SWRC Equation	Notations
Gardner (1958)	$\theta(\psi) = \dfrac{\theta_s}{1 + a_g \psi^{n_g}}$	θ = volumetric water content θ_s = saturated volumetric water content a_g = fitting parameter which is a function of the air-entry value of the soil n_g = fitting parameter related to the gradient of the curve
Brooks and Corey (1964)	$\theta(\psi) = \theta_s$ for $\psi <= \psi_{aev}$ $\Theta_n = \left[\dfrac{\psi}{\psi_{aev}}\right]^{-\lambda_{bc}}$ for $\psi > \psi_{aev}$ where $\Theta_n = \dfrac{\theta(\psi) - \theta_r}{\theta_s - \theta_r}$	ψ_{aev} = air-entry value of soil λ_{bc} = pore size distribution index θ_r = residual water content Θ_n = normalised water content
van Genuchten (1980)	$\Theta_n = \dfrac{1}{\left[1 + (a_{vg}\psi)^{n_{vg}}\right]^{m_{vg}}}$ where $\Theta_n = \dfrac{\theta(\psi) - \theta_r}{\theta_s - \theta_r}$	a_{vg} = fitting parameter related to the air-entry value n_{vg} = fitting parameter related to the gradient of the curve m_{vg} = fitting parameter related to the residual water content
Fredlund and Xing (1994)	$\theta(\psi) = C(\psi)\dfrac{\theta_s}{\left\{\ln\left[e + (\psi/a_f)^{n_f}\right]\right\}^{m_f}}$ where $C(\psi) = 1 - \dfrac{\ln(1 + \psi/\psi_r)}{\ln[1 + (10^6/\psi_r)]}$	a_f = fitting parameter related to the air-entry value n_f = fitting parameter related to the gradient of the curve m_f = fitting parameter related to the residual water content ψ_r = soil suction corresponding to the residual water content θ_r
Pham and Fredlund (2008)	for $1 \leq \psi < \psi_{aev}$ $\theta_1(\psi) = \theta_u - S_1 \log(\psi)$ for $\psi_{aev} \leq \psi < \psi_r$ $\theta_2(\psi) = \theta_{aev} - S_2 \log\left(\frac{\psi}{\psi_{aev}}\right)$ for $\psi_r \leq \psi < 10^6$ kPa $\theta_3(\psi) = S_3 \log\left(\frac{10^6}{\psi}\right)$	S_1, S_2, S_3 = slope of straight line portions of SWRC within each zone θ_u = water content at 1 kPa θ_{aev} = water content at air-entry value $\theta_1, \theta_2, \theta_3$ = water content in line segments 1, 2 and 3 respectively

Table 2.4: Curve fitting equations proposed in the literature for the SWRC.

methods such as finite element or finite difference models. van Genuchten (1980) proposed a three-parameter equation which produces a "S-shaped" curve, or sigmoid". This gives a smooth curve in the region of the air entry value, however due to the nature of the sigmoid curve shape, the van Genuchten equation has a tendency to overestimate the residual water content of a soil sample. This is because the water content tends towards zero as suction tends towards 10^6 kPa, however at high suctions the van Genuchten (1980) equation simulates no change in water content with suction i.e. the curve becomes horizontal. Fredlund and Xing (1994) developed a four parameter equation which has a similar sigmoid shape to the van Genuchten (1980) equation, but gives greater flexibility in the region of the residual water content. It does this by applying a correction factor which directs the SWRC to a water content of zero at a suction of 10^6 kPa. Most recently, Pham and Fredlund (2008) developed a series of equations to represent SWRCs which split the curve into three segments over the suction axis. These zones include suction less than air entry value, suction values between the air entry value and the residual water content, and suctions above the residual water content. This approach gives greater control over the shape of the curve within the three zones, however it is more complicated to use and requires a greater number of parameters to be determined.

Several comparative studies are presented in literature where SWRC equations have been fitted to laboratory data sets, for example Leong and Rahardjo (1997) reviewed seven SWRC equations by analysing a database of soils. For each curve fitting equation, the minimum sum of squared residual values (SSR) was calculated to quantify the performance of each equation. It was shown that the three curve-fitting parameter equations (van Genuchten, 1980; Fredlund and Xing, 1994) performed better than the two parameter equations (Gardner, 1958; Brooks and Corey, 1964). The Fredlund and Xing (1994) equation was found to "perform marginally better" than the van Genuchten (1980) equation. A study by Sillers (1997) reviewed nine SWRC equations by analysing a database of 231 soils. The Akaike criterion (Akaike, 1974), a statistical indicator, was used to assess the performance of the curve-fit using each SWRC equation. The results shows that the Fredlund and Xing (1994) equation with the correction factor performed the best, followed by the van Genuchten (1980) equation. The study also showed that the Fredlund and Xing (1994) correction factor could be applied to other SWRC equations and in each case the quality of the fit could be improved.

The equations presented in this section can be used to fit a curve to measured SWRC data from laboratory experiments. However, undertaking these laboratory experiments can be laborious and time consuming, as explained in Section 2.2.2. Therefore, predicting the SWRC accurately without having to undertake these experiments is a key focus of the academic community. The next section takes a look at methods presented in the literature to predict the SWRC of a soil using standard laboratory tests and index properties.

2.2.4 Estimating the SWRC

Knowledge of a soils drying SWRC is critical if the unsaturated shear strength is to be calculated in the case of dewatering operations. However, in many cases, undertaking a SWRC laboratory test is expensive and time consuming and therefore not feasible during preliminary stages of construction projects. As a result, researchers have developed methods to predict the drying SWRC of a soil using standard laboratory test results, such as particle size distribution, dry density, particle density and voids ratio. The predictive methods are often referred to as PedoTransfer Functions (PTF) (Schaap and Leij, 1998). They can be broadly divided into three categories.

- Functional regression models which correlate basic soil properties to empirical SWRC equation parameters (Benson et al., 2014; Perera et al., 2005; Rawls and Brakensiek, 1985; Vereecken et al., 1989; Schaap et al., 1998).
- Statistical estimates of water contents at various soil suctions (Gupta and Larson, 1979; Schaap et al., 1998).
- Predictive models based on the physical characteristics of the soil (Arya and Paris, 1981; Aubertin et al., 2003; Tyler and Wheatcraft, 1989).

Functional regression models correlate basic physical properties to parameters of a SWRC equation, for example Rawls and Brakensiek (1985) presented regression equations for estimating the parameters of the Brooks and Corey (1964) equation. These equations are correlated to the percentage sand in the soil specimen and the porosity. Vereecken et al. (1989) used a dataset of 40 Belgium soils to derive equations for the parameters of the van Genuchten (1980) equation. It was found that the SWRC could be estimated to

a reasonable degree of accuracy using the grain size distribution, dry density and carbon content. Perera et al. (2005) used functional regression to determine equations for the parameters of the Fredlund and Xing (1994) equation using a database of soils from the United States. The set of equations require parameters derived from the particle size distribution such as D_{10} (particle size at 10% passing) and P_{200} (percent passing the No. 200 sieve). Benson et al. (2014) proposed a set of equations for the van Genuchten a_{vg} and n_{vg} parameters for clean sands. This model requires the dry unit weight, the particle size at 60% passing, D_{60}, and the coefficient of uniformity, C_u. By analysing several soils from literature, it was shown that the predicted a_{vg} and n_{vg} values were within ± 2 percent of the best-fit values. Recently Chai and Khaimook (2020) proposed a model for estimating the parameters of the Fredlund and Xing (1994) equations using the PSD, saturated permeability, and plasticity index. The method aims to link the air-entry value parameter to the saturated permeability of a soil sample, and the rate of desaturation to the slope of the PSD curve.

The second type of pedotransfer function uses statistical analysis techniques on a database of soils. No prior shape of the SWRC is used (i.e. the empirical SWRC equations are not used as a starting point in the analysis). Gupta and Larson (1979) developed an equation which requires the percentage of sand, silt, clay and organic matter, along with the bulk density. A number of regression coefficients were developed which are selected from a table based on a given matric suction. Schaap et al. (1998) used neural network algorithms to analyse the UNSODA database of soils and predict the hydraulic properties of soils using different levels of input data (soil texture, density, porosity). The model produces an estimated water content along with the uncertainty of the prediction in each case. It was shown that the predicted errors and confidence limits were often large, however they may still be accurate enough for most applications during preliminary stages of projects.

The third type of pedotransfer function uses a physio-empirical approach where a grain-size distribution curve is used in the prediction of the SWRC. The Arya and Paris (1981) model was the first of this kind. The method attempts to estimate the pore size distribution from the particle size distribution. The pore radii are then converted to soil suctions through the use of capillary theory. This theory is based on the assumption that the pore size distribution and the particle size distribution are strongly related, with

larger particles producing larger pore sizes than smaller particles. The Arya and Paris (1981) model contains a fitting parameter, α, which can typically be taken as 1.38, but can range between 1.1 for fine textured soils and 2.5 for coarse grained soils (Arya et al., 1982). This fitting parameter was included to account for uncertainties in the prediction of the SWRC. This method requires a well defined particle size distribution, otherwise the accuracy of the predicted curve becomes poor. There are various models presented in the literature which aim to improve the estimate of the Arya and Paris (1981) for heterogeneous soils. Gupta and Ewing (1992) applied the Arya and Paris (1981) model to the PSD to understand how inter-aggregate pores (i.e inter-particle pores within a soil aggregate) may impact the shape of the SWRC and the quality of the prediction. Nimmo (1997) proposed an extended version of the Arya and Paris (1981) model that quantifies the effect of soil structure and fabric on the SWRC. The model splits the pore space into texture-related and structure-related components. The revised model was shown to be an improvement on the Arya and Paris (1981) model by the goodness of fit, indicated by correlation coefficients ranging from 0.908 to 0.998 for the new model, compared with a range of 0.686 in 0.955 for the texture-based model. Tyler and Wheatcraft (1989) adapted the Arya and Paris (1981) model by estimating the α input parameter for different soils rather than adopting a default value. This is achieved by calculating fractal dimensions by linear regression analysis over particles associated with the grain-size fractions.

Fredlund et al. (2002) also proposed a physio-empirical model for predicting the SWRC of a soil from the particle size distribution. The method divides the PSD into small particle groupings of relatively uniform particle sizes. For each uniform particle size, it is hypothesized that there is a unique SWRC. The SWRCs for each particle size are summed together to form one SWRC that describes the whole soil. The primary limitation of this method lies in the ability to 'mix' the individual particle fractions to obtain the overall SWRC. This 'mix' is controlled by a parameter named the assumed packing factor, n_p, which must be approximated for each particle size. The method has been shown to be quite sensitive to this parameter, and more research is required to understand how best to estimate the parameter (Fredlund et al., 2002).

The Modified Kovács Model (Aubertin et al., 2003) is a physio-empirical model based on standard soil properties. It is a modification of an original model proposed by Kovacs (1981). This model makes the distinction between capillary and adhesive forces, and has

been shown to be effective at predicting the SWRC of tailing materials and silts (Aubertin et al., 1998) and later for cohesive and granular soils (Aubertin et al., 2003).

2.2.5 Comparison of SWRC Estimation Methods

A number of studies which compare the performance of the SWRC estimation methods have been presented in the literature. Each study has analysed a database of soils with experimental SWRC testing. The study by Fredlund et al. (2002) compares the method proposed in the paper to the models by Arya and Paris (1981), Tyler and Wheatcraft (1989), Vereecken et al. (1989), Rawls and Brakensiek (1985) and Scheinost et al. (1997) and applies the different techniques to a database of 188 soils. The methods were compared using the following metrics:(i) the squared difference between the measured and estimated air-entry values, and (ii) the squared difference between the measured and estimated maximum slopes of the SWRC. Figure 2.6, reproduced from Fredlund et al. (2002), presents the calculated squared difference for the air-entry value and maximum slope for all six predictive methods, where a low value of squared difference indicates a good fit. The Fredlund et al. (2002) model and Arya and Paris (1981) model show the highest level of confidence in correctly estimating the air-entry value of the soil across the database of soils studied. The air-entry value is typically the most important area of the SWRC when applying a SWRC to unsaturated soil mechanics problems because this occurs over the low suction range of most interest to geotechnical problems. This is followed by the slope of the SWRC. The study showed that models by Vereecken et al. (1989), Fredlund et al. (2002), Scheinost et al. (1997) and Arya and Paris (1981) all performed reasonably well at estimating the slope of the curve.

Table 2. Squared difference between the logarithm of the estimated and measured air-entry values (AEV) for all six PTFs.

PTF AEV	Squared difference
Fredlund et al. 1997 PTF	0.5850
Arya and Paris 1981	0.8620
Scheinost et al. 1997	1.1911
Rawls and Brakensiek 1985	0.7870
Vereecken et al. 1989	1.3281
Tyler and Wheatcraft 1989	3.4380

Table 3. Squared difference between estimated and measured maximum slopes for all six PTFs.

PTF maximum slope	Squared difference
Fredlund et al. 1997 PTF	0.487
Arya and Paris 1981	0.586
Scheinost et al. 1997	0.476
Rawls and Brakensiek 1985	7.850
Vereecken et al. 1989	0.462
Tyler and Wheatcraft 1989	0.988

Figure 2.6: Squared difference results for the air-entry value and maximum slope for the six SWRC predictive methods. Reproduced from Fredlund et al. (2002).

In the study by Chai and Khaimook (2020), the method proposed in the paper is compared to the Arya and Paris (1981) and Perera et al. (2005) models. A dataset of 9 soils from literature was used to verify the proposed model. This was split in four plastic soils and five non-plastic soils. The plastic soils were defined as soils with a plasticity index greater than 8. The absolute relative error (ARE) was calculated to compare results. A low value of ARE indicates a better fit than a high ARE value. The results, reproduced from Chai and Khaimook (2020), are presented in Figure 2.7. For the plastic soils, the Chai and Khaimook (2020) performed well, whilst both the Arya and Paris (1981) and Perera et al. (2005) models perform reasonably. Note that the average values of ARE are largely influenced by the poor performance of each method for soil HR. If soil HR is removed from the average, the Chai and Khaimook (2020) performs best with an ARE value of 0.097 followed by the Arya and Paris (1981) model with 0.188 and the Perera et al. (2005) model with 0.236. For the non-plastic soils, each predictive method performs well, with the Chai and Khaimook (2020) model marginally better than the Arya and Paris (1981) model and Perera et al. (2005) (See Figure 2.7).

Table 6
ARE of the predictions on the literature datasets.

Type of soils	Verification data	Absolute relative error (*ARE*)		
		Proposed model	Perera et al. [30]	Arya and Paris [4]
Plastic	SK-10	0.069	0.078	0.194
	SK-17	0.043	0.188	0.116
	HR	1.538	9.826	5.854
	BN1	0.179	0.441	0.255
	Average	0.457	2.633	1.605
Nonplastic	1010	0.199	0.580	0.332
	1160	0.210	0.758	0.194
	1465	0.223	0.346	0.694
	1467	0.572	0.297	0.286
	3311	0.101	0.317	0.081
	Average	0.261	0.460	0.320

Figure 2.7: Calculated ARE for the Chai and Khaimook (2020) model, Arya and Paris (1981) model and the Perera et al. (2005) model. Reproduced from Chai and Khaimook (2020).

This section has summarised some of the methods presented in literature for predicting the SWRC of soils using standard laboratory tests such as particle size distribution and

dry density. A predicted SWRC is essential if the shear strength of an unsaturated soils is to be estimated without undertaking complex, time consuming and expensive laboratory experiments. The next section documents methods for estimating the shear strength of unsaturated soils which have been presented in the literature.

2.3 Shear Strength of Unsaturated Soils

Knowledge of the the shear strength of soils under unsaturated conditions is critical to the safety of engineered structures. It is particularly important to the stability of slopes which are subjected to repeated changes in moisture content due to changing weather patterns. The previous section of this literature review presented the current accepted understanding of the water content soil suction relationship described by the soil water retention curve (SWRC). This relationship plays a pivotal role in the change in shear strength of unsaturated soils when subjected to changes in water content. This section will present the current knowledge of shear strength theory for unsaturated soils and how the SWRC plays a key part in estimating the shear strength of soils when direct testing methods, such as triaxial tests, are unavailable.

2.3.1 Shear Strength Theories

Theories of shear strength for unsaturated soils have been proposed as extensions to the theories and equations regularly used in saturated soil mechanics. The shear strength of a saturated soil can be described by the Mohr-Coulomb failure criteria and the effective stress parameter, originally proposed by Terzaghi (1936) and regularly used in geotechnical engineering today. It can be expressed by the equation

$$\tau = c' + \sigma' \tan \phi' \tag{2.3.2}$$

where τ is the shear stress on the failure plane at failure, c' is the effective cohesion intercept, ϕ' is the effective angle of internal friction, and σ' is the effective stress which is equal to $(\sigma - u_w)$ where σ is the normal stress on the failure plane at failure and u_w is the pore water pressure at failure. The relationship between shear strength and effective stress is linear when plotted on a graph of effective stress and shear stress. Failure conditions

can be drawn using Mohr circles, with the line tangent to the Mohr circles representing the failure envelope.

The use of effective stress with the Mohr-Coulomb failure criterion has proven to be successful when dealing with saturated soils. However, as was discussed in Section 2.1, the use of effective stress as a stress state variable for unsaturated soils is unsatisfactory. Instead, two stress state variable are required, net total stress $(\sigma - u_a)$ and matric suction $(u_a - u_w)$. The extended Mohr-Coulomb model for unsaturated soils was proposed by Fredlund et al. (1978) and can be expressed as

$$\tau = c' + (\sigma - u_a)\tan\phi' + (u_a - u_w)f_1 \tag{2.3.3}$$

where f_1 is a soil property function defining the relationship between shear strength and soil suction. The form of the f_1 parameter in Equation (2.3.3) allows the shear strength envelope with respect to matric suction to be either linear of curved. The original form of the equation proposed by Fredlund et al. (1978) was linear, where $f_1 = \tan\phi^b$, such that

$$\tau = c' + (\sigma - u_a)\tan\phi' + (u_a - u_w)\tan\phi^b \tag{2.3.4}$$

where ϕ^b is the angle indicating the rate of increase in shear strength with respect to a change in matric suction. The failure envelope for unsaturated soils can be plotted in a three-dimensional manner, as presented in Figure 2.8. The net normal stress is plotted along the horizontal axis, shear stress along the vertical axis, and the matric suction is plotted on the axis into the page. The frontal plane represents the saturated soil conditions where matric suction is zero. The Mohr circles for unsaturated soils are plotted on the net normal stress axis in a same manner as saturated soils are plotted on the effective stress axis. At an elevated matric suction, a second failure envelope along with Mohr circles can be plotted, as shown in Figure 2.8. The surface tangent to both sets of Mohr circles is known as the Mohr-Coulomb failure plane for unsaturated soils. The inclination of this surface is controlled by the parameter $\tan\phi^b$ if the change in shear strength with matric suction is linear. It was originally thought to be linear based on analysis of a limited data set of soils (Fredlund et al., 1978). However, later studies by Gan et al. (1988) and Escario and Jucá (1989) which involved experimental testing of partially saturated soils showed that it was non-linear after the air-entry value of the soil was reached.

Equations for unsaturated shear strength have also been proposed as part of elastoplastic constitutive soil models for unsaturated soils (Alonso et al., 1990; Wheeler and Sivakumar,

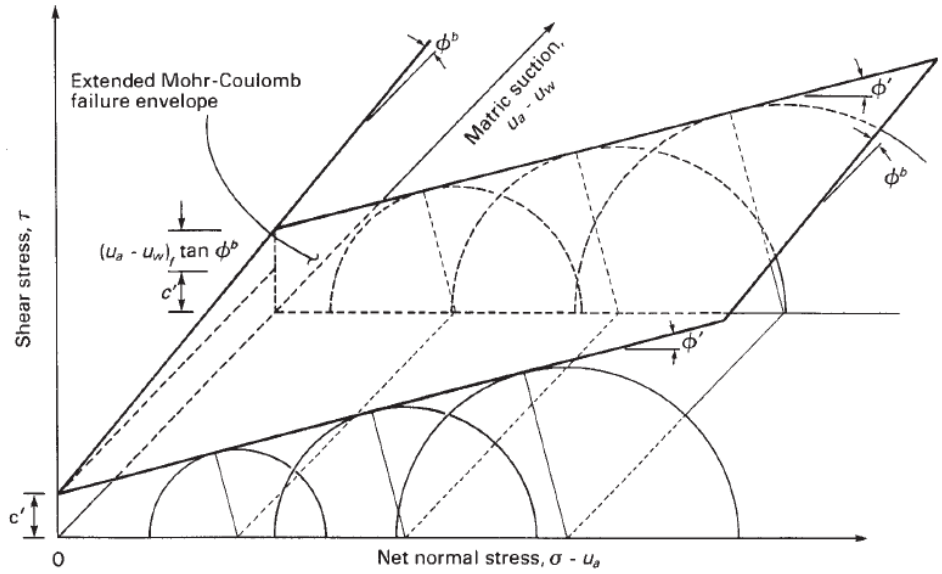

Figure 2.8: Extended Mohr-Coulomb failure envelope for unsaturated soils. Reproduced from Fredlund et al. (2012).

1995; Toll, 1990; Sun et al., 2000; Sheng et al., 2008). The equations for shear strength are written in terms of the $q - p - u$ space used in critical state soil models. The stress state variables used are deviator stress, $q = \sigma_1 - \sigma_3$, mean total stress, $p = (\sigma_1 + \sigma_2 + \sigma_3)/3$ and matric suction, $u = u_a - u_w$. σ_1, σ_2 and σ_3 are the major, intermediate and minor principal stresses respectively. The critical state shear strength equation of the Barcelona Basic Model (Alonso et al., 1990) takes the form

$$q = M(p - u_a) + k(u_a - u_w) \tag{2.3.5}$$

where M is the gradient of the critical state line and k is an elastic constant. Wheeler and Sivakumar (1995) suggested a critical state shear strength equation where each shear strength property is a function of matric suction

$$q = M_s(p - u_a) + \mu_s \tag{2.3.6}$$

where M_s and μ_s are material characteristics that are a function of suction. Sun et al. (2000) suggested a different equation to describe the critical state line

$$q = M(s)[\bar{p} + \bar{\sigma_0}(s)] \tag{2.3.7}$$

where

$$M(s) = M(0) + M_s\bar{\sigma_0}(s) \tag{2.3.8}$$

where $\bar{\sigma_0}(s) = \frac{s}{1+s/a}$, $M(0) \equiv M$, is the slope of the critical state line for saturated soils, M_s is a fitting parameter, and a is constant equal to the maximum stress, $\sigma_0(s)$, when the soil is subject to an infinite suction. Finally Sheng et al. (2008) proposed an alternative shear strength equation as part of the SFG (Sheng, Fredlund, Gens) model. The SFG model describes yield stress, shear strength, and volume change behaviour of unsaturated soils as functions of suction. In this model an apparent tensile strength equation is proposed

$$\bar{p}_0 = \begin{cases} -S & S < S_{sa} \\ -S_{sa} - (S_{sa}+1)\ln\frac{S+1}{S_{sa}+1} & S \geq S_{sa} \end{cases} \tag{2.3.9}$$

where S_{sa} is the saturation suction, which represents the unique transition value of suction between saturated and unsaturated states.

The equations proposed so far are empirical, which means that they require unsaturated shear strength testing to determine the unsaturated shear strength parameters. The following sections reviews some of the methods for testing unsaturated soils using laboratory apparatus. Methods for estimating the shear strength using the SWRC are discussed in a following section.

2.3.2 Testing Methods for Unsaturated Shear Strength

Shear strength testing for unsaturated soils is an extension of procedures undertaken for saturated soils. Both modified triaxial cell apparatus and shear box apparatus can be used to determine the shear strength of an unsaturated soil. These tests can be classified into two groups (Sheng et al., 2011):

- Suction controlled tests using either triaxial or direct shear laboratory equipment. Suction is usually held constant as stresses are applied. These tests can be considered drained as water and air can flow in and out of the specimen in order to maintain suction. The principal components of these tests are shown in Figure 2.9 (a) and (c).
- Constant water content tests using either triaxial or direct shear laboratory equipment. Water content is held constant while suction may change. These tests are less

common because the stress state can not be controlled. The principal components of these tests are shown in Figure 2.9 (b) and (d).

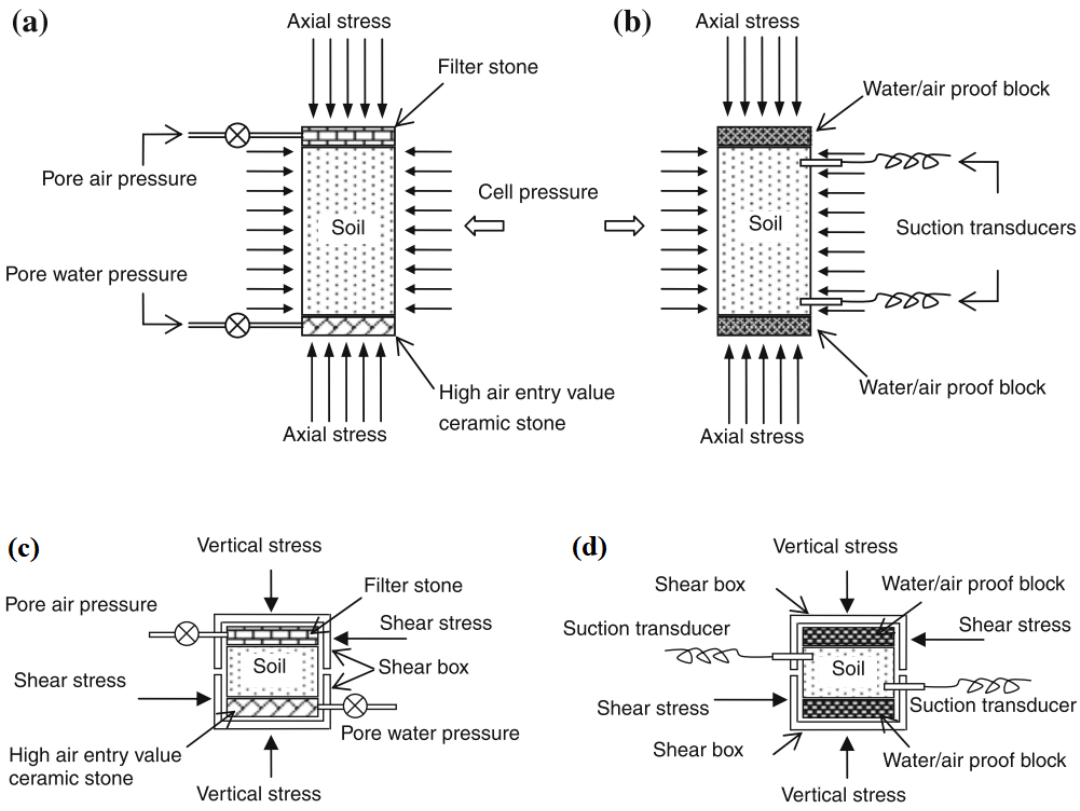

Figure 2.9: Illustration of shear strength tests for unsaturated soils for (a) suction controlled triaxial test (b) undrained triaxial test (c) suction controlled direct shear test and (d) undrained direct shear test. Reproduced from Sheng et al. (2011).

The following observations have come about as a result of experimental shear strength testing of unsaturated soils (Fredlund et al., 1996; Escario and Jucá, 1989; Vanapalli et al., 1996; Wheeler and Sivakumar, 1995; Fredlund et al., 2012):

- Under constant net vertical pressure, an increase in matric suction results in an increase in shear strength.
- Under constant suction, an increase in net vertical stress results in an increase in shear strength
- The relationship between shear strength and matric suction is non-linear.

- The increase in shear strength with suction is greatest at low suctions i.e. below the air-entry value of the soil. This increase flattens out as suction increases and water content tends towards residual conditions.
- Vertical stress has a much greater influence on the change in shear strength than matric suction, however at the near surface, net vertical stresses are likley to be small whereas suctions can vary significantly.

Experimental testing will be discussed in further detail in the following sections as estimated shear strength is compared to measured shear strength for a number of equations presented in the literature.

2.3.3 Estimation of Shear Strength using SWRCs

A soil water retention curve, described in detail in Section 2.2, describes the relationship between matric suction and either water content or saturation. It is known that a decrease in water content causes an increase in shear strength i.e. there is a relationship between the SWRC and the shear strength of a soil.

This sections documents the equations presented in the literature that aim to formulate this relationship as an extension of the saturated Mohr-Coulomb failure model. This model, rather than critical state soil models, has been selected to investigate further because it is most likely to be easily implemented into current soil mechanics practice in the construction industry. Fredlund et al. (1996) proposed a non-linear form of Extended Mohr-Coulomb Equation 2.3.4

$$\tau = c' + (\sigma - u_a)\tan\phi' + (u_a - u_w)\Theta_d^{\kappa}\tan\phi' \tag{2.3.10}$$

where and κ is a fitting parameter and Θ_d is the dimensionless water content defined as θ/θ_s, where θ is the current volumetric water content and θ_s is saturated water content. Garven and Vanapalli (2006) provided an empirical relationship between the fitting parameter κ and plasticity index, PI, of the soil

$$\kappa = -0.0016(PI)^2 + 0.0975(PI) + 1 \tag{2.3.11}$$

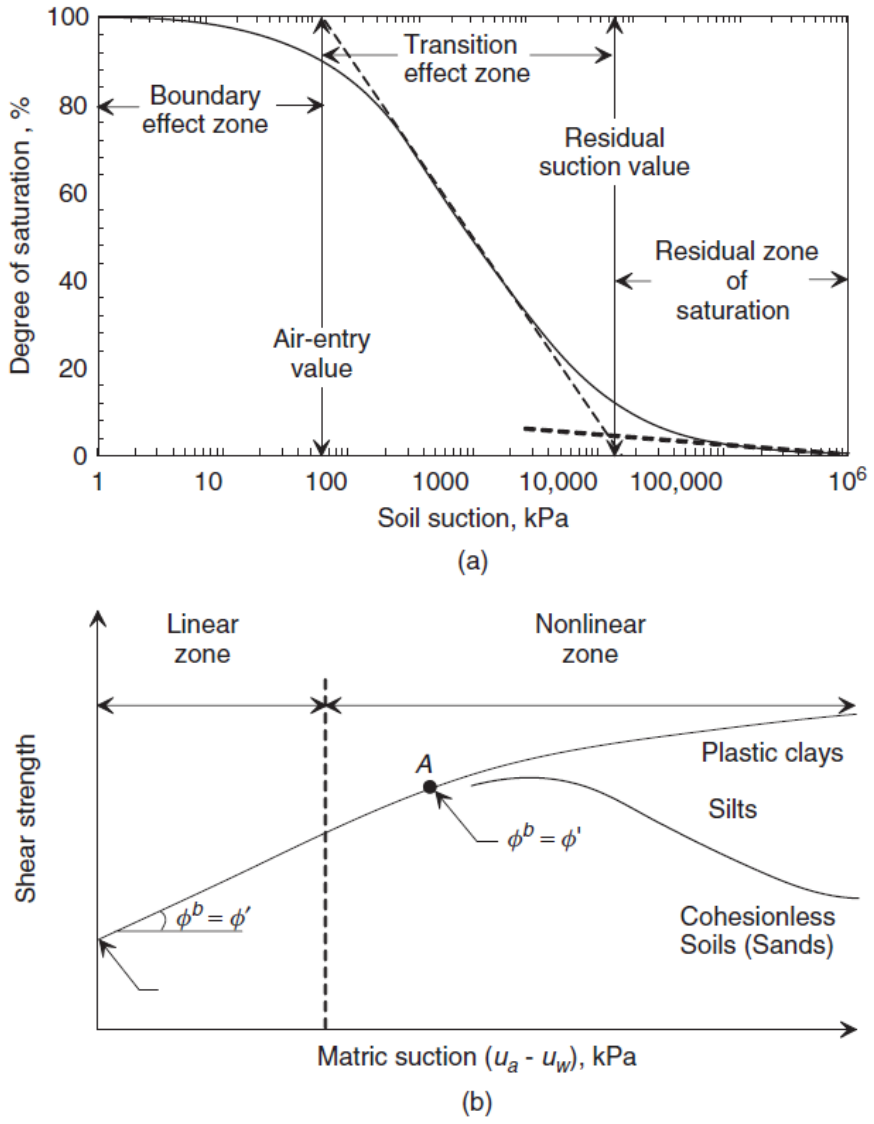

Figure 2.10: Relationship of SWRC to shear strength envelope. Reproduced from Fredlund et al. (2012).

Vanapalli et al. (1996) proposed an equation where a SWRC is normalised between saturated and residual water content conditions

$$\tau = c' + (\sigma - u_a)\tan\phi' + (u_a - u_w)\left(\frac{\theta - \theta_r}{\theta_s - \theta_r}\right)\tan\phi' \tag{2.3.12}$$

where θ_r is the residual water content.

Oberg and Sallfors (1997) proposed an equation that uses the SWRC in the form of degree of saturation, S

$$\tau = c' + (\sigma - u_a)\tan\phi' + (u_a - u_w)S\tan\phi' \tag{2.3.13}$$

Toll and Ong (2003) proposed an equation that can be used in both critical state soil models and in the extended Mohr-Coulomb equation, which is written as:

$$\tau = c' + (\sigma - u_a)\tan\phi' + (u_a - u_w)\left(\frac{S_r - S_{r2}}{S_{r1} - S_{r2}}\right)^k \tan\phi' \tag{2.3.14}$$

where S_r is the degree of saturation, S_{r1} is a reference value which can be taken as 100% saturation, S_{r2} is a reference value which can be taken as the degree of saturation at residual suction, and k is a fitting parameter.

Khalili and Khabbaz (1998) assume that a soil behaves like a saturated soil if the matric suction is less than the air-entry value of the soil. Once the air-entry value is exceeded, the suction component of shear strength is reduced by a factor λ'. The equation takes the form

$$\tau = c' + (\sigma - u_a)\tan\phi' + (u_a - u_w)\lambda'\tan\phi' \tag{2.3.15}$$

where

$$\lambda' = \left[\frac{u_a - u_w}{(u_a - u_w)_b}\right]^{-0.55} \tag{2.3.16}$$

where $(u_a - u_w)_b$ is the air-entry value.

The equations presented here all take a similar form, where a function relating the SWRC is given in place of the $\tan\phi^b$ parameter proposed by Fredlund et al. (1978). Additionally, all the equations can be re-cast into a form of the equation using the Bishop effective stress parameter, χ.

$$\tau = c' + (\sigma - u_a)\tan\phi' + \chi(u_a - u_w)\tan\phi' \tag{2.3.17}$$

The equivalent form of $\tan\phi^b$ and χ for each equation presented is given in Table 2.5.

The following section will review some mechanical testing of unsaturated soils where the estimated and measured shear strength are compared to assess the performance of each equation and suitability of applying each equation in engineering practice.

2.3.4 Comparison of Shear Strength Equations using Mechanical Testing of Unsaturated Soils

There are a number of studies presented in the literature which compare the performance of the shear strength estimation equations using experimental mechanical shear strength

Equation	$\tan\phi^b =$	$\chi =$
Fredlund et al. (1978)	$\tan\phi^b$	$\dfrac{\tan\phi^b}{\tan\phi'}$
Fredlund et al. (1996)	$\Theta_d^\kappa \tan\phi'$	Θ_d^κ
Vanapalli et al. (1996)	$\left(\dfrac{\theta-\theta_r}{\theta_s-\theta_r}\right)\tan\phi'$	$\left(\dfrac{\theta-\theta_r}{\theta_s-\theta_r}\right)$
Oberg and Sallfors (1997)	$S\tan\phi'$	S
Khalili and Khabbaz (1998)	$\left[\dfrac{u_a-u_w}{(u_a-u_w)_b}\right]^{-0.55}\tan\phi'$	$\left[\dfrac{u_a-u_w}{(u_a-u_w)_b}\right]^{-0.55}$

Table 2.5: Equivalent $\tan\phi^b$ and χ for shear strength equations.

testing data (Sheng et al., 2011; Vanapalli and Fredlund, 2000). This section will review some of these studies.

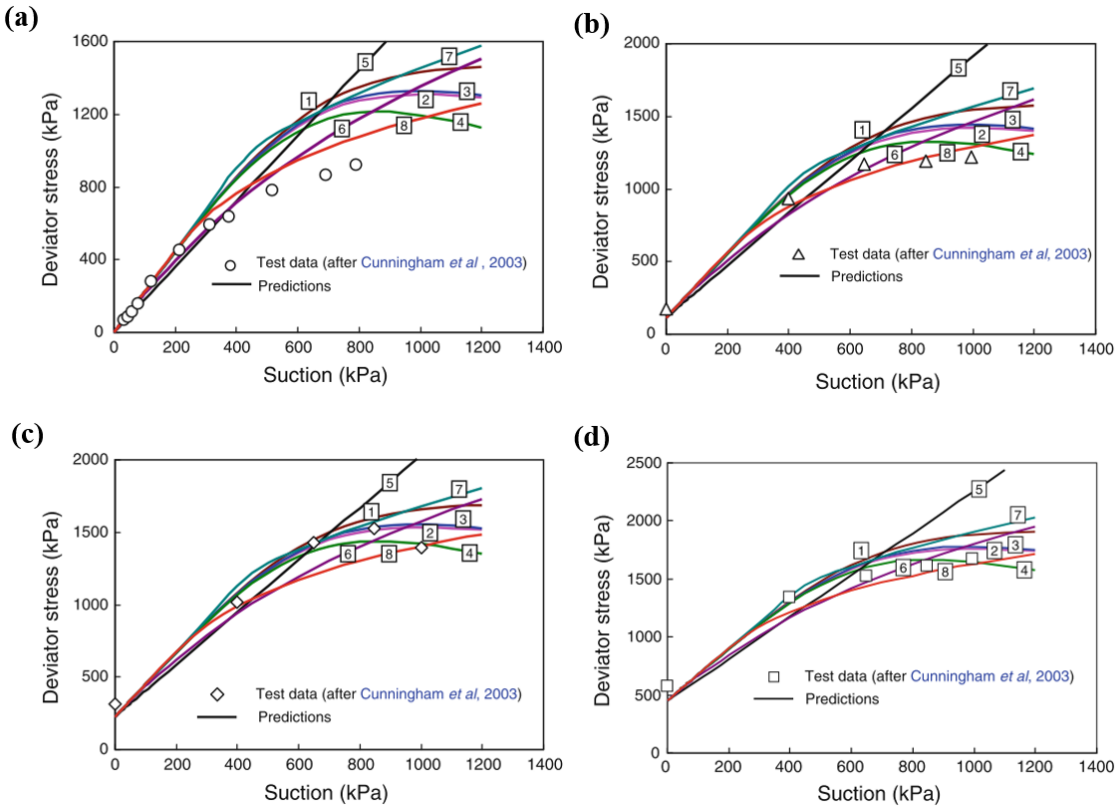

Figure 2.11: Prediction of the triaxial test data on air-dry silty clay for net confining pressures of (a) 0 kPa, (b) 50 kPa, (c) 100 kPa, and (d) 200 kPa. Reproduced from Sheng et al. (2011).

The first is a study by Sheng et al. (2011) which compares eight shear strength equations using a number of experimental testing datasets. The equations compared

are those proposed by Oberg and Sallfors (1997) [1], Fredlund et al. (1996) [2], Vanapalli et al. (1996) [3], Toll and Ong (2003) [4], Alonso et al. (1990) [5], Sun et al. (2000) [6], Khalili and Khabbaz (1998) [7] and Sheng et al. (2008) [8], where the numbers relate to the predicted shear strength curves in Figures 2.11 and 2.12. The two datasets presented in the paper are summarised here. The first was a set of triaxial compression tests undertaken on a reconstituted silty clay provided by Cunningham et al. (2003). The slurry soil was isotropically preconsolidated to 130kPa, before being tested at net confining pressures of 0 kPa (unconfined), 50 kPa, 100 kPa and 200 kPa, as presented in Figure 2.11 (a), (b), (c) and (d) respectively. The results can summarised for each net confining pressure as follows

- Unconfined - all shear strength equations overestimate the shear strength data. The closest prediction is using the equation by Sheng et al. (2008).
- 50 kPa - Closest prediction by Sheng et al. (2011) followed by Toll and Ong (2003). The equations based on the SWRC (Vanapalli et al., 1996; Fredlund et al., 1996) follow the shape of the data but somewhat overestimate the shear strength at low suctions. The shear strength appears to be sensitive to the residual suction, which can be difficult to determine for fine grained soils.
- 100 kPa - The equations based on the SWRC give close predictions of shear strength, particularly the equations by Fredlund et al. (1996) and Vanapalli et al. (1996).
- 200 kPa - The best prediction is given by the Toll and Ong (2003) equation, followed by the equations by Fredlund et al. (1996) and Vanapalli et al. (1996).

In general it was shown that the shear strength equations based on the SWRC fit well to the strength data at higher confining pressures, but less so at confining pressures less than 100 kPa. The second dataset was provided by Thu et al. (2006) which contains shear strength data on compacted kaolin clay (15%) and silt (85%). All soil specimens were compacted to an optimum water content of 22% and tested at net confining pressures of 100 kPa, 200 kPa and 300 kPa. The results can be summarised for each net confining pressure as

- 100 kPa - The closest predictions are by Sheng et al. (2008) and Sun et al. (2000).

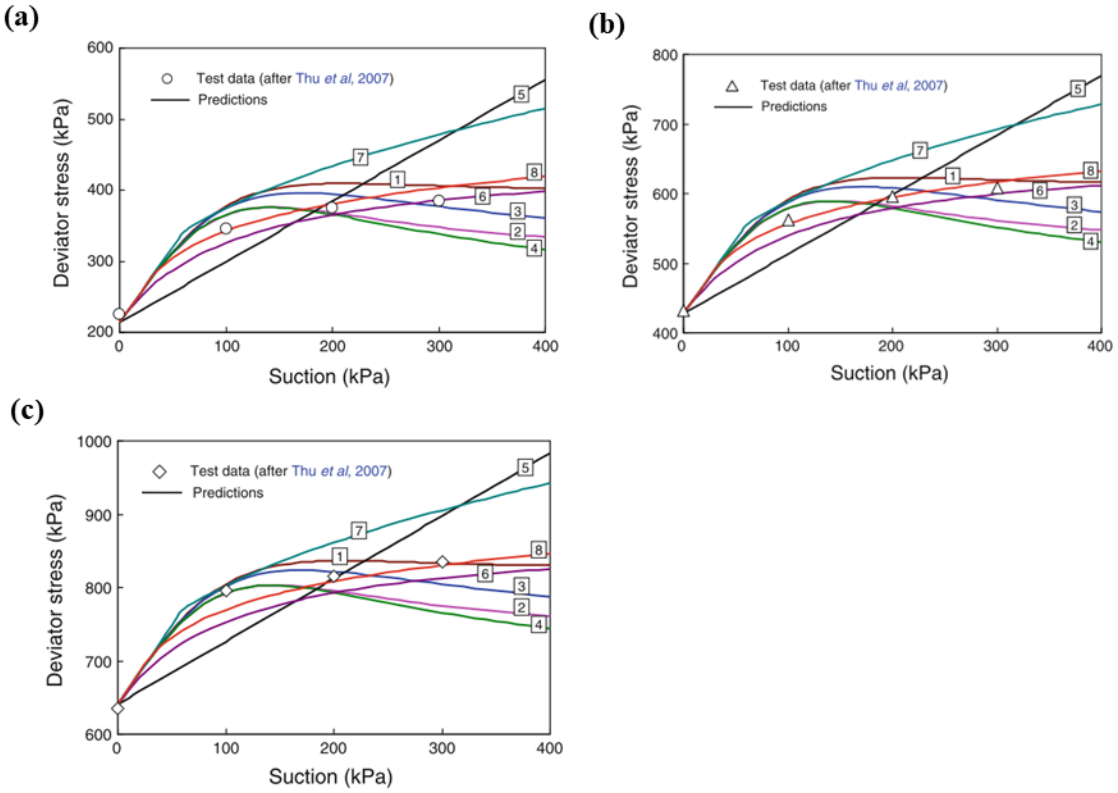

Figure 2.12: Prediction of the triaxial test data on compacted kaolin clay at net confining pressures of (a) 100 kPa, (b) 200 kPa, (c) 300 kPa. Reproduced from Sheng et al. (2011).

The equations that use the SWRC perform best at intermediate suctions between 200 to 300 kPa.

- 200 kPa - The closest predictions are again by Sheng et al. (2008) and Sun et al. (2000). The equations by Fredlund et al. (1996) and Vanapalli et al. (1996) give reasonable predictions at intermediate suctions but underestimate shear strength at high suctions greater than 300 kPa.

- 200 kPa - Again the closest prediction is given by the Sheng et al. (2008) equation. The equations by Sun et al. (2000), Vanapalli et al. (1996) and Fredlund et al. (1996) all give reasonable predictions.

Based on the experimental testing presented in this paper, the equations by Sheng et al. (2008), Sun et al. (2000), Vanapalli et al. (1996), Fredlund et al. (1996) and Toll and Ong (2003) consistently outperform the equations by Alonso et al. (1990), Khalili and Khabbaz (1998) and Oberg and Sallfors (1997), which typically overestimate the shear strength of

the soils as suction increases. It must be noted that the equations by Vanapalli et al. (1996) and Toll and Ong (2003) are sensitive to the selection of residual suction, therefore this parameter must be chosen with care when used in practice. It is clear from looking at the results from each dataset that different equations may perform better for different soils types, therefore as many equations as possible should be utilised in practice if the required parameters cannot be determined from available shear strength data.

Vanapalli and Fredlund (2000) presented a study which compares the shear strength equations by Fredlund et al. (1996), Vanapalli et al. (1996), Oberg and Sallfors (1997) and Khalili and Khabbaz (1998). Three soil samples have been analysed from a dataset of experimental direct shear tests by Escario and Jucá (1989). The soils samples include a Madrid gray clay, red silty clay and Madrid clay sand. Escario and Jucá (1989) measured the SWRC for each soil sample between suctions of 0 kPa and 15,000 kPa. Also the shear strength testing was undertaken up to suctions of 15,000 kPa while the net total stress was held constant at 120 kPa.

Figure 2.13, reproduced from Vanapalli and Fredlund (2000), shows the comparison between the predicted and measured shear strength over the full suction range tested for each of the three soil samples. Figure 2.14 shows the same comparison over a limited suction range which is of most interest during the application of unsaturated soil mechanics to geotechnical engineering problems. In each figure, Procedure 1 refers to the Fredlund et al. (1996) equation, Procedure 2 refers to the Vanapalli et al. (1996) equation, Procedure 3 to the Oberg and Sallfors (1997) equation and Procedure 4 to the Khalili and Khabbaz (1998) equation. The results can be summarised as follows

- Over the full suction range, the Fredlund et al. (1996) equation performs the best of the four procedures. The Vanapalli et al. (1996) follows, however it tends to overestimate the shear strength in the high suction range. This may be due to possible error in estimating the residual suction from the SWRC. Both the Khalili and Khabbaz (1998) and Oberg and Sallfors (1997) equations provide poor predictions in the large suction ranges.
- In the limited suction range, less than 1500 kPa, both equations by Fredlund et al. (1996) and Vanapalli et al. (1996) provide good comparisons for all three soils tested. The Oberg and Sallfors (1997) equation is also poor in the low suction range. The

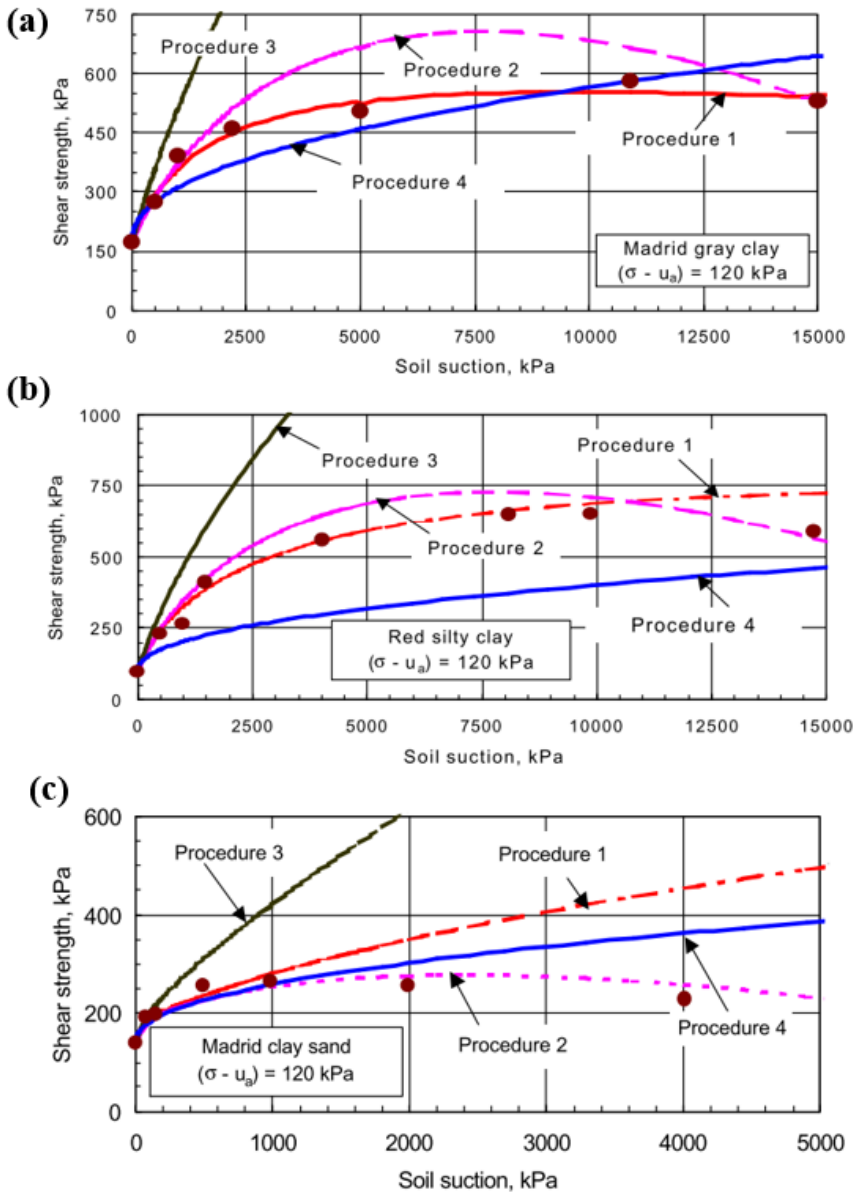

Figure 2.13: Comparison of predicted vs measured shear strength data for the four shear strength equations for the soils (a) Madrid gray clay (b) Red silty clay and (c) Madrid clay sand. Reproduced from Vanapalli and Fredlund (2000).

Khalili and Khabbaz (1998) provides mixed results in the low suction range, where it typically underestimates shear strength. As the low suction range will be of most importance during the application of this theory in groundwater control, Fredlund et al. (1996) and Vanapalli et al. (1996) equations are likely to give the best results.

The results presented by Vanapalli and Fredlund (2000) demonstrate that the shear

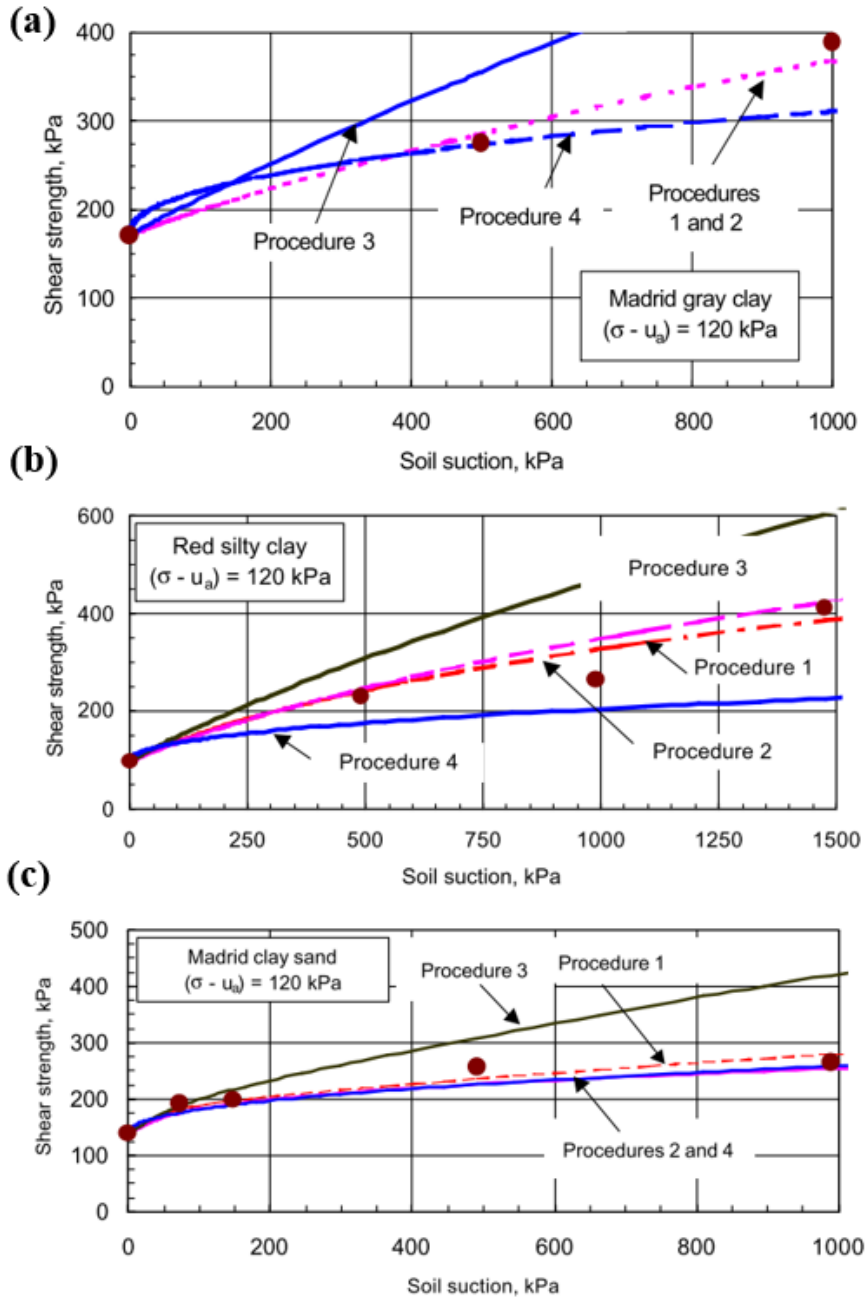

Figure 2.14: Comparison of predicted vs measured shear strength data for the four shear strength equations over the limited suction range of 0 kPa to 1500 kPa for the soils (a) Madrid gray clay (b) Red silty clay and (c) Madrid clay sand. Reproduced from Vanapalli and Fredlund (2000).

strength of an unsaturated soil can be reasonably predicted in the low to medium suction range (less than 1500kPa) using the SWRC and the equations by Vanapalli et al. (1996) and Fredlund et al. (1996). As the suction increases, the error between the predicted

and measured shear strength is more likely to increase. The error in the predicted shear strength when using the Vanapalli et al. (1996) model may be attributed to the error in estimating the residual suction of the soil. This is particularly the case for fine grained soils such as clay, as demonstrated by the Madrid clay in Figure 2.13. The following section will look at how some of these concepts can be applied in geotechnical engineering practice.

2.4 Application of Unsaturated Shear Strength in Practice

The application of unsaturated soil mechanics in engineering practice is still relatively limited. Applying unsaturated soil mechanics is of most interest to slope stability problems, where changes in negative pore water pressure can greatly influence the factor of safety of a slope. Other problems include the bearing capacity of soils when designing foundations and the stability of retaining walls. For all these problems, it is common practice within the construction industry to use saturated soil mechanics, as this is the conservative approach. Engineers may feel uncomfortable applying unsaturated soil mechanics for a number of reasons, these include: (i) a lack of understanding of the theory of unsaturated shear strength (ii) uncertainty in the negative pore-water pressure profile above the water table (iii) a lack of computer software which can model unsaturated soil behaviour and (iv) a perception that negative pore-water pressures can not be relied upon due to climatic and seasonal variations in rainfall (Fredlund et al., 2012). This section of the literature review presents a couple of case studies where unsaturated shear strength has been used successfully during slope stability analyses.

There are several methods in which unsaturated shear strength can be used in a slope stability analysis. The first is to use a modified geotechnical modelling software which uses the non-linear unsaturated shear strength equations proposed by Fredlund et al. (1996). The second approach is to use standard geotechnical modelling software (i.e. a saturated soil mechanics model) and split the soil above the water table into a number of layers. The total cohesion in each layer is calculated as the effective cohesion plus the cohesion due to matric suction. This is referred to as the total cohesion method (Ching et al., 1984). A third method is to use Bishop stress method, where the unsaturated effective stress is calculated from suction and water content. This is the approach used by the PLAXIS

geotechnical finite element software to model unsaturated soils.

The first example is a case study from Hong Kong presented by Ching et al. (1984) which uses the total cohesion method. An existing 60 degree slope is located behind a row of residential buildings. The slope has been protected from rainfall infiltration by a lime plaster cement across its surface, however failures in this surface have been observed leading to the study of its stability. The soil consists of colluvium, completely weathered granite, highly weathered granite, and fully competent granite bedrock. The groundwater table is located between around 50m below the ground surface and roughly follows the ground surface profile. Triaxial tests were undertaken to assess the shear strength parameters, ϕ', c' and ϕ^b. In situ measurements of soil suction were conducted using tensiometers. From this, matric suction profiles with elevation were developed, as shown in Figure 2.15.

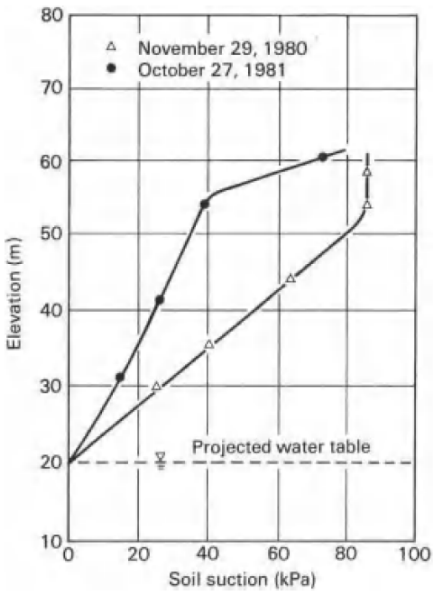

Figure 2.15: In situ measurements of matric suction. Reproduced from Ching et al. (1984).

The soil stratum was split into a number of soil layers 5.0m thick, each given an independent soil cohesion based on a matric suction profile. A number of slope stability analyses were then undertaken based on a series of matric suction profiles that are a percentage factor of the hydrostatic profile. For each analysis the result is given in terms of the slope factor of safety. The results are presented in Figure 2.16. If using only saturated soil mechanics, i.e. not taking into consideration matric suction, then the calculated factor of safety was 0.864, indicating unstable slope conditions. However, at the time the paper

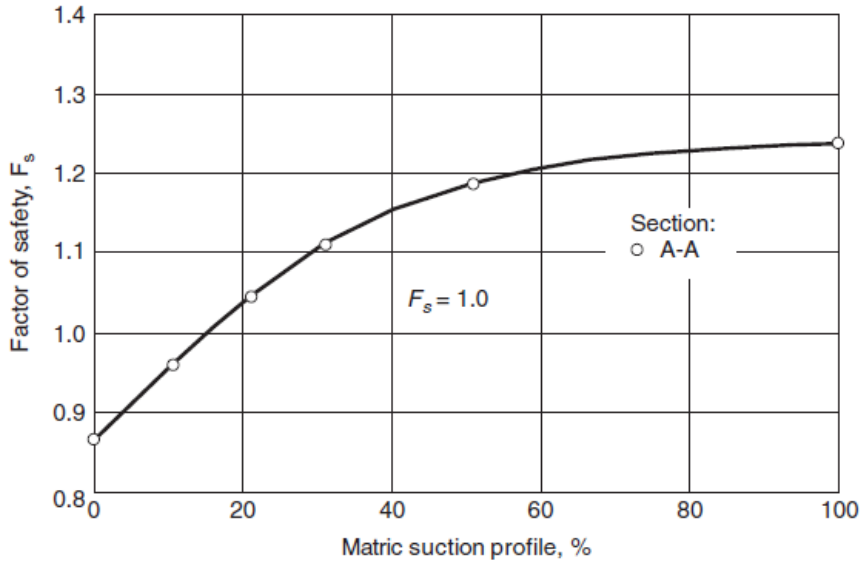

Figure 2.16: Calculated factors of safety considering various matric suction profile as a percentage of hydrostatic conditions. Reproduced from Fredlund et al. (2012)

was written, the slope was stable, indicating that the matric suction is playing a role in the stability of the slope. A factor of safety of 1.0 is calculated when the matric suction profile simulated is 10-20% of the hydrostatic matric suction profile. Above a factor of 10% the factor of safety continues to increase before it starts to level off at around 60% of the hydrostatic matric suction profile. Above 60%, the additional suction does not translate into additional shear strength, meaning factor of safety no longer increases. This case study demonstrates that matric suction plays an important part in the stability of slopes, and clearly demonstrates that as suction increases, shear strength increases, leading to an improvement in the factor of safety of the slope.

The second example uses the approach where the extended shear strength equation for unsaturated soils is used during a numerical analysis (Ng, 1988). This example is based on a typical steep slope of approximately 60 degrees in Hong Kong. Again the role of matric suction is shown by computing the factor of safety of the slope. In this instance however a moisture flux boundary condition is applied to the slope surface to simulate a sudden heavy rainfall event. The geology is similar to the previous example, where colluvium overlays weathered granite. The ϕ^b angle for each soil was assumed to be a percentage of the effective angle of internal friction, ϕ', ranging from 25%, 50%, 75% and 100%. The unsaturated hydraulic conductivity function was derived from the saturated

soil permeability and the SWRC. The infiltration of rainfall into the soil was specified as a moisture flux boundary condition equivalent to 10% of the average annual rainfall in Hong Kong. The analysis is time dependant, with the results calculated at various time steps as the water infiltrates into the slope. Figure 2.17 shows the changing negative pore water pressure profile with time along a vertical section though the slope.

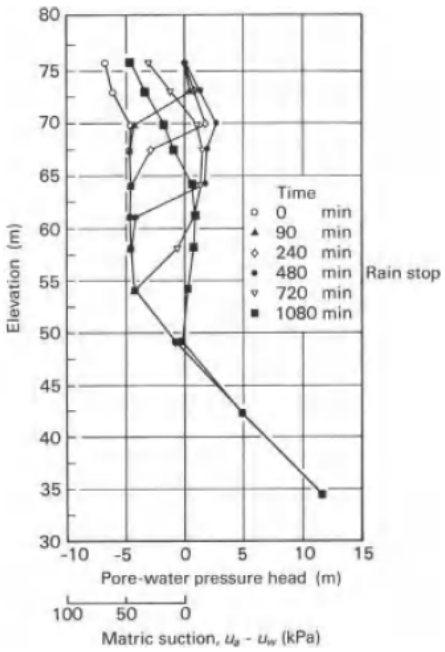

Figure 2.17: Matric suction profile along vertical section through the slope at various elapsed times. Reproduced from Ng (1988).

The results are presented in Figure 2.18 as the factor of safety vs elapsed time for each ratio of ϕ^b to ϕ' simulated. Where negative pore pressures are ignored, i.e. $\phi^b/\phi' = 0$, the factor of safety is close to 0.9, indicating unstable slope conditions. However, observations of a stable slope on site indicate that it must be greater than 1.0. The factor of safety ranges from 1.0 to 1.4 when ϕ^b/ϕ' varies between 0.25 to 1.0. As time progresses it can be seen that the factor of safety of the slope decreases as the water infiltrates into the slope. The decrease in factor of safety becomes more substantial as ϕ^b/ϕ' increases, with the greatest decrease in factor of safety when $\phi^b = \phi'$. This can attributed to the fact that the critical slip surface is shallow and the mobilized shear resistance is significantly influenced by matric suctions. The factor of safety begins to increase after 480 minutes when the rainfall stops and the water infiltrates deeper into the soil, however the rate of increase in factor of safety is slower than the decrease during the onset of rainfall.

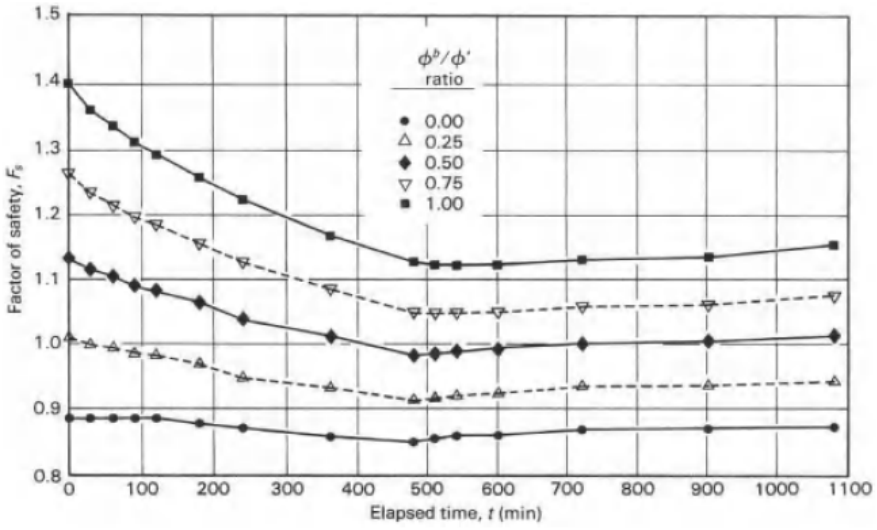

Figure 2.18: Calculated factors of safety at various elapsed times for a range of ϕ^b to ϕ' ratios. Reproduced from Ng (1988).

These case studies demonstrates how critical matric suction can be to the factor of safety of unsaturated slopes. It is common practice during geotechnical design to ignore the effects of matric suctions, however these examples show that this may often be too conservative and explains why many slopes fail design standards such as Eurocode when they can be clearly observed as stable in practice. This can lead to over conservative slope designs which require unnecessary reinforcement such as soil nails, soil anchors or geotextile mesh, or more hard engineering solutions such as retaining walls. The change in factor of safety due to rainfall presented in the second case study demonstrates that variable pore water pressure conditions must be considered during the design of unsaturated slopes, as this will have implications for the design requirements during the lifetime of the structure.

2.5 Summary

The objective of this MScR research project is to develop a process to estimate the change in shear strength of a soil due to the lowering of the water table as a consequence of a dewatering operation. It is also key to understand how this change in shear strength may increase the stability of a temporary battered slope. This literature review has presented the current understanding of the key concepts, theories and studies on the topics that are fundamental to this research objective. As the groundwater table is lowered,

the soil becomes unsaturated, and negative pore water pressures, i.e. matric suctions, develop. It is this development of matric suctions that pull the soil particles together which leads to an increase in shear strength of the soil. This soil behaviour is described by the branch of geotechnical engineering called unsaturated soil mechanics. This first section of this literature review discussed the concept of stress state variables, and how it is considered best practice to use two stress state variables, net total stress ($\sigma - u_a$) and matric suction ($u_a - u_w$), as proposed by Fredlund and Morgenstern (1977), rather than using an unsaturated effective stress parameter, as originally proposed by Bishop (1959). This is because the effective stress parameter was experimentally shown to not be a stress state variable, but rather a constitutive equation linking stress state variables (Morgenstern, 1979).

Matric suction plays a fundamental part in the behaviour of soils as they desaturate. The change in water content of a soil with matric suction is described by the soil water retention curve (SWRC). There has been a significant amount of research into the SWRC as it is been proven to be an essential component when applying unsaturated soil mechanics in practice. For a given soil there can be any number of possible soil water retention curves depending on the conditions tested. If the soil is being dried or wetted, this will lead to separate drying and wetting curves. There is also an infinite number of possible scanning curves which lie between these drying and wetting curves. The void ratio of the soil also has an impact on the SWRC. Soil samples can be compacted to different densities, which will have the effect of shifting the SWRC along the suction axis. A number of different methods for determining the SWRC in the laboratory were discussed, along with methods for measuring the soil suction in the field. There are a number of soil databases available to the academic community and industry which contain laboratory testing of unsaturated soils. The UNSODA database contains over 1,000 soil samples with a laboratory measured SWRC (Nemes et al., 2001). There have been numerous attempts to find an empirical equation that can produce a best fit curve to measured SWRC data. The most commonly cited in literature are the equations by van Genuchten (1980) and Fredlund and Xing (1994). It was shown by Leong and Rahardjo (1997) that the Fredlund and Xing (1994) equation performs marginally better than the van Genuchten (1980) equation. Laboratory experiments used to derive a SWRC can be time consuming and expensive to undertake, and as a result are not widely used in the UK construction industry. Therefore, there have

been a number of attempts to estimate a SWRC of a soil using only standard laboratory test data. These include particle size distributions, dry density, particle density, voids ratio and plasticity information. A number of methods including Arya and Paris (1981); Fredlund et al. (2002); Perera et al. (2005); Rawls et al. (1982); Gupta and Larson (1979); Aubertin et al. (2003) have been shown to give reasonable predictions, however this often depends on the soil data set presented. The methods typically aim to translate the particle size distribution to the SWRC by estimating the pore size distribution. This can be difficult because factors such as particle arrangement, packing density and stress history can impact the SWRC but do not influence the shape of the PSD (Fredlund et al., 2002).

With a SWRC for a soil sample, the unsaturated shear strength can then be assessed. The shear strength of a soil is critical to the stability and safety of any engineered soil structure. It is well known that in the unsaturated zone, as the matric suction increases the strength of the soil also increases. This can be easily observed by feeling the ground on a warm summers day, where the ground is often dried out and hard, compared to a cold and wet winters day when the ground is comparably soft. This is also commonly observed on construction sites when the groundwater table is lowered. The theory behind these observations, and how this is related to the SWRC, have been presented in this literature review. The first equation proposed for unsaturated shear strength was by Fredlund et al. (1978), which is an extension of the Mohr-Coulomb equation for saturated soils. The original equation by Fredlund et al. (1978) is linear, meaning that shear strength increases with matric suction on a linear scale. The rate of change of shear strength with matric suction is governed by the $\tan \phi^b$ parameter. It was later shown by Gan et al. (1988) and Escario and Jucá (1989) that the relationship between matric suction and shear strength is linear when the suction is less than the air-entry value of the soil, but then becomes non-linear as suction increases beyond the air-entry value. As such Fredlund et al. (1996) proposed a non-linear version of the equation, which requires a fitting parameter κ. There have also been a number of unsaturated shear strength equations proposed for more advanced soil models, such as the critical state Barcelona Basic Model proposed by Alonso et al. (1990). The unsaturated shear strength of soils can be tested in the laboratory using modified shear strength testing apparatus such as a direct shear box and triaxial cell. Like SWRC determination, unsaturated shear strength testing can be very time consuming and expensive, therefore a number of equations have been proposed to

estimate the unsaturated shear strength of a soil. Several of these require the SWRC, such as the models by Vanapalli et al. (1996); Fredlund et al. (1996); Oberg and Sallfors (1997). Each of these equations take the same form, but with a unique expression for the $\tan \phi^b$ parameter. The fitting parameter κ in the equation by Fredlund et al. (1996) can be estimated using the plasticity index of the soil (Garven and Vanapalli, 2006). A number of studies have been presented which assess the performance of these equations by comparing predictions to the results of mechanical experimental testing of unsaturated soils. It was found that the equations by Fredlund et al. (1996) and Vanapalli et al. (1996) both give reasonable predictions, particularly in the low to medium suction range (below 1500 kPa). The equation by Oberg and Sallfors (1997) was shown to perform less well than the others.

With an understanding of unsaturated soil mechanics, in particular the SWRC and the extended Mohr-Coulomb equation for shear strength, these concepts can be used in engineering practice. Of particular importance to groundwater control operations is to understand how the strength of soils increase as the groundwater table is lowered. This has most significance in relatively shallow excavations when there are temporary battered slopes. It is also of great importance to understand the stability of existing natural and engineered slopes across the world, whether this is in urban environments or rural regions, as slope failures can have huge human and economical costs. In this literature review two case studies have been presented which show how unsaturated soil mechanics can be used in practice to assess the stability of two existing engineered slopes in Hong Kong (Ching et al., 1984). It was shown that if matric suction is ignored, i.e. applying only saturated soil mechanics, both slopes would have a factor of safety of less than 1.0, indicating unstable and unsafe slopes. However, we know from observations that these slopes are stable, therefore we can conclude that matric suction must be contributing to the stability of the slope. This demonstrates that it can be highly conservative to ignore the influence of matric suction in slope design. When matric suctions were included, the factor of safety of the slopes increased to between 1.0 and 1.4. The second case study simulated a sudden rainfall event, which showed that a sudden decrease in matric suction can lead to a lowering of the factor of safety, however the factor of safety will increase again with time as the water front flows deeper into the soil. These two case studies have highlighted the importance of assessing the matric suction profile when analysing the stability of slope.

Particular consideration should be taken to the changing matric suction profile in the slope due to changes in water content, which could due be to groundwater abstraction during a groundwater control operation or water infiltration through the surface during rainfall.

The following Chapter will build on the knowledge of the SWRC presented in this Literature Review and present the methodology and analysis undertaken during this MScR project to estimate the SWRC of a soil using only standard laboratory test data. It will document the first crucial stage of estimating the unsaturated shear strength of a soil when extensive laboratory testing cannot be undertaken.

Chapter 3

Estimation of the Soil Water Retention Curve

To achieve the research objective put forward in the introduction, it is critical that the SWRC is well understood theoretically and can be estimated using standard laboratory test data. It is also vitally important that the confidence of any prediction is understood and quantified, as this could lead to significant errors in estimated suction and therefore shear strength during preliminary design calculations of construction projects.

The objective of this chapter is to present the methodology undertaken to develop a procedure for estimating the Soil Water Retention Curve (SWRC) of a soil which can be used by geotechnical engineers in practice. The beginning of the chapter describes the data selection process, along with a description of how the data has been preprocessed before analysis. Following this is the core data analysis that has been undertaken. This includes fitting best-fit curves to both the particle size distribution data and soil water retention data for each soil of the dataset. The SWRC is then estimated from standard index properties such as the PSD and density using three methods presented in literature. To assess how well each predictive method performs, statistical analysis is undertaken, where the error between the predicted and true SWRC is calculated. Using this information, the 5th and 95th percentiles of suction error are calculated, which are used as a metric for understanding the spread of the suction error across the dataset. Towards the end of the chapter, it is shown how the 5th and 95th percentiles of suction error can be used as

confidence limits during the analysis of soils by geotechnical engineers in practice.

The end result from the analysis documented in this chapter is a set of software tools which can be used to estimate the SWRC of a soil using standard laboratory test data. Along with this are confidence limits to quantify the possible error in the prediction. This provides a valuable tool for practising geotechnical engineers during the design stage of projects where it is vital to understand the possible error in estimated soil parameters, and the implications this may have on design of a structure and its future stability.

3.1 Data Selection

The first section of the methodology presented in this chapter documents the data selection process undertaken and the preprocessing of this data into a suitable format for data analysis.

3.1.1 Selection of Soil Database

The Unsaturated Soil Hydraulic Database (UNSODA) (Nemes et al., 2001) contains a large number of unsaturated soil samples with data which is suitable for this study. The database is freely available to download online, making it ideal for selecting a sample dataset of soils. It includes the required particle size distribution, dry density and soil water retention data. The Hydraulic Properties of European Soils (HYPRES) database (Lilly et al., 1999) is not freely available to download online, and could not be sourced elsewhere, therefore it was not included as part of this study.

3.1.2 Description of UNSODA Database

The UNSODA database consists of 790 number soil samples of global origin (Nemes et al., 2001). The soil samples within the database have been classified using the United States Department of Agriculture Soil Classification System (USDA-SCS) (Nemes et al., 2001). Soils are classified into 12 textural classes based on the percentage of sand, clay and silt within the sample. The textural classes are named: sand (S), loamy sand (lS), sandy loam

(sL), sandy clay loam (scL), sandy clay (sC), loam (L), clay loam (cL), clay (C), silty clay (siC), silty clay loam (sicL), silt loam (siL), silt (Si). All 790 samples are presented on the USDA-SCS textural triangle in Figure 3.1.

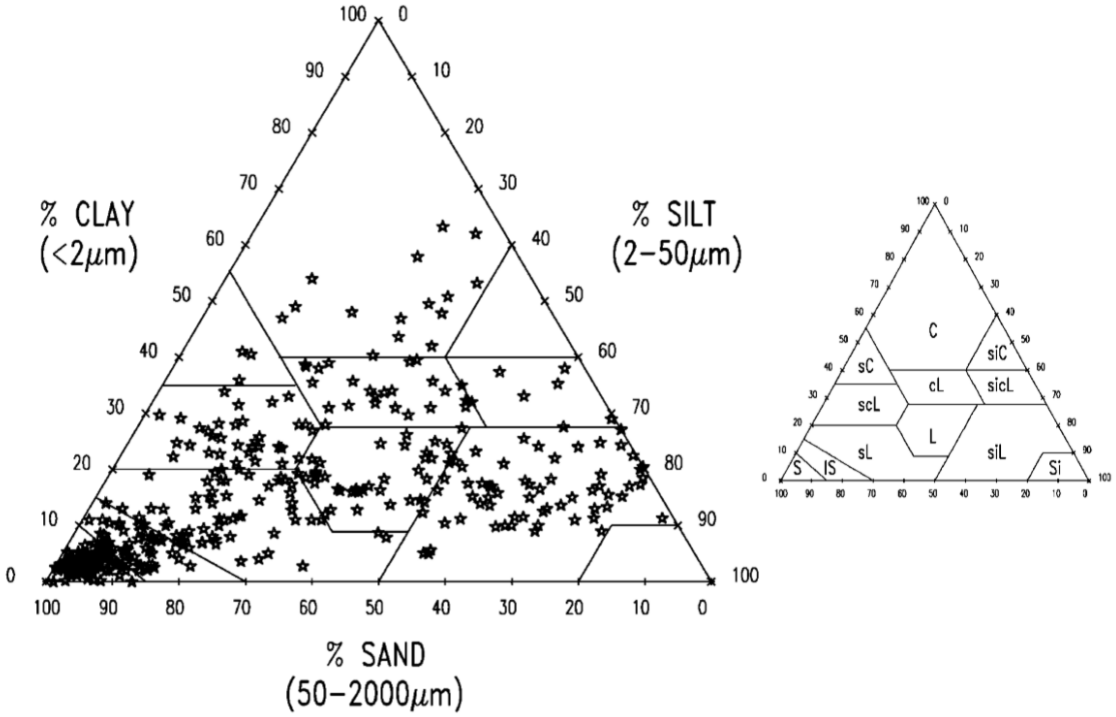

Figure 3.1: Distribution of the soil datasets in UNSODA V2.0 across the USDA-SCS soil textural triangle (reproduced from Nemes et al. (2001)).

The soil samples are reasonably spread across the textural triangle, with a bias towards the sand corner of the triangle (Figure 3.1). The number of soils within each of the USDA textural are presented in Table 3.1.

Texture	No. Soils	Texture	No. Soils	Texture	No. Soils
Sand	185	Silt	3	Clay	39
Loamy Sand	60	Silt Loam	141	Clay Loam	36
Sandy Loam	133	Silty Clay	24	Loam	69
Sandy Clay	3	Silty Clay Loam	30	Sandy Clay Loam	30

Table 3.1: Number of soils in each textural class of the UNSODA database.

Table 3.2 shows the data fields for each soil in the UNSODA database which that are useful during the data analysis part of this study.

Data	Unit
Texture	-
Dry Density	g/cm^3
Particle Density	g/cm^3
Porosity	-
Particle Size Distribution	
Particle Size	μm
Particle Fraction	-
Soil Water Retention	
Pressure Head	cm
Volumetric Water Content	-
Soil Water Retention Testing Method	-

Table 3.2: Data types included in UNSODA database suitable for use in the development of the SWRC estimation procedure.

The soil water retention data provided is for laboratory drying and wetting experiments plus field drying and wetting measurements. The database also contains data for hydraulic conductivity, water diffusivity data, sample origin, organic matter content and others.

Although the database has a large quantity of useful data, it does have some limitations. Primarily the database has been developed by the United States Department of Agriculture, which means that it was designed for describing and classifying agricultural soils. These soils are typically found within the upper few metres of the ground. Therefore they may not always represent the engineering soils encountered on construction sites within the United Kingdom and across the globe. Secondly, there is no geotechnical soil testing data, such as liquid limit and plastic limit from Atterberg limit tests, or shear strength data from triaxial testing. However, despite these limitations, the database of soils is still incredibly valuable because it contains a comprehensive dataset of soil water retention data along with index properties.

3.1.3 Selection of Sample Data Set

A subset of soils from within the UNSODA database have been selected for this study. A subset was chosen to enable quicker data analysis and interpretation of results. This subset is a total of 102 soils which have been selected based on the criteria outlined below:

- Soils commonly encountered on UK construction sites. Soil categories selected based on experience of working with these kind of soils during groundwater control projects Thomas et al. (2020) i.e. soils from the USDA textural classes: sand, sandy clay, clay, clay loam and silt.
- Soils which have a particle size distribution test with a least 5 No. measured points for granular soils (sand and silt), and 3 measured points for cohesive soils (sandy clay, clay and clay loam). At least 3 points are required to ensure that a best-fit curve can be fit to the raw data by undertaking a regression analysis. 5 points are required for the granular soils because the slope of the curve tends to be steeper, making it harder to achieve a good fit for these soils.
- Soils which contain at least 10 measured points of water content on a laboratory drying soil water retention curve test. At least 10 points are required for the regression analysis to ensure a good fit. The measured suction points tends to be more closely spaced together than PSD points, therefore more points are required to ensure a good fit over most of the suction range.
- Soils which contain a test result for dry density. This is a required property for most SWRC predictive models.

3.1.4 Data Preprocessing

The data for each of the 102 soils has been preprocessed prior to undertaking any analysis. This involved converting from units used in agriculture to units used within geotechnical engineering. In addition pressure head has been converted to total soil suction, ψ. Volumetric water content, θ remains unchanged, however it is converted to degree of saturation, S, later in the data analysis. The converted properties and units are shown in Table 3.3.

Data	Symbol	Unit Converted
Dry Density	ρ_d	Mg/m^3
Particle Density	P_d	Mg/m^3
Porosity	ϕ	-
Particle Size Distribution		
Particle Size	PS	mm
Particle Fraction	PF	-
Soil Water Retention		
Total Soil Suction	ψ	kPa
Volumetric Water Content	θ	-

Table 3.3: Unit conversion of soil data from database prior to data analysis

The Unified Soil Classification System (USCS) is a soil classification system used in engineering and geology to describe the texture, grain size and plasticity of a soil (ASTM International, 2006). This system is typically used in the United Kingdom construction industry along with the British Soil Classification System (BSCS) (BSI, 2015). For the purpose of this study, the soil categories of the USDA-SCS have been mapped to the most appropriate USCS soil category, however it must be noted that the classification map is not like for like, as the USCS system classifies soils based on plasticity information for cohesive soils and particle grading for granular soils, whereas the USDA system is based solely on the ratio of sand/silt/clay.

USDA SCS		USCS	
Name	Symbol	Name	Symbol
Sand	S	Poorly Graded Sand	SP
Sandy Clay	sC	Clayey Sand	SC
Silt	Si	Silt	ML
Clay Loam	cL	Clay of Low Plasticity	CL
Clay	C	Clay of High Plasticity	CH

Table 3.4: Soil Classification Map: USDA to USCS

The classification map presented is to give the reader, who is more likely to understand the USCS system, a good understanding of the UNSODA soils analysed in this study. The

soil classification map presented in Table 3.4 is based on the study by García-Gaines and Frankenstein (2015).

3.2 Soil Data Analysis

With a sample dataset of soils selected and preprocessed, the core data analysis for each soil of the sample dataset now follows. The following subsections document the method of analysis undertaken. This includes finding a best-fit curve for both the PSD and SWRC, and then predicting the SWRC using methods presented in literature.

3.2.1 Regression Analysis of Particle Size Distribution

To estimate the soil water retention behaviour of a soil, knowledge of the particle size distribution is essential. This is because the soil water retention curve of a soil is directly linked to the pore size distribution of the soil, and the pore size distribution is influenced by the particle size distribution (Fredlund et al., 2012). Determining the relationship between the two is the main area of uncertainty when predicting a SWRC using a PSD. This is due to factors such as grain shape, soil density and consolidation which impact the pore size distribution of the soil but are not reflected in the particle size distribution.

For each soil in the dataset, a particle size distribution is available. A curve is fit to the particle size distribution data by undertaking a non-linear regression analysis of the modified Fredlund and Xing SWRC equation for particle size distribution data (Fredlund et al., 2012). The equation is

$$P_p(d) = \frac{1}{\left\{ \ln\left[e + (a_{gr}/d)^{n_{gr}}\right]\right\}^{m_{gr}}} \times \left\{1 - \left[\frac{\ln(1 + d_r/d)}{\ln(1 + d_r/d_m)}\right]^7\right\} \tag{3.2.1}$$

where $P_p(d)$ is the percentage by mass of particles passing a particular particle size, a_{gr} is the parameter designating the inflection point on the grain size distribution curve, n_{gr} is the parameter related to the steepest slope on the grain-size distribution curve, m_{gr} is the parameter related to the shape of the grain-size curve as it approaches the fine-grained region, d_r is the parameter related to the particle size in the fine grained region and is referred to as the residual particle size, d is the diameter of any particle size under

consideration, and d_m is the diameter of the minimum allowable size particle.

The non-linear regression analysis was undertaken using the "curve-fit" algorithm from the Python Scipy package. This package is a Python based ecosystem of open-source software for mathematics, science, and engineering (SciPy.org, 2019). The software package was adopted because of its ease of use when programming in Python. The "curve-fit" algorithm uses the Trust Region Reflective least-squares algorithm to determine the curve fitting parameter values, a_{gr}, n_{gr} and m_{gr}, and d_r which give the best-fit curve to the particle size data. The value of d_m is fixed at 0.00001mm as recommend by the authors Fredlund et al. (2012).

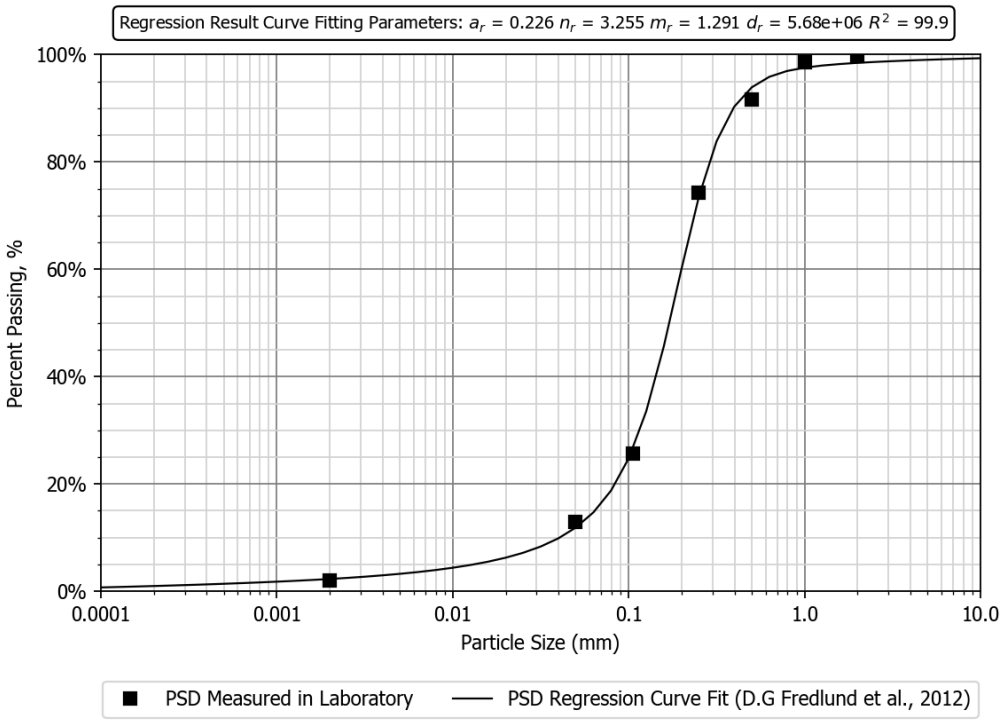

Figure 3.2: Example of the best-fit PSD curve determined by non-linear regression using the raw PSD data for sandy soil with code 1014.

Using the resulting curve fitting parameters values, a, n, m, and d_r, the best-fit curve is plotted along with the raw particle size distribution data for all soils in the dataset. An example is shown in Figure 3.2 for soil code 1014, which is a soil within the sand textural class. For the resulting curve fitting parameters for each soil in the dataset, the reader should see Table A.1 of Appendix A and Figures C1 to C102 of Digital Appendix C.

3.2.2 Regression Analysis of Soil Water Retention Data

A non-linear curve fit regression analysis has been undertaken on the soil water retention data for each soil of the dataset. The Fredlund and Xing (1994) equation has been selected as the theoretical equation to fit to the measured data. This is because the Fredlund and Xing (1994) equation provides the greatest flexibility for the shape of the curve in the region of the air entry value (i.e at low suction area of curve) and at the residual water content section of the curve at high suctions. The Fredlund and Xing (1994) SWRC equation is

$$\theta(\psi) = C(\psi)\frac{\theta_s}{\left\{\ln\left[e + (\psi/a_f)^{n_f}\right]\right\}^{m_f}} \tag{3.2.2}$$

where

$$C(\psi) = 1 - \frac{\ln(1 + \psi/\psi_r)}{\ln[1 + (10^6/\psi_r)]} \tag{3.2.3}$$

where $\theta(\psi)$ is the volumetric water content to be found for a given value of total soil suction ψ, θ_s is the saturated volumetric water content, a_f is the fitting parameter related to the air-entry, n_f is the fitting parameter related to the rate of water extraction from the soil once the air-entry value has been exceeded, m_f is the fitting parameter related to residual water content conditions and $C(\psi)$ is the correction factor which is a function of suction corresponding to residual water content, where ψ_r is the soil suction corresponding to the residual water content θ_r.

The non-linear regression analysis was undertaken using the "curve-fit" algorithm which is part of the Python Scipy package (SciPy.org, 2019). The curve-fit algorithm uses the Trust Region Reflective least-squares method to determine the parameters values which give the best-fit curve to the measured soil water retention data. This method of analysis enable bounds to be placed on the parameters values. This ensures realistic parameter values are found, whilst ensuring the regression algorithm does not fail. The bounds placed on the parameters are presented in Table 3.5.

Using the resulting curve fitting parameters values, θ_s, a_f, n_f, m_f, and ψ_r, the best-fit curve is plot along with the raw soil water retention data for all the 102 No. soils. An example is shown in Figure 3.3 for soil code 1014, which is a soil within the sand textural class. For the resulting curve fitting parameters for each soil in the dataset, along with the calculated coefficient of determination, R^2, the reader should see Table A.2 of Appendix A

SWRC Parameter	Lower Bound	Upper Bound
θ_s	0.1	1.0
a_f	0.1	1000
n_f	0.1	50
m_f	0.1	50
ψ_r	0.1	10,000

Table 3.5: Parameter bounds during SWRC regression analysis.

and Figures C1 to C102 of Digital Appendix C.

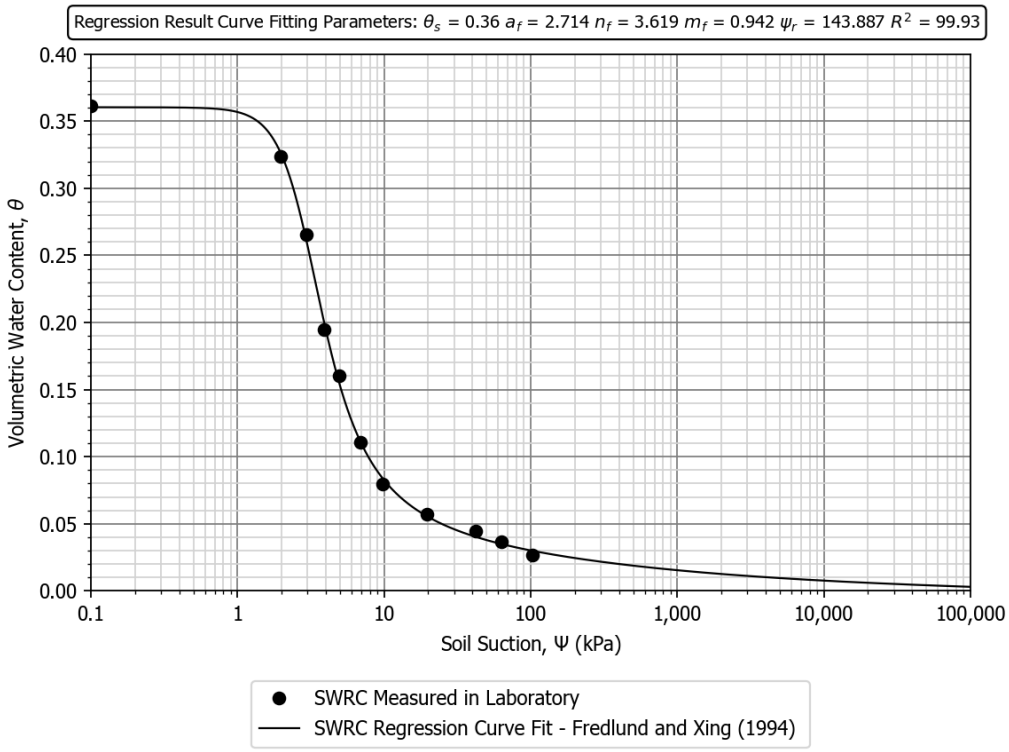

Figure 3.3: Example of the best-fit SWRC (Fredlund and Xing, 1994) determined by non-linear regression using the raw soil water retention data for soil code 1014 of the sand texture class.

3.2.3 Estimation of the SWRC using the Arya and Paris (1981) Model

Background Theory

The Arya and Paris (1981) model is a physio-empirical model for predicting soil water retention behaviour from typical laboratory soil testing data. It is based on the assumption that the SWRC is essentially a pore-size distribution curve, which can be derived from the particle size distribution, dry density, and particle density of a soil sample.

The following equations outline the steps to derive the SWRC as presented by Arya and Paris (1981). The cumulative particle size distribution curve, as shown in Figure 3.4, is split into n number intervals. The solid mass, W_i, within each interval is computed as the difference in cumulative percentages between the boundaries of the intervals (i.e. particle size), divided by 100. This results in values of W_i such that the sum of all W_i is unity

$$\sum_{i=1}^{n} W_i = 1 \tag{3.2.4}$$

The pore volume for each interval size is calculated by

$$V_{v_i} = \frac{W_i e}{\rho_p}; \quad i = 1, 2, ..., n \tag{3.2.5}$$

where V_{v_i} is the pore volume associated with the solid mass in the i^{th} particle-size interval, ρ_p is the particle density, and e is the void ratio, which can be calculated from

$$e = \frac{\rho_p - \rho_d}{\rho_d} \tag{3.2.6}$$

where ρ_d is the measured dry density of the soil sample, or

$$e = \frac{\phi}{1 - \phi} \tag{3.2.7}$$

where ϕ is the soil porosity.

The pore volumes, V_{v_i}, calculated for each interval size are cumulatively summed. The volumetric water content is calculated by

$$\theta_{v_i} = \sum_{j=1}^{j=i} \frac{V_{v_j}}{V_b}; \quad i = 1, 2, ..., n \tag{3.2.8}$$

where θ_{v_i} is the volumetric water content represented by a pore volume for which the largest size pore corresponds to the upper limit of the i^{th} particle-size interval, and the

sample bulk volume V_b is given by

$$V_b = \frac{1}{\rho_d} \tag{3.2.9}$$

The average volumetric water content, $\theta^*_{v_i}$ for the midpoint of the particle-size interval is calculated by

$$\theta^*_{v_i} = \frac{\theta_{v_i} + \theta_{v_{i-1}}}{2} \tag{3.2.10}$$

The mean particle radius, R_i, which corresponds to the midpoint of a given particle-size interval, is given by

$$R_i = \frac{d_i/2 + d_{i-1}/2}{2} \tag{3.2.11}$$

The mean pore radius r_i for the assemblage formed by the particles in the i^{th} particle-size interval is calculated by

$$r_i = R_i\sqrt{4en_i^{1-\alpha}/6} \tag{3.2.12}$$

where n_i is the number of spherical particles given by

$$n_i = \frac{3W_i}{4\pi R_i^3 \rho_p}. \tag{3.2.13}$$

The parameter α in Equation (3.2.12) is an empirical constant with a value typically within the range 0.9 to 1.4 (Vaz et al., 2005; Fredlund et al., 2012). Table 3.6 gives some values of α for a range of soil types as recommended by Arya and Paris (1981).

USDA Texture	α
Sand	1.285
Sandy Loam	1.459
Loam	1.375
Silt Loam	1.150
Clay	1.160

Table 3.6: Values of alpha proposed by Arya and Paris (1981).

Once the pore radii have been derived using the above equations, the soil water potential ψ_i can be calculated

$$\psi_i = \frac{2\sigma\cos(\Theta)}{\rho_w g r_i} \tag{3.2.14}$$

where σ is the surface tension of water, Θ is the contact angle (assumed as $\Theta = 0$), ρ_w is the density of water, g is acceleration due to gravity, and r_i is the mean pore radius.

Verification

Programming of the Arya and Paris (1981) model has been undertaken in order to estimate the SWRC for each soil within the dataset. The model has been programmed using the Python programming language. This subsection documents the verification of the Arya and Paris (1981) model by comparing results with data published in literature.

The data used for this verification is derived from a scientific report by Arya, Richter, and Davidson (1982). The soil is from a dataset of American soils and the soil sample presented in the report is a sandy loam soil from New Jersey. For this soil, the particle size distribution, dry density and particle density are provided as shown in Table 3 of Arya et al. (1982). In addition, values calculated during each calculation step are presented, along with the final value of suction head ψ_i for each value of volumetric water content, θ_{v_i}. The particle size distribution for this soil is depicted in Figure 3.4. Particle size has been converted to units of mm from μm, and a best-fit curve has been found using the method documented in Section 3.2.1.

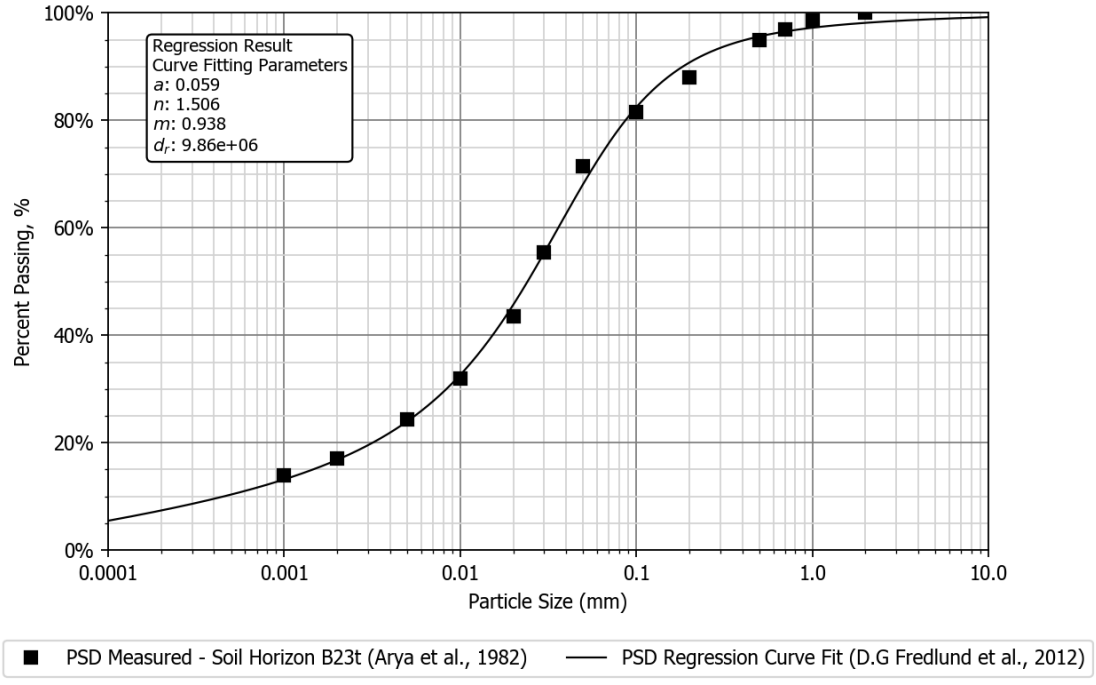

Figure 3.4: Particle size distribution for soil B23t from Arya et al. (1982).

The particle size distribution, dry density, and particle density are then input to the model and the SWRC is estimated. The results from the model verification for each

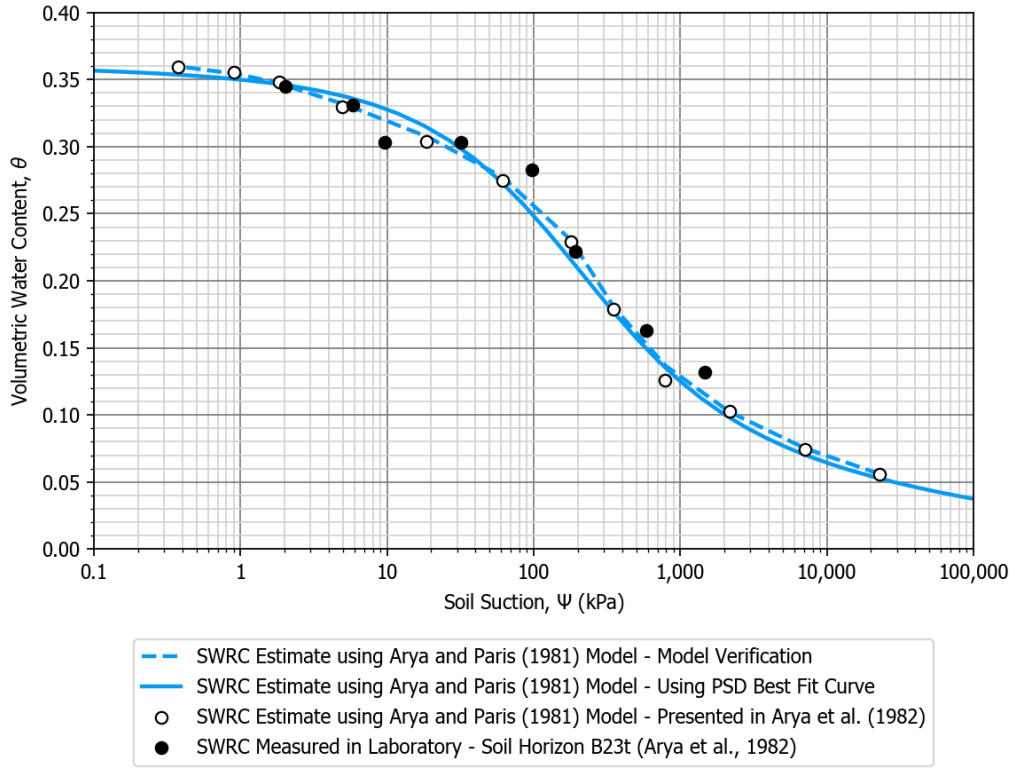

Figure 3.5: Measured and Estimated SWRC for soil B23t from Arya et al. (1982).

calculation stage are presented in Table 3.7. Suction, ψ is presented in units of kPa but also presented as suction head in units of cm, for direct comparison to the original results in Arya et al. (1982).

The results are presented in graphical form as a plot of suction, ψ (kN/m^2) vs volumetric water content, θ_{v_i} in Figure 3.5. The blue dashed line represents the estimated SWRC using the raw PSD data, whilst the white circles depict the estimated SWRC as presented in Arya et al. (1982). The black circles represent the measured SWRC, which were collected using a tension table over the low suction range and a pressure plate apparatus for the high suction range. It can be seen in Figure 3.5 that the blue line is a near perfect fit for the white points. This verifies the programming of the Arya and Paris (1981) model using the Python script, which means the script can be used for the analysis of the 102 No. selected soils in the dataset.

In addition to using the raw PSD data for the calculation of the SWRC using the Arya and Paris (1981) model, the PSD best-fit curve is used (solid blue line in Figure 3.5). This enables the estimation of the SWRC over the full range of suction and can give a smoother

$PS(mm)$	$\Sigma W_i(-)$	$W_i(-)$	$\theta_{v_i}(m^3/m^3)$	$\theta^*_{v_i}(m^3/m^3)$	$R_i(m)$	$R_i^3(m^3)$	$n_i(1/g)$	$n_i^{1-\alpha}(-)$	$r_i(m)$	$\psi(kN/m^2)$	$\psi_i(cm)$
0.002	0.170	0.030	0.062	0.056	7.50E-07	4.22E-19	6.41E+09	1.88E-04	6.32E-09	2.28E+04	2.32E+05
0.005	0.244	0.074	0.088	0.075	1.75E-06	5.36E-18	1.24E+09	3.50E-04	2.02E-08	7.16E+03	7.29E+04
0.01	0.320	0.076	0.116	0.102	3.75E-06	5.27E-17	1.30E+08	8.26E-04	6.63E-08	2.17E+03	2.22E+04
0.02	0.435	0.115	0.158	0.137	7.50E-06	4.22E-16	2.46E+07	1.56E-03	1.82E-07	7.92E+02	8.07E+03
0.03	0.555	0.120	0.201	0.179	1.25E-05	1.95E-15	5.54E+06	2.74E-03	4.03E-07	3.58E+02	3.65E+03
0.05	0.715	0.160	0.259	0.230	2.00E-05	8.00E-15	1.80E+06	4.20E-03	7.97E-07	1.81E+02	1.84E+03
0.1	0.815	0.100	0.295	0.277	3.75E-05	5.27E-14	1.71E+05	1.03E-02	2.34E-06	6.16E+01	6.28E+02
0.2	0.880	0.065	0.319	0.307	7.50E-05	4.22E-13	1.39E+04	2.67E-02	7.54E-06	1.91E+01	1.95E+02
0.5	0.950	0.070	0.344	0.332	1.75E-04	5.36E-12	1.18E+03	6.81E-02	2.81E-05	5.13E+00	5.23E+01
0.7	0.970	0.020	0.351	0.348	3.00E-04	2.70E-11	6.67E+01	2.03E-01	8.31E-05	1.73E+00	1.77E+01
1	0.985	0.015	0.357	0.354	4.25E-04	7.68E-11	1.76E+01	3.36E-01	1.52E-04	9.51E-01	9.69E+00
2	1.000	0.015	0.362	0.360	7.50E-04	4.22E-10	3.20E+00	6.43E-01	3.70E-04	3.90E-01	3.97E+00

Table 3.7: Calculation of SWRC using the Arya and Paris (1981) model. Results from Python programming script.

curve, particularly where there are few PSD data points. The closeness between the two estimated SWRCs demonstrates the suitability of using the curve-fit PSD curve in the estimation of the SWRC. With the Arya and Paris (1981) model verified as shown in this section, analysis of the selected 102 No. soils in the dataset can be undertaken using the same procedure, as shown in the following section.

Estimation of SWRC for Dataset

The SWRC estimation procedure using the Arya and Paris (1981) model, as verified in the subsection above, is applied to each soil of the dataset. Instead of using the raw particle size distribution data, the best-fit curve for the PSD is used. The PSD curve has been generated using 50 calculation points. If the number of calculation points is greater than 50, then the Arya and Paris (1981) model does not function correctly and the SWRC curve becomes offset on the suction axis. This was observed when verifying the model using the PSD best-fit curve. This issue arises when calculating the average volumetric water content (Equation 3.2.10) when using small particle size intervals. As a result of using 50 calculation points, the calculated SWRC can at times be angular in places, particularly where the change in the gradient of the curve is sharp.

The estimated soil water retention curve is calculated using the dry density and the particle density. Where the particle density is omitted from the database, an average value

of 2.65 Mg/m^3 is used. The estimated SWRC for a soil from each of the five textural classes analysed (sand, clay, silt, sandy clay and clay loam) are presented in Figures 3.6 and 3.7. The corresponding PSD for these soils are presented in Figures C1, C23, C46, C81 and C54 of Digital Appendix C. The predicted SWRC for every soil in the dataset is presented in Figures C1 to C102 of Appendix C.

The Root Mean Squared Logarithmic Error (RMSLE) is calculated to assess the relative difference between the predicted SWRC and the measured SWRC across the soils in the dataset. RMSLE is utilised as the error metric over Root Mean Square Error (RMSE) because RMSLE does not penalise big differences in suction as the curve tends towards the high suction range of the SWRC. The RMSLE is calculated as

$$RMSLE = \sqrt{\frac{1}{n}\sum_{i=1}^{n}(\log(\hat{\psi}+1) - \log(\psi+1))^2} \tag{3.2.15}$$

where n is the number of sample points, $\hat{\psi}$ is the predicted suction using the Arya and Paris (1981) model and ψ is the suction derived from the best-fit curve regression analysis. The number of sample points, n is 19, which is based on the suction difference calculated at saturations from 0.05 to 0.95 at intervals of 0.05. A low value of RMSLE indicates a small difference between the predicted and measured SWRC, and a high value a large difference.

	Soil 1014	Soil 1134	Soil 2361	Soil 3214	Soil 2433
RMSLE	0.256	1.689	0.328	1.179	0.575

Table 3.8: Calculated RMSLE for each soil presented in Figure 3.6.

For the soils presented in Figure 3.6, the RMSLE calculated is presented in Table 3.8. For the sand and clay soils, the SWRC prediction performed wells with a RMSLE value below 0.35. For the clay loam soil, the performance of the SWRC prediction was average, with a RMSLE value above 0.5. However, for the silt and sandy clay soils, the predicted SWRC was poor, with an RMSLE greater than 1.0, and a significant difference between the predicted and measured suction. This is most noticeable in the offset of the predicted curve for the sandy soil, and the gradient of the curve for the silty soil. This highlights the difficulty in estimating the SWRC from the particle size distribution and dry density. The shape of the SWRC estimated using the Arya and Paris (1981) model closely resembles the shape of the PSD curve. However, in the cases where the measured SWRC has a notably

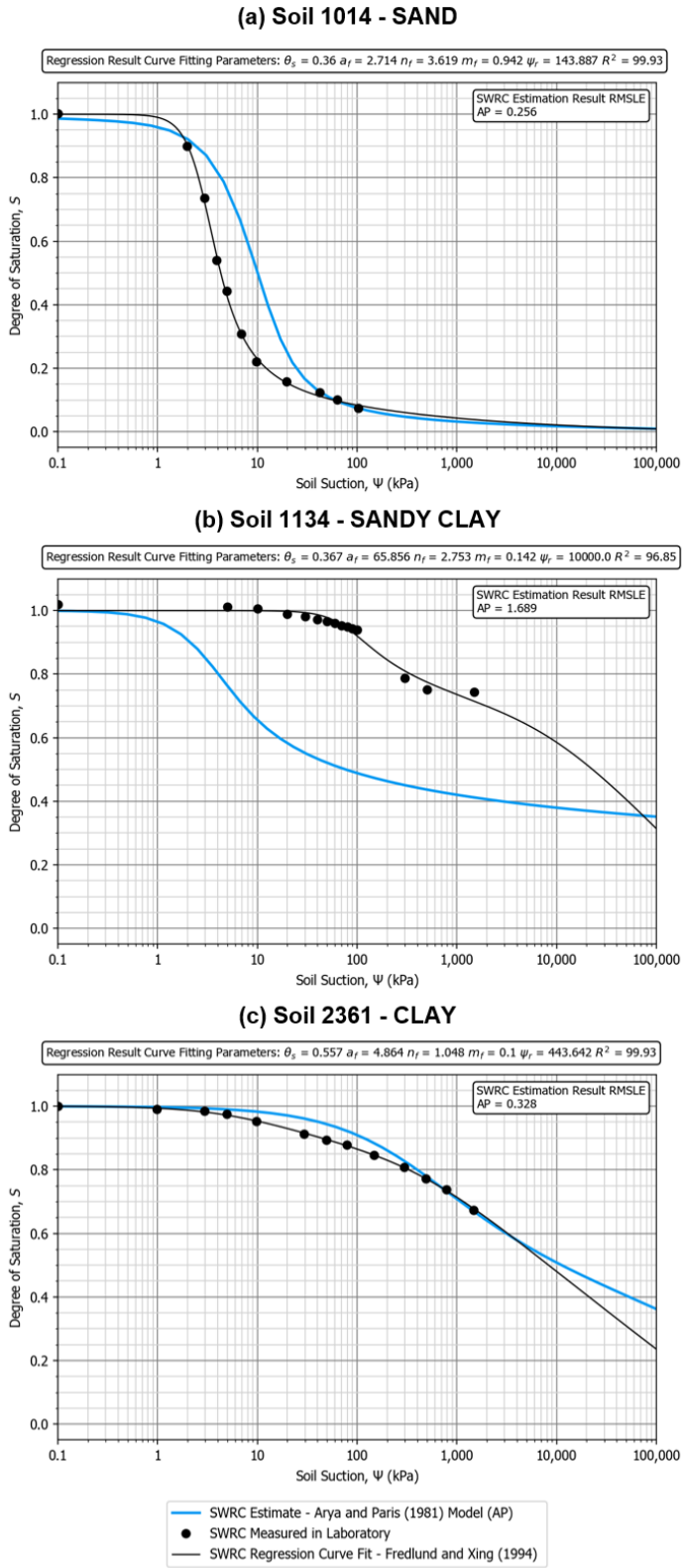

Figure 3.6: Estimated SWRC using the Arya and Paris (1981) model (blue) vs Measured SWRC (black) for (a) Soil 1014 Sand (b) Soil 1134 Sandy Clay (c) Soil 2361 Clay.

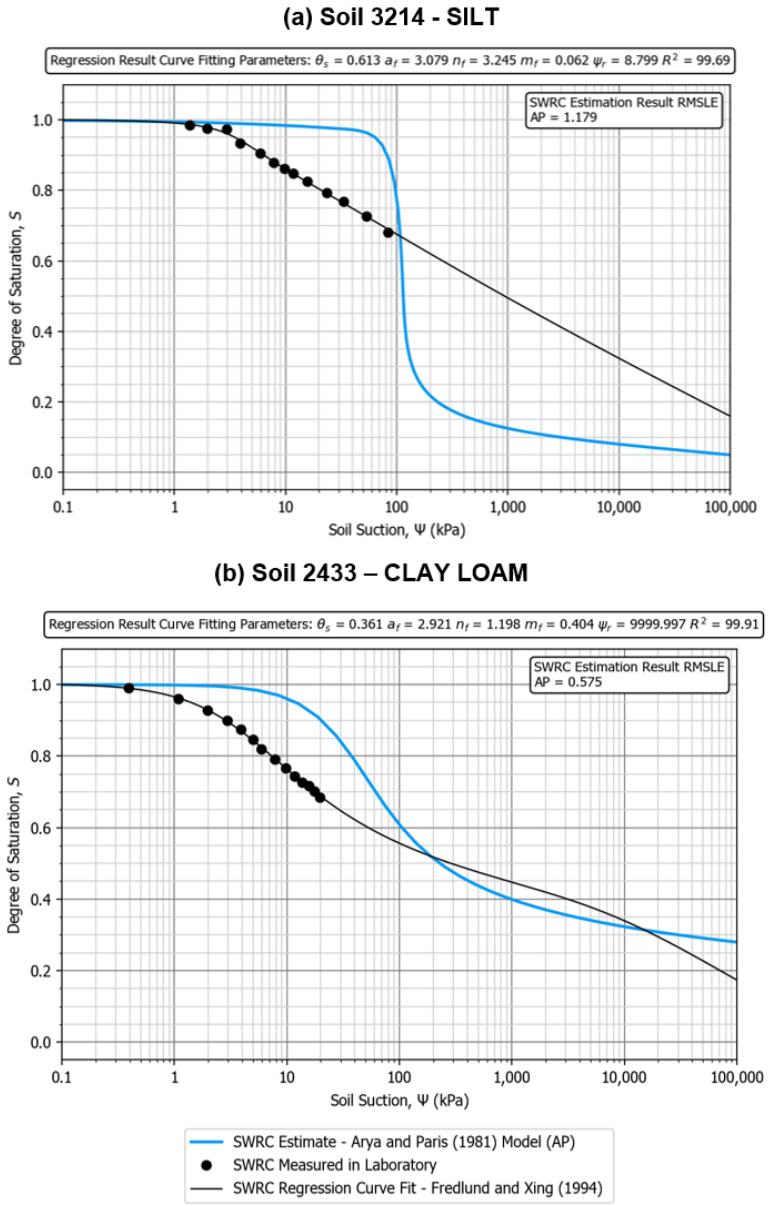

Figure 3.7: Estimated SWRC using the Arya and Paris (1981) model (blue) vs Measured SWRC (black) for (a) Soil 3214 Silt (b) Soil 2433 Clay Loam.

different shape to PSD curve, the estimation procedure performs poorly. This is maybe due to factors influencing the SWRC which are not reflected in the shape of the PSD curve, such as grain shape and roughness, particle arrangement and pore distribution, and the SWRC testing methodology.

The minimum, mean, maximum, and standard deviation of the calculated RMSLE for all analysed soils within the four textural classes are presented in Table 3.9. The mean

Textural Class	No. Soils	Min RMSLE	Mean RMSLE	Max RMSLE	Standard Deviation, σ
Sand	73	0.078	0.608	1.801	0.306
Sandy Clay	2	1.494	1.592	1.689	0.138
Silt	2	0.662	0.921	1.179	0.325
Clay	8	0.125	0.650	1.318	0.465
Clay Loam	17	0.440	0.932	1.677	0.329

Table 3.9: Calculated variability in RMSLE across each textural class when predicting the SWRC using the Arya and Paris (1981) Model.

RMSLE for the sand, silt and clay textural classes is within the range of 0.6 to 0.7, which suggests that the Arya and Paris (1981) model performs reasonably wells at estimating the SWRC for these soils. For the sandy clay, silt and clay loam soils, the mean RMSLE is above 0.8, which suggests that this method performs on average poorly. However it must be noted that there are only two soil samples within the sandy clay and silt categories, therefore strong conclusions about the suitability of the Arya and Paris (1981) model for estimating the SWRC cannot be derived for these two categories.

The section has presented the analysis undertaken on the 102 number soil dataset to predicted the SWRC using the Arya and Paris (1981) model. The next section presents a similar analysis using the Modified Kovacs model (Aubertin et al., 2003), which is a model for estimating the SWRC using solely particle size distribution data.

3.2.4 Estimation of the SWRC using the Modified Kovács Model

Background Theory

The Modified Kovács Model (MK) (Aubertin et al., 2003) is a predictive model based on the physical properties of a soil. It is a modification of the original model proposed by Kovacs (1981) and makes the distinction between capillary and adhesive forces, which both act together to generate suction within the pore matrix of a soil. However, in the original Kovacs (1981) model, a number of key parameters were not well defined making it difficult to apply the model in practice. Aubertin et al. (1998) made some modifications to this model, and applied it to a dataset of soils including tailings and silts. The model was then later extended to include a range of soil materials, from coarse sands to clayey

soils (Aubertin et al., 2003).

The equations for the Modified Kovács Model are briefly described below, as given in Aubertin et al. (2003). The degree of saturation is divided into two components, adhesive and capillary, and is described by the equation

$$S = \frac{\theta}{\phi} = 1 - \langle 1 - S_a \rangle (1 - S_c) \tag{3.2.16}$$

where S is any degree of saturation, θ is any volumetric water content, ϕ is the initial porosity of the soil, S_c is the degree of saturation associated with the capillary component, and S_a is the degree of saturation associated with the adhesive component. The Macaulay brackets $\langle . \rangle$ are used to define a ramp function, which is defined as

$$\langle x \rangle = 0.5(x + |x|) \tag{3.2.17}$$

which sets x i.e. $1 - S_a$ to zero if it is calculated to be negative. Equation (3.2.16) defines the degree of saturation in two parts, the capillary saturation, S_c and the adhesive saturation, S_a. Capillary saturation is thought to dominate the water absorption in the low suction range, whilst adhesive saturation dominates in the high suction range (Fredlund et al., 2012). The capillary saturation, S_c is defined as

$$S_c = 1 - \left[\left(\frac{h_{c0}}{\psi} \right)^2 + 1 \right]^m \exp \left[- m(h_{c0}\psi)^2 \right] \tag{3.2.18}$$

where h_{c0} is the equivalent capillary height which is related to an equivalent pore diameter and the solid surface area, ψ is the soil suction represented as a head or length, and m is the pore-size coefficient, which is unitless.

The adhesive component of saturation, S_a is empirically related to soil suction through the following equation

$$S_a = a_c \left(1 - \frac{\ln(1 + \psi/\psi_r)}{\ln(1 + \psi_0/\psi_r)} \right) \frac{(h_{c0}/\psi_n)^{2/3}}{e^{1/3}(\psi/\psi_n)^{1/6}} \tag{3.2.19}$$

where a_c is the adhesion coefficient, e is the voids ratio, ψ_n is the normalisation parameter introduced to maintain consistency in the units ($\psi_n = 1$cm when ψ is in units of cm) and ψ_0 is the suction head equal to 10^7cm of water corresponding to a dry soil condition.

The four parameters, h_{c0} (cm), ψ_r (cm), m and a_c are required when solving the MK model. These parameters are defined in Table 3.10 for both granular and cohesive soils.

Parameter	Granular Soils (Sand, Silt)	Cohesive Soils (Clay, Clay Loam, Sandy Clay)
h_{c0}	$\frac{0.75}{[1.17\log(C_u)+1]eD_{10}}$	$\frac{0.15\rho_s}{e}w_L 1.45$
ψ_r	$0.86h_{c0}^{1.2}$	$0.86h_{c0}^{1.2}$
m	$\frac{1}{C_u}$	0.00003
a_c	0.01	0.0007

Table 3.10: Equations for Modified Kovacs Model (Aubertin et al., 2003). D_{10} is the diameter corresponding to 10% passing on the particle size distribution curve, C_u is the coefficient of uniformity equal to D_{60}/D_{10}, ρ_s is the density of the soil particles (kg/m^3), and w_L is the liquid limit (%).

Verification of Model

Programming of the MK model (Aubertin et al., 2003) has been undertaken in order to estimate the SWRC for each soil within the dataset. The model has been programmed using the Python programming language. This subsection documents the verification of the programming of the MK model by comparing results with data published in literature.

The data used for this verification is from the scientific paper by Aubertin et al. (2003) and is shown in Figure 3.8. The soil is a fine, uniform and dense sand and the data for this soil is from Bruch (1993).

For this soil the particle size distribution has not been provided, however parameters derived from the PSD have been, such as D_{10} and C_u. In addition, the void ratio, e has been provided. The SWRC as presented in Aubertin et al. (2003) is plotted as suction, ψ (cm) vs volumetric water content, θ (-) (Figure 3.8). The white diamonds represent the measured SWRC from a laboratory experiment (no method of testing was given by the authors), the black dashed line through these points is the best-fit curve, and the black solid line is the predicted SWRC using the MK model.

To verify the model programming undertaken, the predicted SWRC has been extracted from Figure 3.8 as a series of points using a web-based image plot digitiser. The soil suction is converted from units of cm to units of kPa, to align with the units used by the Python

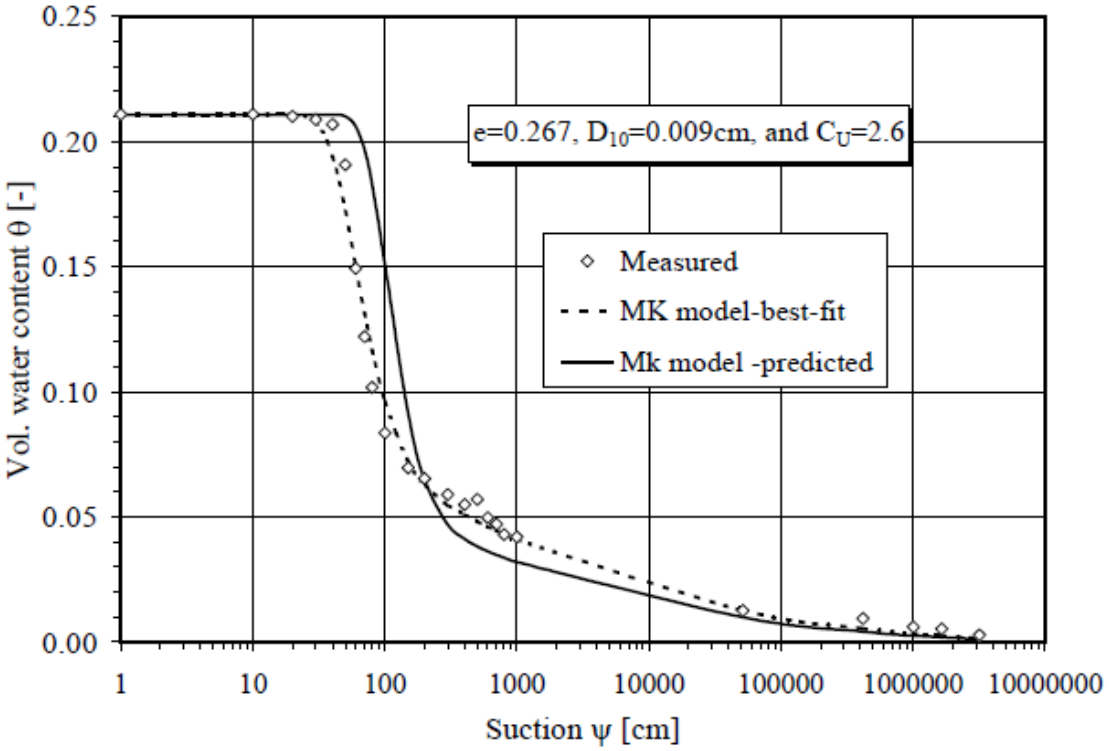

Figure 3.8: Soil parameters and the SWRC measured and predicted as presented by Aubertin et al. (2003).

script.

The void ratio, e, D_{10} and C_u are input to the model and the SWRC is estimated. The results from the model verification are shown in Figure 3.9. The predicted SWRC using the Python program is plotted in Figure 3.9 as a green line. The predicted SWRC as presented by Aubertin et al. (2003) is plotted as white circles, whilst the measured suction is plotted as black circles. It can be seen from Figure 3.5 that the green line is a near perfect fit for the white points, which verifies the programming of the MK model using the Python script. The following section presents the analysis of all dataset soils using this method.

Estimation of SWRC for Selected Soils

The SWRC estimation procedure using the MK model (Aubertin et al., 2003), as verified in the subsection above, is applied to all the granular soils within the selected dataset.

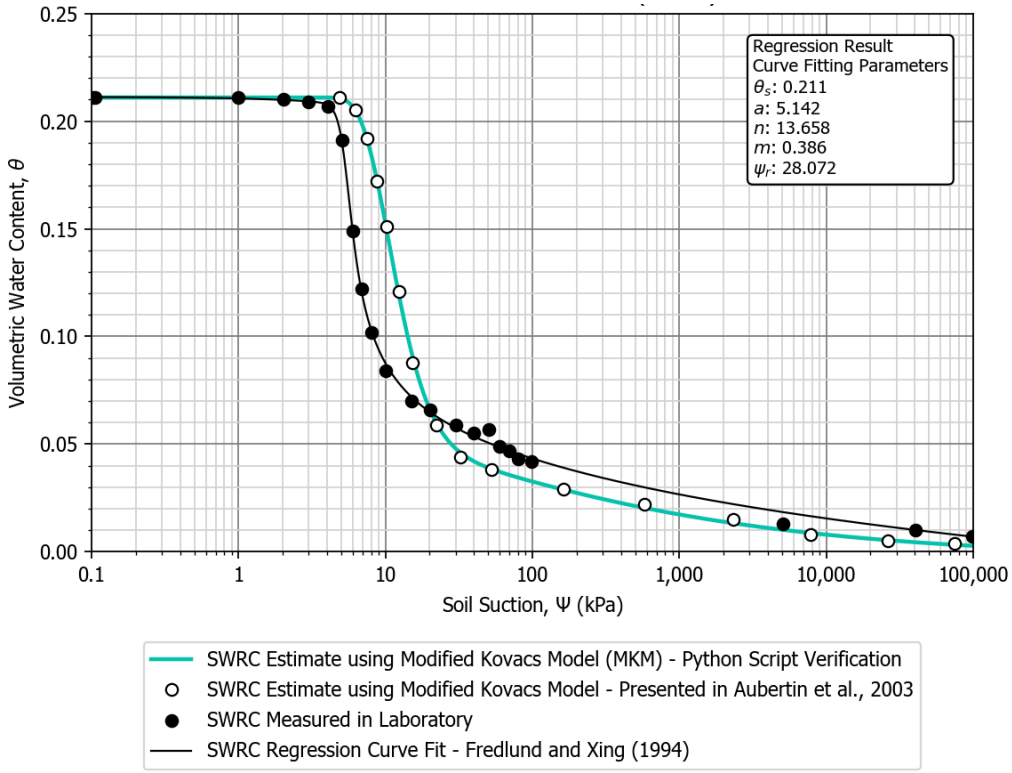

Figure 3.9: Predicted SWRC using Python script (green line) vs predicted SWRC as presented by Aubertin et al. (2003) (white circles). Measured SWRC shown by black circles, with the best-fit SWRC shown by the black line.

Unfortunately, because the UNSODA database was developed for agricultural purposes, there are no Atterberg Limit test data, specifically liquid limit, w_L for cohesive soils. This means that the MK mode cannot be used to estimate the SWRC for the cohesive soil samples within the dataset. Therefore, the MK model has been used for any soil sample within the sand and silt textural classes. This come to a total of 75 No. soils.

To determine the input parameters for the MK model, the best-fit PSD curve is used. The D_{10} and C_u values are calculated algorithmically from the best-fit PSD curve using linear interpolation. In addition, the void ratio is calculated from the porosity, which in turn is calculated from the dry density and particle density of the soil. Where the particle density is omitted from the database, an average value of 2.65 Mg/m^3 is used.

The estimated SWRC for a soil from each of the two granular textural classes analysed (sand, silt) are presented in Figure 3.10. The estimated SWRC for each soil in the dataset is presented in Figures C1 to C102 of Digital Appendix C.

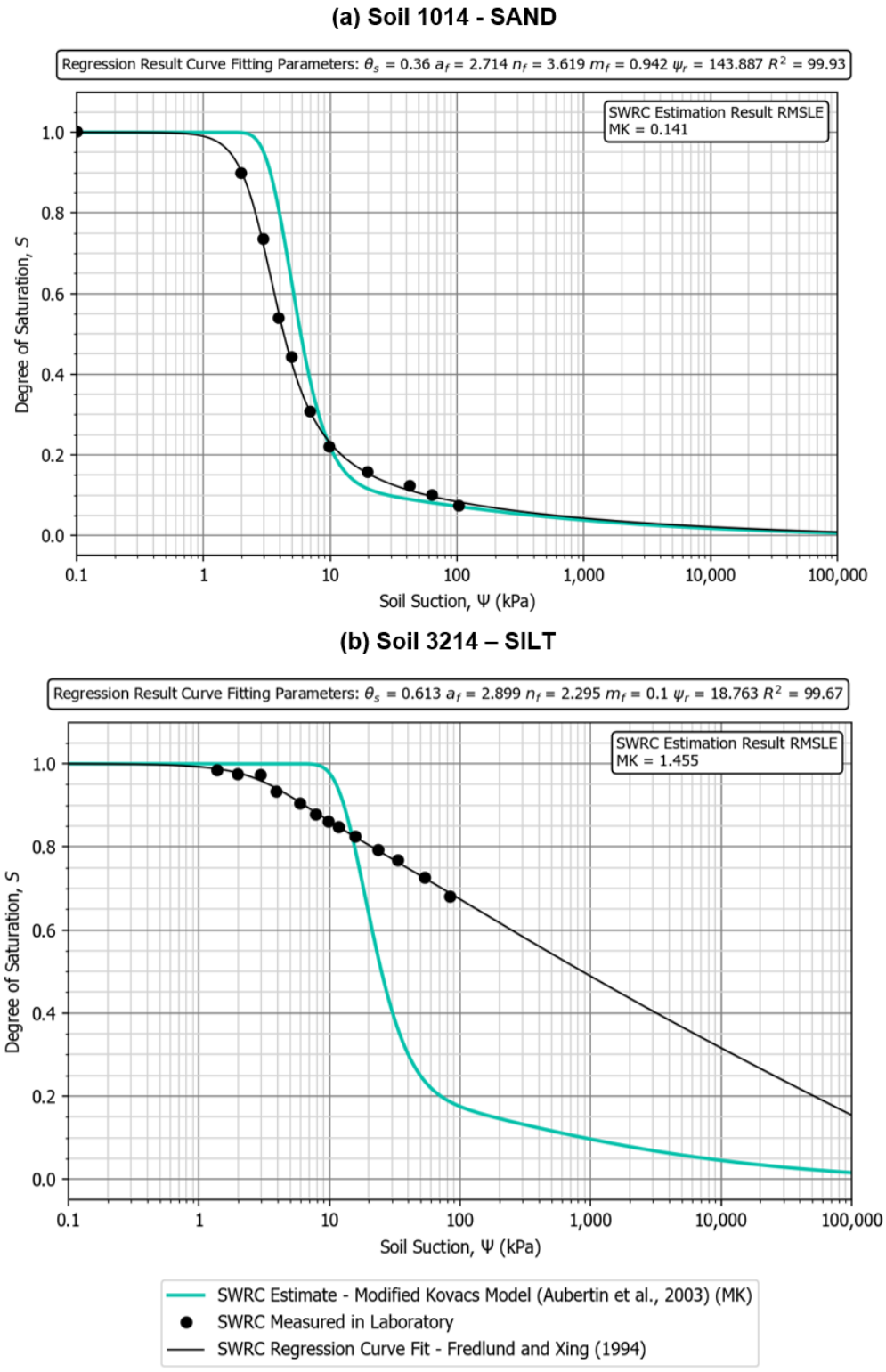

Figure 3.10: Estimated SWRC using the MK model (Aubertin et al., 2003) (green) vs Measured SWRC (black) for (a) Soil 1014 Sand (b) Soil 3214 Silt.

The Root Mean Squared Logarithmic Error (RMSLE) (Equation (3.2.15) of Section 3.2.3) is calculated to assess the relative difference between the predicted SWRC and the measured SWRC across the soils in the dataset. A low value of RMSLE indicates a small difference between the predicted and measured SWRC, whereas a high value indicates a large difference.

For the soils presented in Figure 3.10, the RMSLE calculated is 0.141 for Soil 1014 (sand), and 1.455 for Soil 3214 (silt). For the sand soil, the SWRC prediction performs well with a RMSLE value below 0.23. Overall the predicted curve was a good fit for the observed data, however the gradient is slightly steeper than the observed curve, and the air-entry value is offset by approximately 1-2kPa from the measured suction. For the silt soil, the SWRC prediction was poor, which resulted in a RMSLE value greater than 1.0. The estimated air entry value was significantly offset by approximately 30kPa, and the gradient was steeper than the measured SWRC. The corresponding PSD for these soils are presented in Figures C1 and C81 of Digital Appendix C.

The minimum, mean and maximum calculated RMSLE for the analysed soils within each of the two granular textural classes are presented in Table 3.11. The mean RMSLE for the sand textural class is 0.548, which suggests that the MK model (Aubertin et al., 2003) performs reasonably well at estimating the SWRC for these soils. The mean RMSLE for the silt textural class is 0.936, which suggests that the MK model performs less well for silts than sands. However there are only two soil samples within the silt category, meaning there is not sufficient data from the silt category to derive strong conclusions about the suitability of the MK model for estimating the SWRC for these soils.

Textural Class	**No. Soils**	**Min RMSLE**	**Mean RMSLE**	**Max RMSLE**	**Standard Deviation, σ**
Sand	73	0.081	0.548	2.567	0.408
Silt	2	0.417	0.936	1.455	0.734

Table 3.11: Calculated variability in RMSLE across each textural class when predicting the SWRC using the Modified Kovács Model Aubertin et al. (2003).

This section has presented the SWRC prediction analysis using the Modified Kovács Model (Aubertin et al., 1998). The following section presents a similar analysis using the Perera et al. (2005) model, which is a functional regression type model which estimates parameters for the Fredlund and Xing (1994) SWRC equation using the PSD.

3.2.5 Estimation of the SWRC using the Perera et al. (2005) Model

Background Theory

The Perera model (PM) (Perera et al., 2005) is a SWRC predictive model which correlates soil index properties to parameters of the Fredlund and Xing (1994) equation. The model is a development of the Zapata et al. (2000) model developed at Arizona State University. It was developed as part of a project entitled "Environmental Effects in Pavement Mix and Structural Design Systems (NCHRP 9-23)".

As part of the project a database of plastic and non-plastic soils were collected from beneath highway pavements in 30 locations in the United States. The soils with a weighted PI of less than 1.0 were categorised as non-plastic soils. The Weighted PI (wPI), is referred to as the product of P200 (percentage passing the Number 200 (0.074mm) sieve) and the PI of the soil. The soils that exhibited wPI greater than or equal to 1.0 were categorized as plastic (PI) soils. The samples were then subject to extensive laboratory testing, and compiled with another database collected earlier by Zapata et al. (2000).

By means of a statistical multiple regression program, the best correlations between the Fredlund and Xing (1994) parameters a, n, m and ψ_r, and the PSD and index parameters were determined and expressed as equations. These equations are defined below for non-plastic soils (Perera et al., 2005).

$$a = 1.14\alpha - 0.5 \tag{3.2.20}$$

where

$$\alpha = -2.79 - 14.1\log(D_{20}) - 1.9 \times 10^{-6} P_{200}^{4.34} + 7\log(D_{30}) + 0.055 D_{100} \tag{3.2.21}$$

D_{20} is the particle diameter corresponding to 20% passing on the PSD curve, D_{30} is the particle diameter corresponding to 30% passing on the PSD curve, P_{200} is the percentage passing the No. 200 sieve (opening 0.074mm), and

$$D_{100} = 10^{\left[\frac{40}{s_1} + \log(D_{60})\right]} \tag{3.2.22}$$

where D_{60} is the particle diameter corresponding to 60% passing on the PSD curve and

$$s_1 = \frac{30}{[\log(D_{90}) - \log(D_{60})]} \tag{3.2.23}$$

where D_{90} is the particle diameter corresponding to 90% passing on the PSD curve. Perera et al. (2005) suggest that a is limited to a minimum 1.0 because in some extreme cases computed values of a can be negative, which would lead to erroneous results.

The n parameter is calculated by

$$n = 0.936\beta - 3.8 \tag{3.2.24}$$

where

$$\beta = \left\{5.39 - 0.29 \ln\left[P_{200}\left(\frac{D_{90}}{D_{10}}\right)\right] + 3D_0^{0.57} + 0.021P_{200}^{1.19}\right\}s_1^{0.1} \tag{3.2.25}$$

where

$$D_0 = 10^{\left[\frac{-30}{s_2} + \log(D_{30})\right]} \tag{3.2.26}$$

where

$$s_2 = \frac{20}{[\log(D_{30}) - \log(D_{10})]} \tag{3.2.27}$$

where D_{10} is the particle diameter corresponding to 10% passing on the PSD curve.

The m parameter is calculated by

$$m = 0.26e^{0.758\chi} + 1.4D_{10} \tag{3.2.28}$$

where

$$\chi = \log s_2^{1.15} - \left(1 - \frac{1}{n}\right) \tag{3.2.29}$$

and $\psi_r = 100$ (kPa)

For plastic soils, the equations are as follows

$$a = 32.835 \times \ln(P_{200}PI) + 32.438 \tag{3.2.30}$$

$$n = 1.421 \times (P_{200}PI)^{-0.3185} \tag{3.2.31}$$

$$m = -0.2154 \times \ln(P_{200}PI) + 0.7145 \tag{3.2.32}$$

where P_{200} is in decimal form, PI is the plasticity index and $\psi_r = 500$ kPa.

Verification of Model

Programming of the Perera et al. (2005) (PM) model has been undertaken in order to estimate the SWRC for each soil within the dataset. The model has been programmed using the Python programming language. This subsection documents the verification of the programming of the PM model by comparing results with data published in literature.

The data used for this model verification is from a scientific paper by Chai and Khaimook (2020). The soil analysed by Chai and Khaimook (2020) was sand soil 1467 from the UNSODA database, which is part of the dataset analysed in this study. Chai and Khaimook (2020) proposed a new equation for predicting the SWRC, whilst comparing their results to the PM model.

For this soil the, particle size distribution and porosity of the soil sample are provided as part of the UNSODA database. The PSD for this soil is depicted in Figure 3.11. The PSD best-fit curve, along with the straight line fit connecting the measured points, are presented together on this figure.

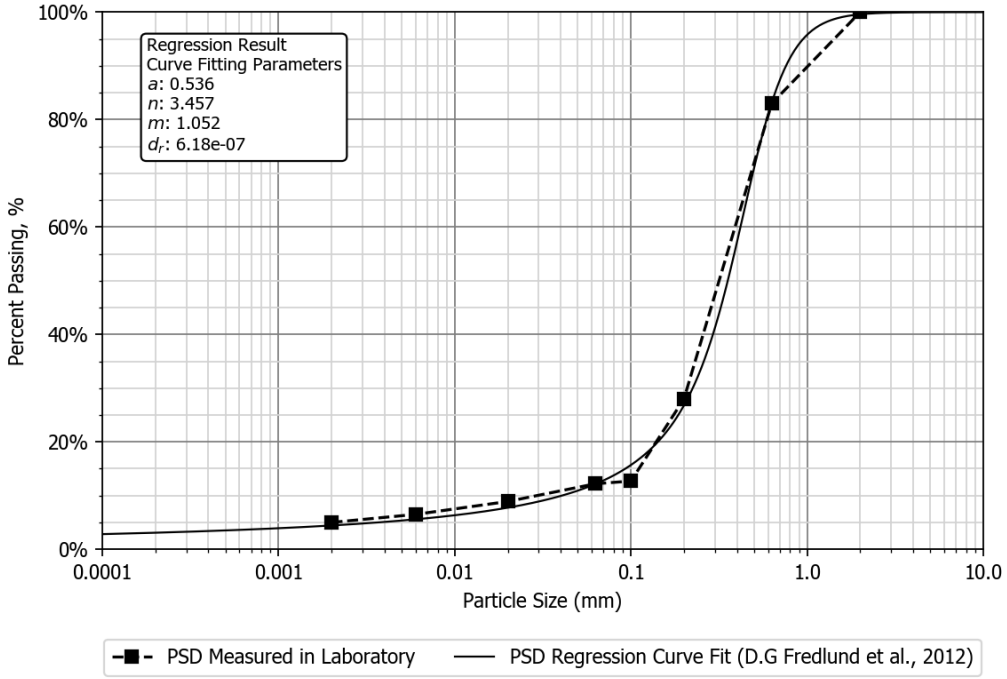

Figure 3.11: Particle Size Distribution for sand Soil 1467.

To verify the model programming undertaken, the predicted SWRC has been extracted from Figure 12 (d) of Chai and Khaimook (2020) as a series of points using a web-based

image plot digitiser. The measured SWRC points have been converted from volumetric water content to degree of saturation using a porosity of 0.312 taken from the database.

The PSD and porosity are input to the Python script and the SWRC is estimated using the PM method. For the purpose of the model verification, the D values are calculated using linear interpolation between the measured PSD points, rather than using the best-fit curve, as this was the approach used by Chai and Khaimook (2020). Table 3.12 presents the calculated input parameters derived from the PSD.

D_{10} (mm)	D_{20} (mm)	D_{30} (mm)	D_{60} (mm)	D_{90} (mm)	P_{200} (%)
0.029	0.139	0.209	0.390	1.014	12.36

Table 3.12: Input Parameters derived from PSD for Soil 1467.

The results from the model verification for each calculation stage are presented in Table 3.13, and the predicted SWRC using the Python program is plotted in Figure 3.12 as a red line. The predicted SWRC as presented in Chai and Khaimook (2020) is plotted as white circles, the measured suction is plotted as black circles, and the best-fit curve to the measured data is plotted as the black line.

s_1	D_{100} (mm)	α	a	s_2	D_0 (mm)	β	n	χ	m	ψ_r (kPa)
72.30	1.394	4.49	4.62	23.47	0.011	6.57	2.35	1.00	0.60	100.0

Table 3.13: Calculated parameter values for the Perera et al. (2005) model for Soil 1467.

It can be seen from Figure 3.12 that the red line is a near perfect fit for the white points, which verifies the programming of the PM model using the Python script. The following section presents the analysis which can now be used in the analysis of dataset of soils using this method.

Estimation of SWRC for Selected Soils

The SWRC estimation procedure using the PM model (Perera et al., 2005), as verified in the subsection above, is applied to all the granular soils within the selected dataset. There is no plasticity index, PI, data for the cohesive soils (Clay, Clay Loam and Sandy Clay) in the dataset, which means that the PM model cannot be used to estimate the SWRC

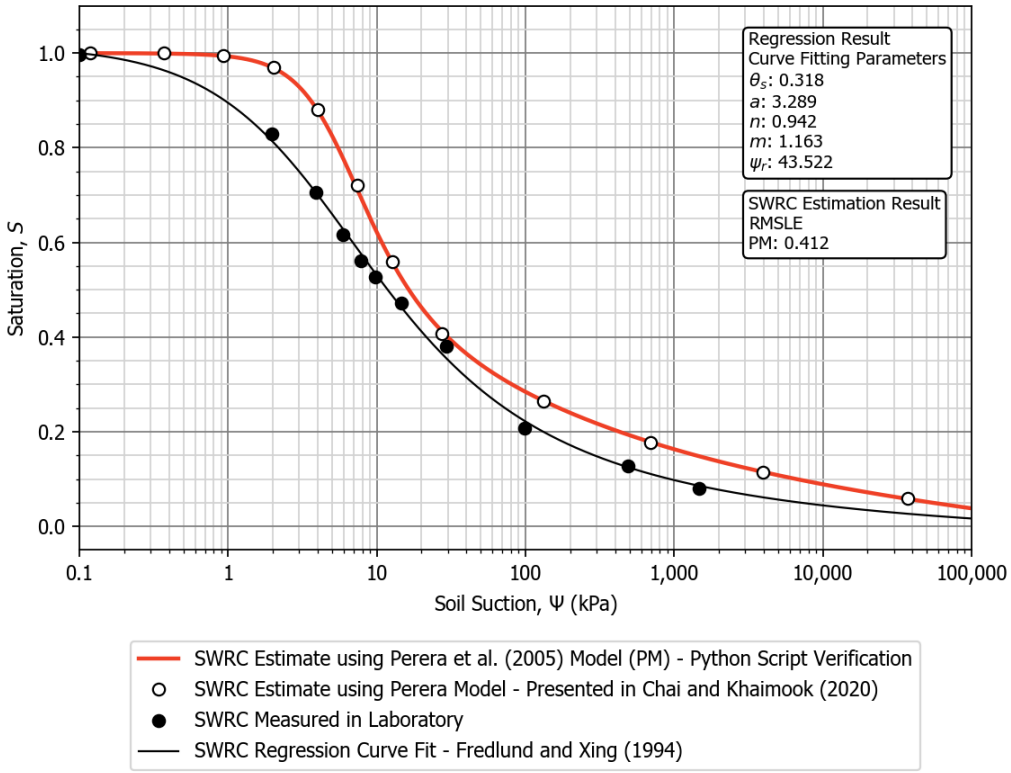

Figure 3.12: Predicted SWRC using Python script (red line) vs predicted SWRC as presented by Chai and Khaimook (2020) (white circles). The measured SWRC is plotted as black circles along with the best-fit curve which is plotted as the back line.

for these soil samples. Therefore, the PM model has been used for each soil sample within the sand and silt textural classes. This comes to a total of 75 No. soils.

To determine the input parameters for the PM model, the best-fit PSD curve is used. The D values (D_{10}, D_{20}, D_{30}, D_{60}, D_{90}) and P_{200} are calculated from the best-fit curve. In addition, the porosity has been used to calculate the saturated water content. The estimated SWRC for a soil from each of the two granular textural classes analysed (sand soil 1014, silt soil 3214) are presented in Figure 3.13.

The Root Mean Squared Logarithmic Error (RMSLE) (Equation 3.2.15 of Section 3.2.3) is calculated to assess the relative difference between the predicted SWRC and the measured SWRC across the soils in the dataset. For the soils presented in Figure 3.13, the RMSLE calculated is 0.565 for Soil 1014 (sand), and 1.057 for Soil 3214 (silt). For the sand soil, the SWRC prediction is average with a RMSLE greater than 0.5. Overall the shape of the predicted curve is a close fit to the observed data, however the predicted

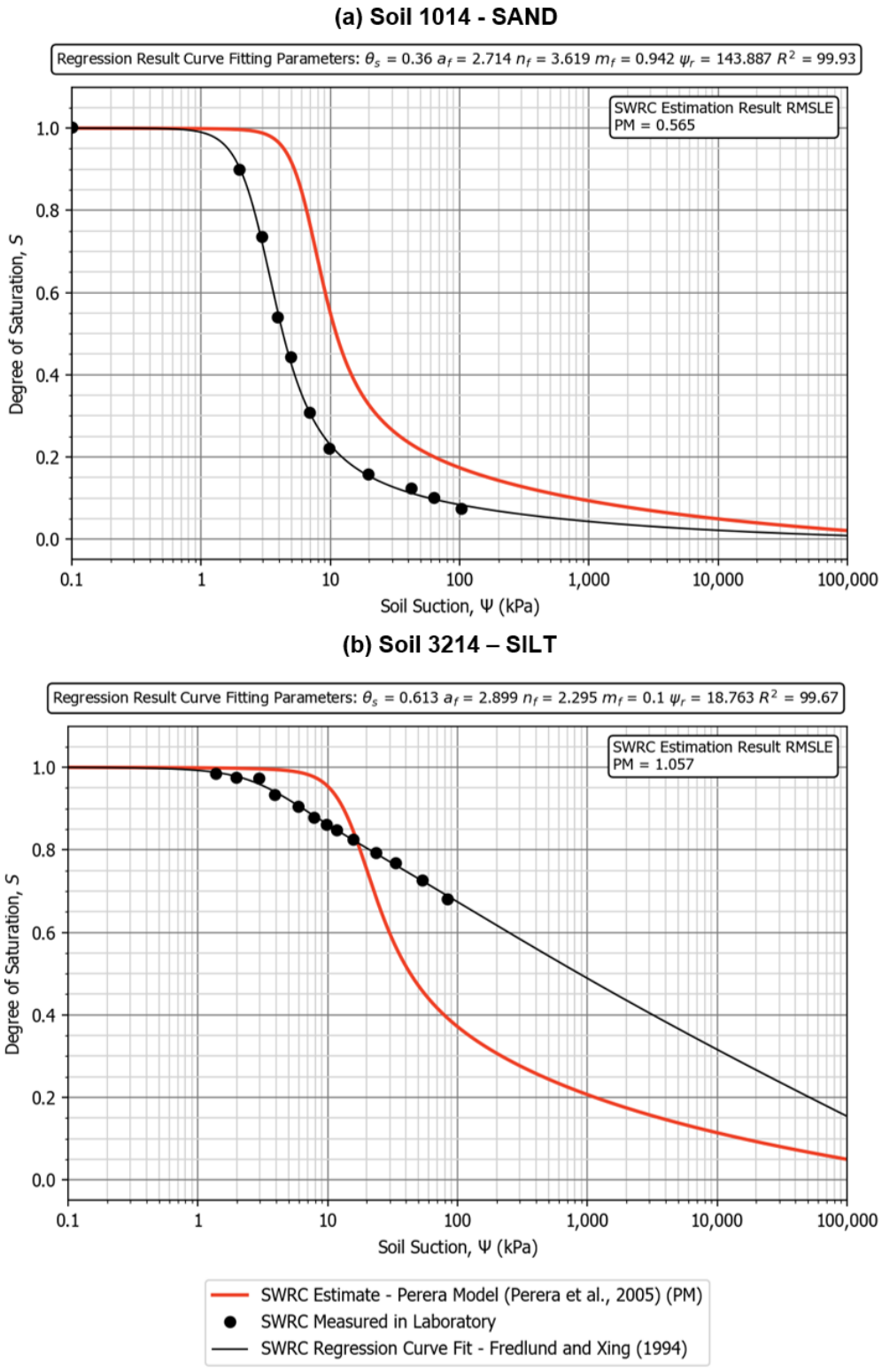

Figure 3.13: Estimated SWRC using the PM model (Perera et al., 2005)(red) vs Measured SWRC (black) for (a) Soil 1014 Sand (b) Soil 3214 Silt.

Textural Class	No. Soils	Min RMSLE	Mean RMSLE	Max RMSLE	Standard Deviation, σ
Sand	73	0.066	0.433	1.785	0.316
Silt	2	0.397	0.727	1.057	0.467

Table 3.14: Calculated variability in RMSLE across each textural class when predicting the SWRC using the Perera Model.

curve has a significant offset from the measured curve, with the air-entry value being offset by approximately 2kPa. For the silt soil, the predicted SWRC resulted in a RMSLE value greater than 1.0, suggesting a poor prediction overall. The estimation was reasonable in the high degree of saturation region near the air-entry value, however the curve becomes largely offset between a saturation of 0.6 and 0.2. The corresponding PSD for these soils are presented in Figures C1 and C81 of Digital Appendix C.

The minimum, mean and maximum calculated RMSLE for the analysed soils within each of the two granular textural classes are presented if Table 3.14. The mean RMSLE for the sand textural classes is 0.433, which suggests that the PM model (Perera et al., 2005) performs reasonably wells at estimating the SWRC for these soils. The RMSLE for silts is higher at 0.727. However, it must be noted that there are only two soil samples within the silt category, which is not sufficient data to derive strong conclusions about the suitability of the PM model for estimating the SWRC.

3.2.6 Summary of Soil Data Analysis

This section presented the analysis undertaken on a dataset of soils including sands, silts, sandy clays, clay loams and clays. The objective of this analysis was to predict the SWRC of a soil using several methods presented in the literature (Arya and Paris, 1981; Aubertin et al., 2003; Perera et al., 2005), and compare the result to the measured laboratory SWRC data. It was shown that by calculating the RMSLE, all three methods performed reasonably well at predicting the SWRC of sands. There were insufficient datasets to draw conclusions on the performance of each method for silt soils. For cohesive soils (clay, clay loam and sandy clay), only the Arya and Paris (1981) model could be used because plastic limit and liquid limit are not included in the UNSODA database.

The following section of this Chapter presents some statistical analysis undertaken to

gain further insight to the error of the SWRC predictive methods. In particular how each method performs over the full range of degree of saturation. In addition, it is shown how confidence limits have been developed from this analysis. The aim of this is to develop a tool which can be used in practice by geotechnical engineers where it is necessary to estimate the SWRC of a soil and have an understanding of the possible error in the prediction.

3.3 Statistical Analysis

To assess how well each SWRC predictive method performs, analysis has been undertaken on the error between the predicted SWRC and the measured SWRC. This error is named herein as the suction error, ψ_e, and is the difference between the logarithmic of the predicted suction and the logarithmic of the measured suction at a given degree of saturation value. It is calculated as follows:

$$\psi_e = \log(\hat{\psi}) - \log(\psi) \tag{3.3.33}$$

where $\hat{\psi}$ is the predicted suction (using one of the predictive methods documented above) and ψ is the measured suction (best-fit Fredlund and Xing (1994) curve). It is important to measure the suction error in logarithmic terms because suction increase on a logarithmic scale. If suction error was measured on a liner scale, then large errors in suction towards residual conditions would dwarf the errors towards the air-entry value. This would make it impossible to study the error between the predicted and measured suction over the full degree of saturation range.

For each soil within the dataset, the predicted and measured SWRC is split into 19 intervals on the degree of saturation axis (i.e. from 0.05 to 0.95). Intervals of saturation were chosen at 0.05 as this gave the clearest visualisation of error when plotted in graphical form. At each of these saturation values, the suction error is calculated. To understand the performance of a SWRC predictive method, the calculated suction error for all soils within the dataset is plotted on a graph of suction error, ψ_e vs degree of saturation, S. An example of this type of plot is shown in Figure 3.14 for the Arya and Paris (1981) model for all 102 soils. The markers indicate the textural class of the soil. Sand soils are plotted using yellow circles, clay loams are plotted using magenta diamonds, sandy clays

are plotted using orange triangles, clay soils are plotted with red squares and silts are plotted with blue hexagons.

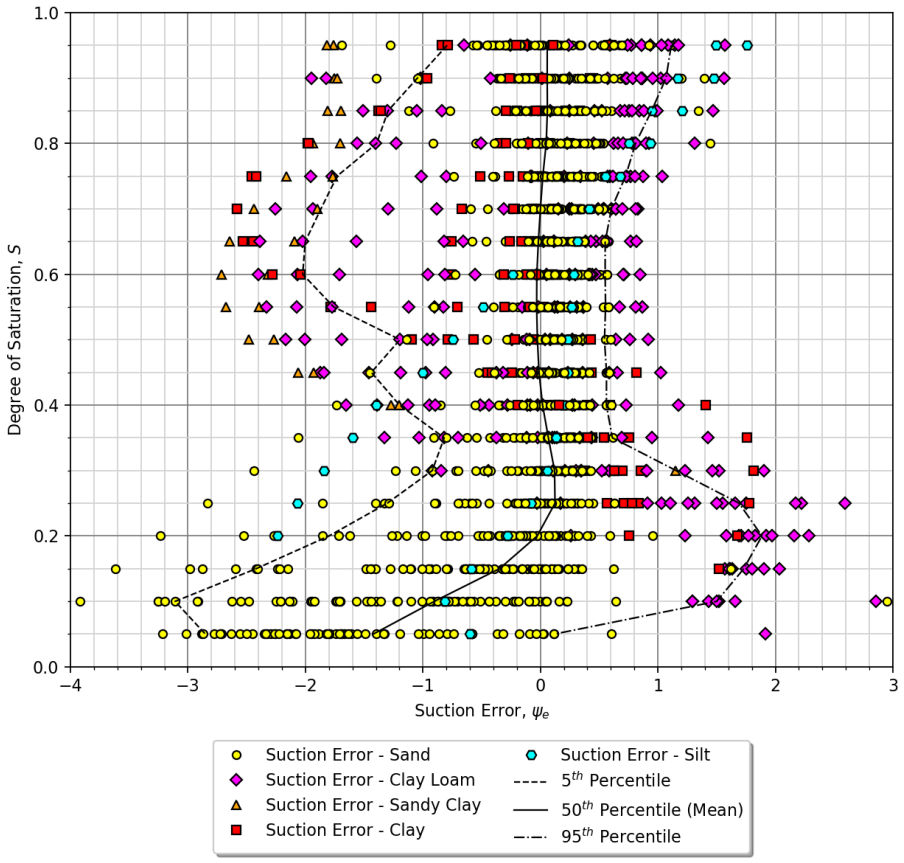

Figure 3.14: Distribution of suction error between the predicted SWRC using the Arya and Paris (1981) model and the best-fit curve for the measured SWRC. Based on all 102 No. analysed soils from the dataset.

For a point on the graph in Figure 3.14, if the suction error is positive, the predicted suction was calculated to be greater than the measured suction best-fit curve at that degree of saturation value. Likewise, where the suction error is negative, the predicted suction was calculated to be less than the measured suction best-fit curve.

The solid black line on Figure 3.14 is the calculated mean suction error. This is calculated by summing the suction error for all 102 No. soils at a given degree of saturation value, then dividing by the total number of soils. This is then repeated at all saturation values. The mean suction error is the centre of the distribution of suction error at a given saturation value. It therefore highlights if the predictive method on average overestimates or underestimates the suction at that saturation value. For example, in Figure 3.14, we

can see that between saturation values of 0.40 and 0.80, the mean suction error for the Arya and Paris (1981) is close to zero, suggesting that the model neither over predicts or under predicts the SWRC on average. Below a saturation of 0.2 however, the mean suction error becomes negative, suggesting on average the Arya and Paris (1981) model under predicts suction at low saturation values.

In addition to the mean suction error, the 5^{th} and 95^{th} percentiles of the suction error have been calculated at each degree of saturation value. The percentiles were calculated using the Numpy percentile algorithm from the Scipy python package (SciPy.org, 2019). The percentiles have been plotted as dashed lines in Figure 3.14. Between these two percentile lines lie 90% of the calculated soil suction errors. This gives an indication of the spread of the suction error within the dataset. For example, if the lines are close together, the spread of the suction error is low, meaning the predicted suction is typically close to the measured suction. This give confidence that the predictive model is a reliable method for predicting the SWRC. If however the percentile lines are far apart, this indicates a large spread in suction error within the dataset, meaning the predicted suction is often far from the measured suction. This gives less confidence that the predictive method is reliable at estimating the SWRC. Therefore the calculated percentile lines can be used as a guide to the confidence in the predicted suction at a given degree of saturation value.

In Figure 3.14 we can see that the percentile lines are influenced by the cohesive soils within the dataset, notably the clay loams. For example, it is clear that the Arya and Paris (1981) model often under predicts the suction between saturations of 0.40 and 0.95 for the cohesive soils. The shape of the 5^{th} percentile curve reflects this by being further from the mean in this range. A similar effect is also observed in the low saturation range below 0.40, where the Arya and Paris (1981) model often over predicts the suction of cohesive soils. It is clear for the data in Figure 3.14 that the predictive model performs differently for granular and cohesive soils. For a practising geotechnical engineer who knows the type of soil they are working with, it is more appropriate to calculate the percentile lines for granular and cohesive soils separately. The following subsections present the calculated suction error and percentile lines for each of the SWRC predictive models, with the soils grouped into cohesive and granular soils.

3.3.1 Analysis of Suction Error for Granular Soils using the Arya and Paris (1981) Model

A graph of suction error, ψ_e vs degree of saturation, S for the 75 No. granular soils that have been analysed using the Arya and Paris (1981) model. This plot is presented in Figure 3.15.

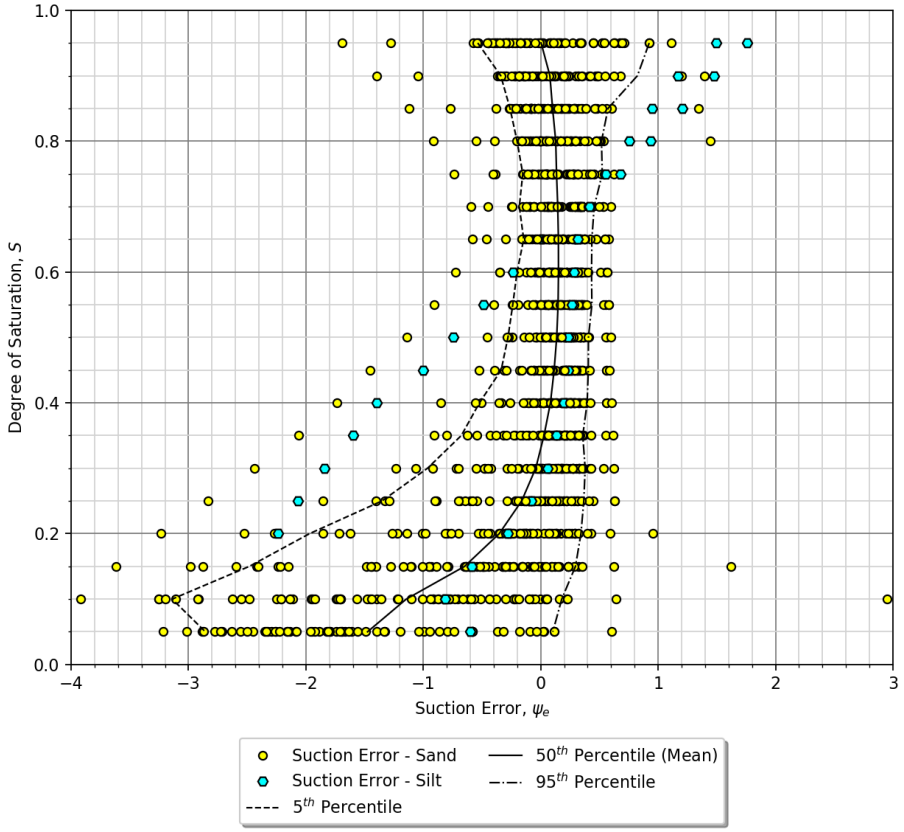

Figure 3.15: Distribution of suction error between the predicted SWRC using the Arya and Paris (1981) model and the best-fit curve for the measured SWRC. Based on all 75 No. analysed granular soils from the dataset.

Firstly, the most noticeable difference to Figure 3.14 is that the percentile lines are much closer together, particularly in the degree of saturation range between 0.35 to 0.95. This indicates that the Arya and Paris (1981) model is generally good at estimating the SWRC for granular soils in this degree of saturation range. The mean suction error is above 0 by about 0.1, suggesting that the model on average over predicts the suction in this range by a small amount. This generally results in the predicted SWRC being offset to the right of the measured SWRC by approximately 1-10 kPa. Below a saturation of

0.35, the percentile lines spread further apart and tend towards a negative suction error. This means that the Arya and Paris (1981) model typically underestimates the suction for granular soils in this range. Some possible explanations for this error include:

- There is a lack of measured SWRC points in the high suction, low saturation range i.e. the best-fit SWRC curve may not accurately represent the real SWRC in this region. Small differences in the residual degree of saturation can lead to large suction errors.
- The dry density and PSD alone may not be sufficient to calculate the pore size distribution, and therefore predict the SWRC accurately in this range i.e. other factors may be influencing the SWRC in this region, such as grain shape, grain packing and volume change as suction increases.

The calculated mean suction error and the 5^{th} and 95^{th} percentiles are given in Table B.1 of Appendix A for the analysis of the 75 No. granular soils using the Arya and Paris (1981) model.

3.3.2 Analysis of Suction Error for Cohesive Soils using the Arya and Paris (1981) Model

A graph of suction error, ψ_e vs degree of saturation, S has been plotted for the 27 No. cohesive soils that have been analysed using the Arya and Paris (1981) model. This plot is presented in Figure 3.16.

It clear from looking at Figure 3.16 that the Arya and Paris (1981) model performs worse for cohesive soils than granular soils. This is most noticeable in the spread of the suction error, where the 5^{th} and 95^{th} percentiles are located further from the mean than for granular soils. For example, at a saturation value of 0.6, the 5^{th} percentile of suction error for the cohesive soil group is -2.38. For the granular soil group it is -0.15. We can see from Figure 3.16 than on average, the Arya and Paris (1981) model under predicts the suction between saturations of 0.37 and 0.95. This is because for a number of soils, the predicted SWRC is offset by a large amount to the left of the measured SWRC. The predicted SWRC in Figure 3.6 (b) is an example of this for a sandy clay. The likely

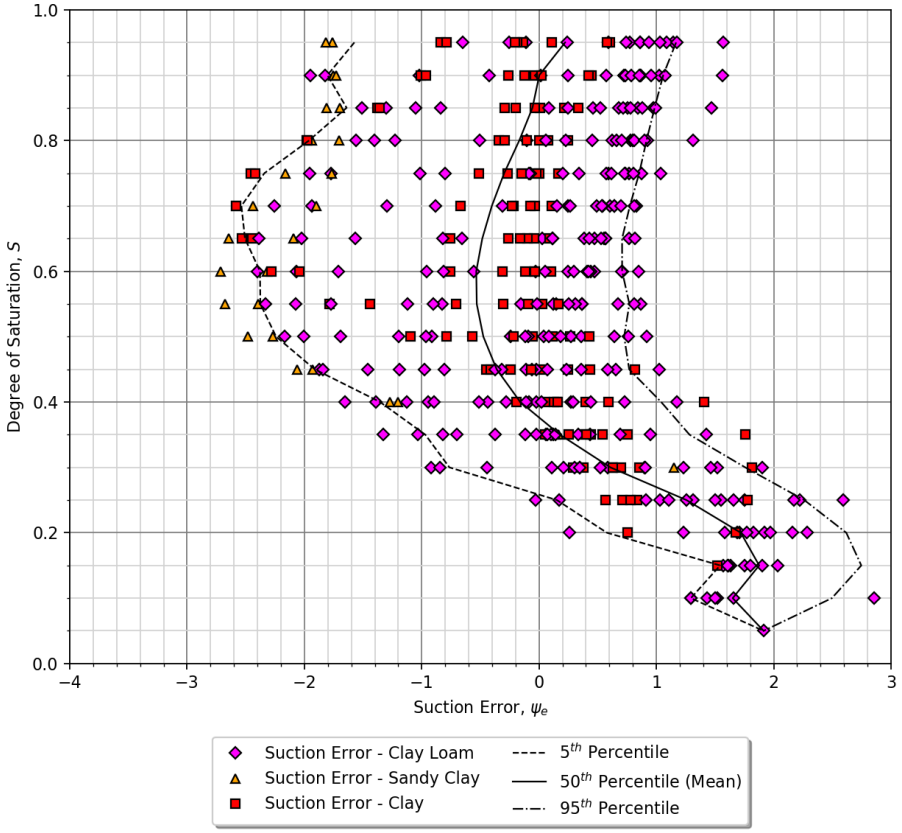

Figure 3.16: Distribution of suction error between the predicted SWRC using the Arya and Paris (1981) model and the best-fit curve for the measured SWRC. Based on all 27 No. analysed cohesive soils from the dataset.

explanation for this offset is the shape of the particle size distribution curve. For clay soils with a high content of granular material, such as sand and silt, the area of the PSD curve where the gradient increases (equivalent to the air-entry value of the SWRC) may be in the region of particle sizes between 0.1 to 1.0mm. If this is the case, the air-entry value calculated using the Arya and Paris (1981) model may be in the region of 1 to 10kPa, which is typical of sand soils. However, the measured air-entry value is typically in the region of 10-100kPa for these types of soils. The air-entry value is typically related to the largest pore size in the soils. For these cohesive soils with granular content, the gaps between the largest particles are likely filled with fine clay particles, which will reduce the size of the largest pores, effectively shifting the air-entry value of the SWRC to the right towards higher suctions. This analysis demonstrates that the approach used by Arya and Paris (1981) to convert the PSD to pore size distribution is less effective for cohesive soils, particularly if there is a considerable proportion of larger diameter particles such as in the

case of the sandy clays samples.

Below a saturation of 0.37, the mean suction error becomes positive, meaning the Arya and Paris (1981) method tends to over predict the suction at low saturation values. However, for most cohesive soils analysed in the dataset, there are few recorded suction measurements at saturations below 0.5. This is probably in part due to the nature of cohesive soils, which often have high residual saturations, and the SWRC testing procedure, as the time it takes to reach low saturations increase the more fine grained the soil becomes.This means that the best-fit SWRC probably does not represent the true SWRC at the low saturation, high suction end of the SWRC. The calculated mean suction error and the 5^{th} and 95^{th} percentiles are given in Table B.2 for the analysis of the 27 No. cohesive soils using the Arya and Paris (1981) model.

3.3.3 Analysis of Suction Error for Granular Soils using the Modified Kovács Model (Aubertin et al., 2003)

A graph of suction error, ψ_e vs degree of saturation, S for the 75 No. granular soils that have been analysed using the Modified Kovács (MK) Model (Aubertin et al., 2003). This plot is presented in Figure 3.17.

The suction error plot follows a similar pattern to the plot for the Arya and Paris (1981) model presented in Figure 3.15. The percentile lines are close to the mean suction error between saturations of 0.35 and 0.95, suggesting the MK model is a reliable model for predicting the SWRC of granular soils in this suction range. The mean suction error above a saturation of 0.45 is positive between 0 and 0.2. This suggests that the model on average over predicts the air-entry value, which means the predicted SWRC is typically offset to the right of the measured SWRC by approximately 1-5 kPa. Below a saturation of 0.35, the percentile lines spread further apart and tend towards a negative suction error. This means that the MK model usually underestimates the suction for granular soils in this range. It appears that using information from the PSD alone is not sufficient to model the SWRC at low saturations. In particular, the rate of change in the gradient of the curve as it tends towards the residual saturation. In many of the predicted SWRC using the MK model, the change in gradient of the curve at low saturations occurs sharply, between

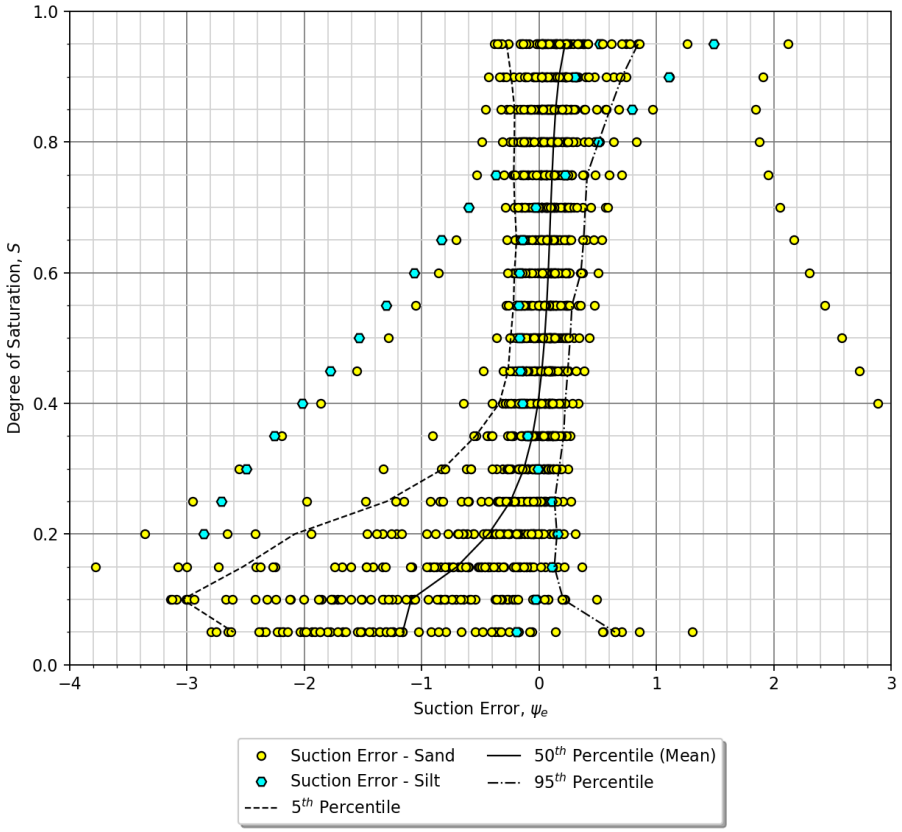

Figure 3.17: Distribution of suction error between the predicted SWRC using the MK model and the best-fit curve for the measured SWRC. Based on all 75 No. analysed granular soils from the dataset.

the suction range of 5 to 15kPa, whereas many of the measured SWRC change gradient over a greater suction range, between 3 to 100kPa. The predicted SWRC tends to follow the shape of the PSD, which indicates other factors such as grain arrangement may be influencing the SWRC in this region. The calculated mean suction error and the 5^{th} and 95^{th} percentiles are given in Table B.3 for the analysis of the 75 No. granular soils using the MK model.

3.3.4 Analysis of Suction Error for Granular Soils using the Perera Model (Perera et al., 2005)

A graph of suction error, ψ_e vs degree of saturation, S for the 75 No. granular soils that have been analysed using the Perera Model (PM) (Perera et al., 2005). This plot is presented in Figure 3.18.

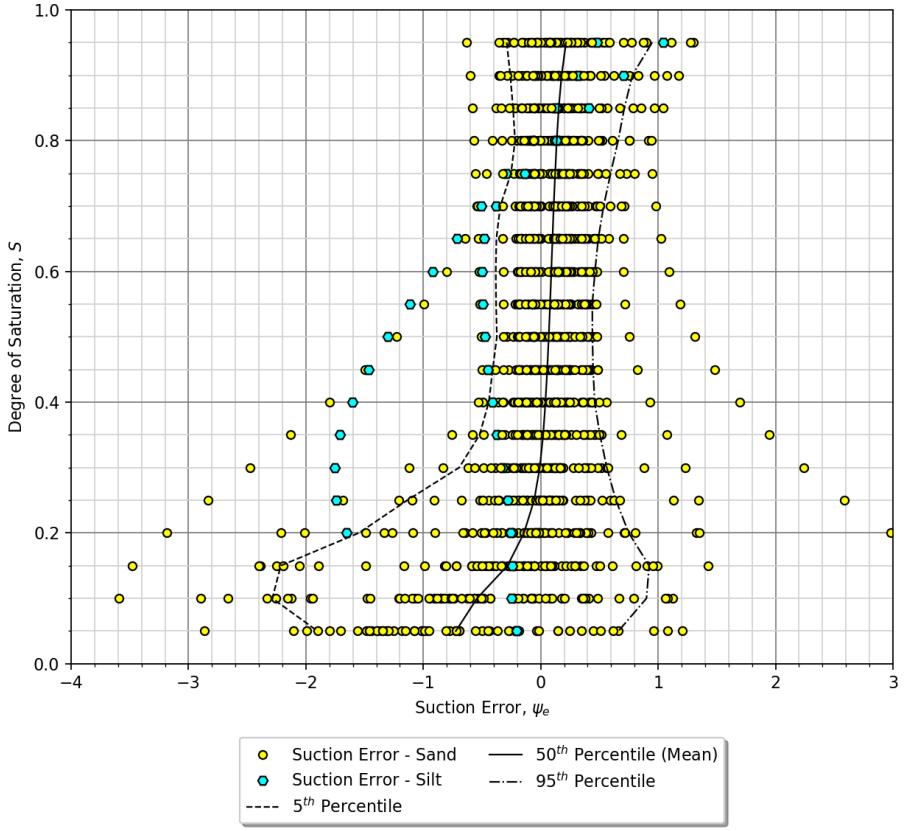

Figure 3.18: Distribution of suction error between the predicted SWRC using the PM model and the best-fit curve for the measured SWRC. Based on all 75 analysed granular soils from the dataset.

The suction error plot follows a similar pattern to the plot for the Arya and Paris (1981) (AP) model presented in Figure 3.15 and the Modified Kocács (MK) model presented in Figure 3.17. Figure 3.19 presents a comparison of the percentile lines and mean suction error for all three predictive methods. The percentile lines are close to the mean suction error between saturations of 0.35 and 0.95, however they are not as close to the mean line as the AP and MK models. This suggests that the PM model is a reliable model for predicting the SWRC of granular soils, however it does not perform as well as the other two models within this saturation range. The mean suction error in this range is also positive, between the value of 0.0 and 0.2. This suggests that the model on average over predicts the air-entry value, which results in the predicted SWRC being offset to the right of the measured SWRC by approximately 1-5 kPa. This is very similar to how the MK model behaves in this saturation range.

Below a saturation of 0.35, the percentile lines spread further apart and tend towards a

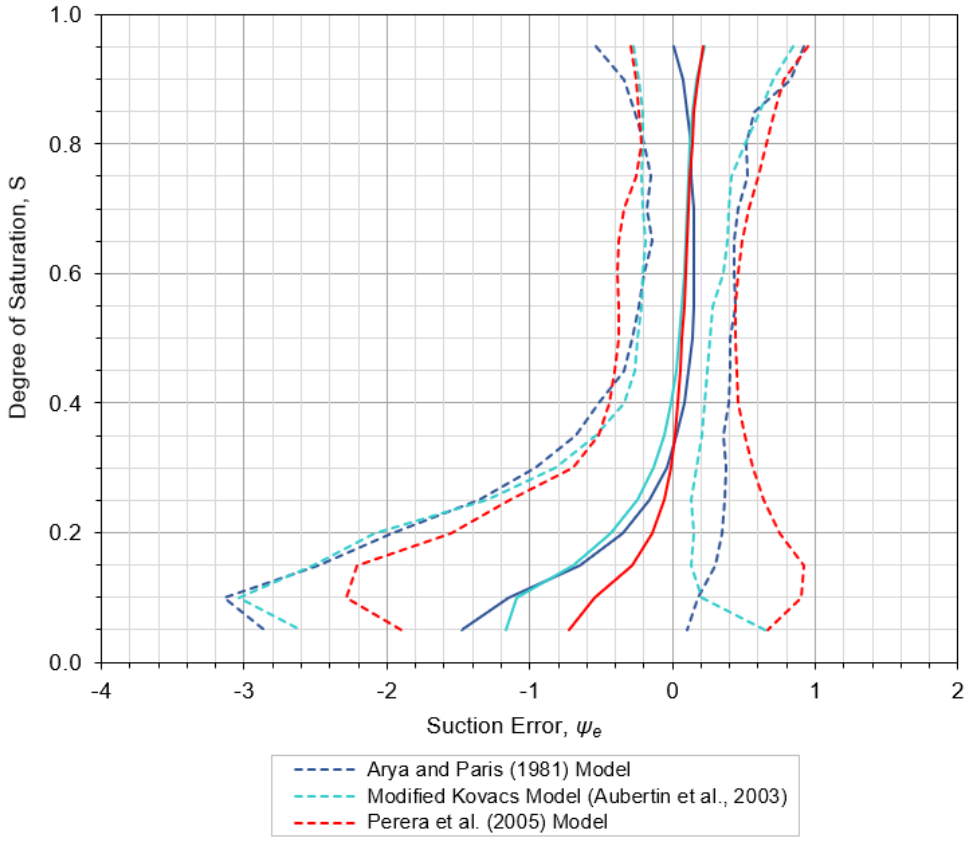

Figure 3.19: Comparison of 5th and 95th percentiles, and the mean suction error for all three SWRC predictive methods.

negative suction error, which means that the PM model often underestimates the suction for granular soils in this range. However, the mean suction error is considerably less than both the AP model and the MK model at these low values of saturation. By looking at the SWRC predictions for all the soils (Figures C1 to C102 of Digital Appendix C), the shape of the curve in the low saturation range is modelled much more accurately than the other two methods. Therefore the PM model is the best performing predictive method for estimating the SWRC in the low saturation range. The fact that the PM model was developed by undertaking a regression of measured SWRC for a database of soils may partly explain why this is the case i.e. it is not solely based on the data derived from the PSD. The calculated mean suction error and the 5th and 95th percentiles are given in Table B.4 for the analysis of the 75 No. granular soils using the PM model.

The statistical analysis presented so far quantifies the likely range of error in the SWRC predictive methods for granular and cohesive soils. The following section describes how

the calculated 5^{th} and 95^{th} percentiles can be converted to confidence limits when used to predict the SWRC of soils in practice.

3.3.5 Use of Confidence Limits in Practice

To utilise the soil analysis undertaken in this chapter, the calculated percentile lines can be converted to confidence limits when predicting the SWRC of soils in practice. Based on the analysis of the dataset of soil, the limits indicate that for 90% of soils, the true SWRC would lie between these lines. This process has been developed into software developed in Microsoft Excel, and is described by the following list and the flow chart in Figure 3.20:

- Collect index properties of the soil for which the SWRC is to be predicted (PSD, dry density, particle density and porosity/void ratio).
- Determine if the soil is cohesive (plastic) or granular (non-plastic) in nature. The method proposed by Perera et al. (2005) could be used, where soils with a weighted PI of less than 1.0 are categorized as non-plastic soils. The Weighted PI (wPI) is referred to as the product of P200 (percentage passing the Number 200 sieve, expressed as a decimal) and the plasticity index, PI, of the soil (expressed as a percentage). The soils that exhibit wPI greater than or equal to 1.0 are categorized as plastic soils. Where the D_{10} value cannot be determined from the PSD because the soil has a large fines content, then the soil should be analysed as a cohesive soil.
- If the soil is cohesive (plastic), predict the SWRC using the Arya and Paris (1981) model.
- If the soil is granular (non-plastic) then predict the SWRC using all three methods presented here. The MK model should be used first, followed by the AP model then the PM model. If the lower saturation range is of most significance for the proposed analysis, then the PM model should be used as the primary method of SWRC prediction.
- For each method, calculate the lower confidence limit (LCL) at each saturation value using the 95^{th} percentile values for the chosen predictive method using the following

equation

$$LCL = 10^{(\log(\hat{\psi})-(\psi_{e95}-\psi_{e50}))} \tag{3.3.34}$$

where LCL is the lower confidence limit in units of kPa, $\hat{\psi}$ is the predicted suction, ψ_{e50} is the mean or 50^{th} percentile of suction error, and ψ_{e95} is the 95^{th} percentile of suction error.

- Then calculate the upper confidence limit at each saturation value using the 5^{th} percentile values for the chosen predictive method using the following equation

$$UCL = 10^{(\log(\hat{\psi})+(\psi_{e50}-\psi_{e5}))} \tag{3.3.35}$$

where UCL is the upper confidence limit in units of kPa and ψ_{e5} is the 5^{th} percentile suction error.

The calculated confidence limits give a possible range of suction that the real SWRC may lie in based on the analysis of the database. An example of the calculated confidence limits for the PM model are presented in Figure 3.21 for soil code 1467, which is a sand soil.

We can see from Figure 3.21 that the real (measured) SWRC, presented as the black circles, lies within the upper and lower confidence limits over the majority of the suction range i.e. less than 1,000kPa. The measured SWRC lies just outside lower confidence limit above 1000 kPa. This demonstrates that this approach can be used to give guidance on the likely position of the SWRC when analysing soils in engineering practice. To explore further how the findings from this chapter can be used in practice, the procedure will be validated using a number of soils available in the literature, including a North East glacial till soil sample from the BIONICS embankment project (Toll et al., 2016). These results are presented and discussed in detail in Chapter 5.

3.4 Observations

This chapter has documented the development of a procedure to estimate the SWRC of a soil based on standard index properties. These properties can be derived from standard laboratory tests and include porosity/void ratio, particle size distribution, and dry density.

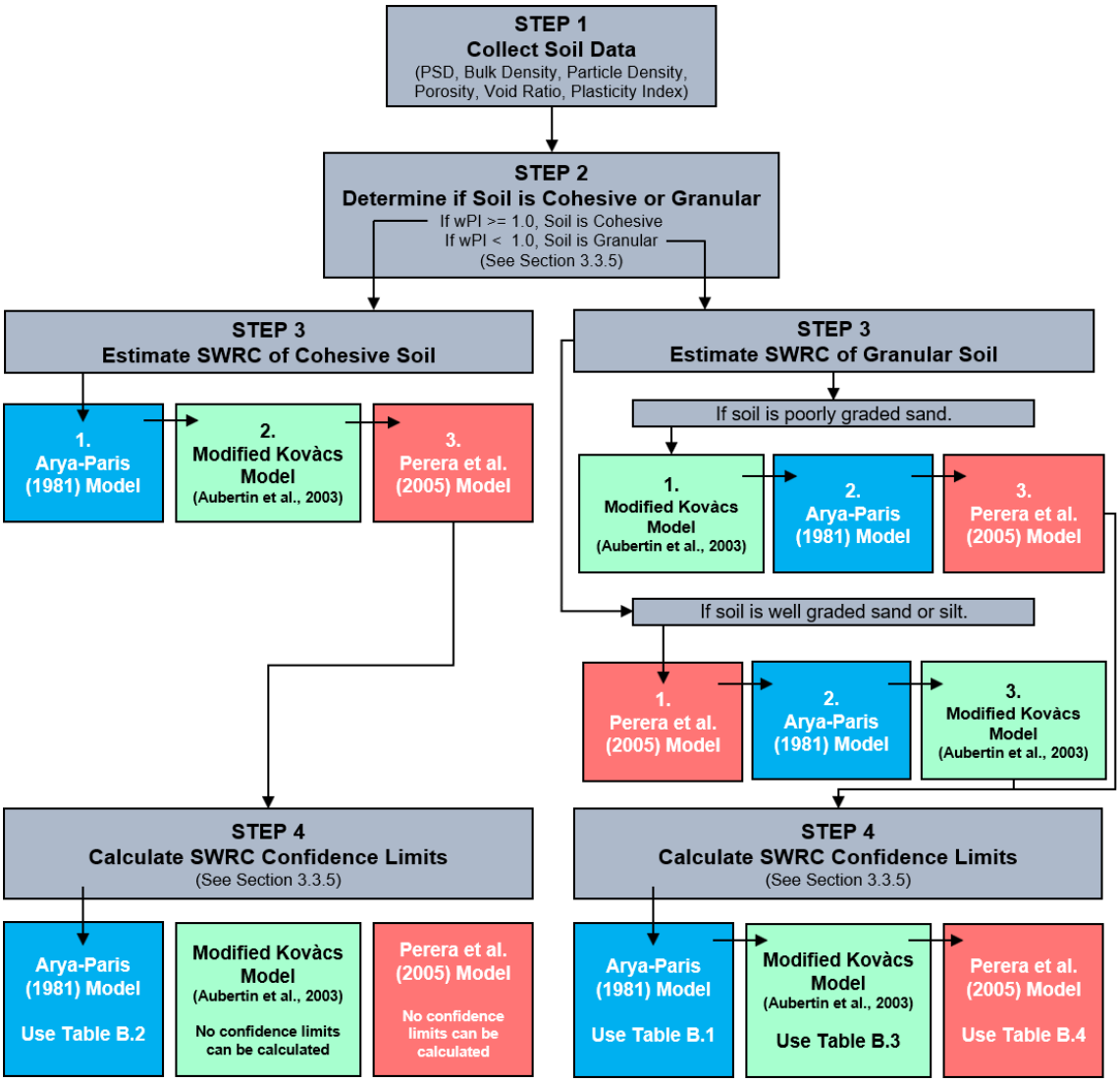

Figure 3.20: Flowchart summarising SWRC Estimation procedure.

As part of the procedure, a dataset of 102 No. soils was selected from the UNSODA database, comprising a selection of granular and cohesive soils. Each soil within the dataset contains index properties along with a laboratory measured drying soil water retention curve (SWRC).

For each soil in the dataset, the best fit curve was found for the SWRC by undertaking a multiple regression analysis using the Fredlund and Xing (1994) equation. Three SWRC predictive methods from literature, the Arya and Paris (1981) model, Modified Kovács (MK) Model (Aubertin et al., 2003) and the Perera Model (PM) (Perera et al., 2005), were programmed into a computer script and used to estimate the SWRC for each soil in the dataset. Due to a lack on Atterberg limit test data within the database, the MK

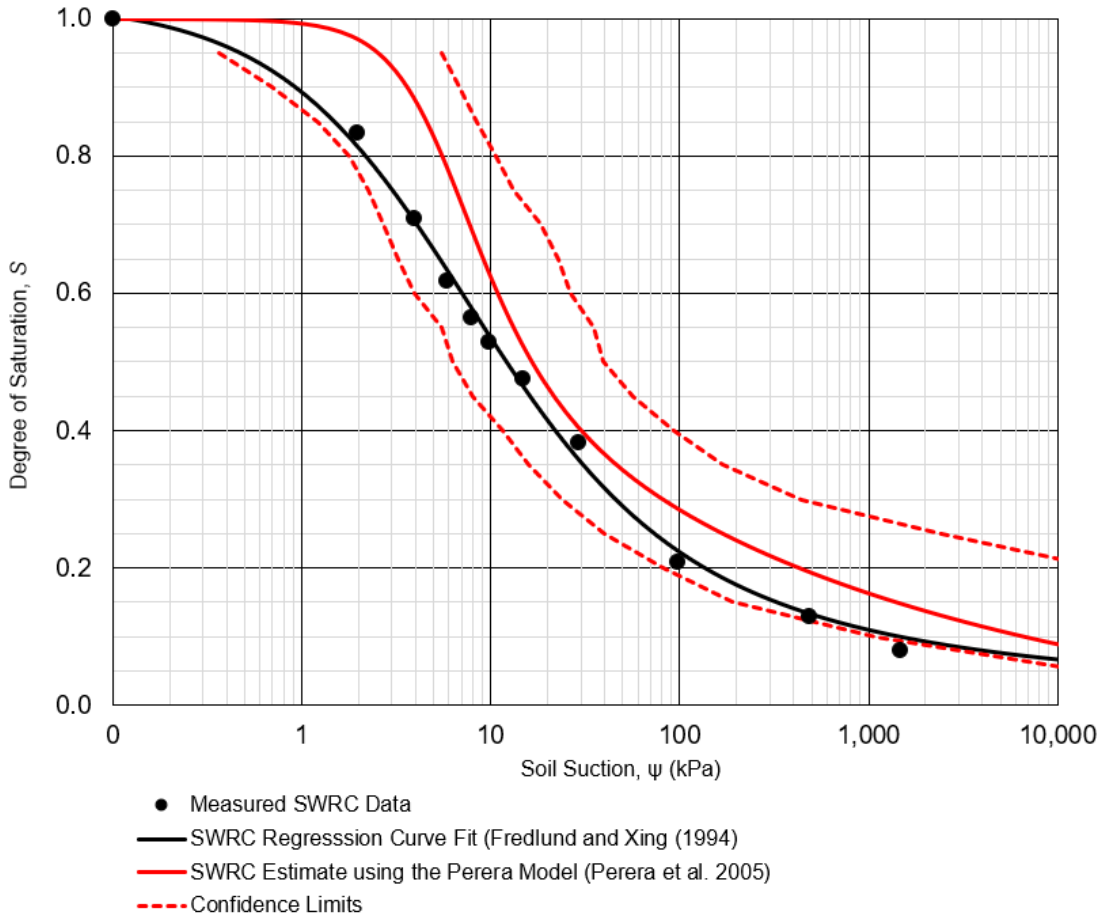

Figure 3.21: Calculated upper and lower confidence limits for the Perera Model for sand soil 1467.

and PM models could not be used to analyse the cohesive soils within the dataset. The programming of the predictive methods was verified by comparing results from the script with results presented in literature.

To assess how well the predictive methods performed, the error in the suction between the predicted and measured SWRC at selected saturation values was calculated. This is then plotted on a graph of suction error vs degree of saturation. At each saturation value, the mean suction error, 5^{th} percentile and 95^{th} percentile were calculated. These metrics provide an indication of the performance of the predictive method at various saturation levels. The results from this analysis can be summarised for the granular soils as:

- The AP, MK and PM models are all good at predicting the SWRC within the saturation range of 0.95 to 0.40.

- The range between the 5^{th} and 95^{th} percentile lines is smallest for the MK model, followed by the AP model and then the PM model, suggesting the MK is the best model for predicting the SWRC in the saturation range 0.4 to 0.95.
- All three predictive model on average overestimate the suction in the upper saturation range between 0.95 to 0.40.
- All three of the predictive models on average underestimate the suction in the lower saturation range between 0.40 and 0.05.
- The shape of the SWRC in the low saturation range is best modelled by the PM model.
- The range between the 5^{th} and 95^{th} percentile lines is closest to zero for the PM model in the low saturation range, followed by the MK model and then the AP model, suggesting the PM is the best model for predicting the SWRC in the low saturation range.
- The models developed using a physical approach (AP and MK) perform poorly in the low saturation range. This suggests the PSD alone does not correlate well to the SWRC at low saturations. Other factors may influence the SWRC in this zone, such as the soil particle arrangement, particle shape, particle roughness or volume change as suction increases.

The findings from the analysis of the cohesive soils are as follows:

- Only the AP model could be used for the prediction of the SWRC for these soils because of a lack of Atterberg limit testing data in the database.
- In general the AP model performs poorly for these soils. Often the predicted SWRC is considerably offset from the measured SWRC along the suction axis.
- On average the AP model underestimates suction in the high saturation range between 0.95 and 0.40.
- The PSD may not correlate well to the SWRC when the soil is fine grained with a large proportion of granular material. The physical approach of the AP model estimates the air-entry value based on the coarse material in the PSD, but does not

take into consideration the arrangement of these particles and how this impacts the pore size distribution. Therefore the AP model can largely over or under-estimate the air-entry value of a cohesive soil, which has the impact of shifting the SWRC horizontally along the suction axis.

- On average the AP model overestimates suction in the low saturation range between 0.40 and 0.05.
- A lack of measured suction points below a saturation of 0.5 means that the best-fit measured SWRC is unlikely to be a true representation of the SWRC in the region of the curve. Therefore no real conclusions can be determined on the ability of the AP model to predict the SWRC in the high suction portion of the SWRC curve.

The 5^{th} and 95^{th} percentiles of suction error for each predictive method can then be converted to confidence limits of suction in kPa when predicting the SWRC of a soil in practice. This procedure was shown for the sand soil 1467 from the dataset, where the Perera Model (Perera et al., 2005) confidence limits were presented on a plot along with the predicted and measured SWRC. It was shown that the real (measured) SWRC was within the confidence limits for the predictive method over the majority of the suction range. See Chapter 5 for the validation of this procedure using a North East glacial till which was not included as part of the analysis presented in this Chapter.

Chapter 4

Validation of SWRC Estimation Procedure

Chapter 3 presented the methodology and analysis that led to the development of a procedure for estimating the SWRC of a soil using standard laboratory soil testing data. It was shown how calculated confidence limits could be used to give a likely range of error in the SWRC prediction. An understanding of the possible error in the predicted SWRC, and the associated strength capacity of the soil is essential if this procedure is to be utilised by geotechnical engineers working on construction projects.

This chapter documents the validation of the procedure by presenting analysis of three soil samples which were not included in the original soil analysis presented in Chapter 3. For the process to be valid and of use by geotechnical engineers in practice, the predicted SWRC should lie within the two calculated confidence limits. The first is a North East Glacial Till soil (Durham Boulder Clay) which has been studied intensively as part of the BIONICS (Biological & Engineering Impacts of Climate Change on Slopes) project between the Universities of Bristol, Dundee, Durham, Loughborough, Nottingham Trent and Newcastle upon Tyne (Toll et al., 2016). The second is a clean sand from the Vashon Advance Outwash Sand formation from Washington State, USA, which was presented in a study by Likos et al. (2010). The procedure outlined in Section 3.3.5 and by the flowchart in Figure 3.20, is used for each soil. The flowchart has been developed to guide the user through the process. Once soil data has been collected, the user must determine if the soil

is Cohesive or Granular. This can be done by assessing the weighted Plasticity of the soil, as shown previously in Section 3.3.5. Once this is know the user can estimate the SWRC of the soil using the three models. The flow chart can be used to give preference to the order at which the user should review the models, as it was shown using the statistical analysis that some soils perform better for certain soil types. Thirdly the flow chart shows that the SWRC confidence limits should be calculated last and used to assess the error in the SWRC prediction.

This chapter is concluded by summarising some of the limitations of the procedure along with some recommendations for future use by geotechnical engineers.

4.1 Durham Lower Boulder Clay

4.1.1 Step 1 - Collect Soil Data

The first soil sample considered is a North East Glacial Till from the BIONICS embankment. The BIONICS embankment was built at Nafferton farm in North East England (Hughes et al., 2009) for the purpose of understanding the impact of climate change and changing weather patterns on UK transport infrastructure. The glacial till is from the Durham Lower Boulder Clay, a common fill material representative of earthworks construction in the UK (Toll et al., 2012).

The material comprises 39% sand, 34% silt and 27% clay, which means that it is classified as a clay loam soil under the USDA soil classification system and a sandy clay under the USCS classification system. The properties of this soil are presented in Table 4.1.

The particle size distribution for the soil is presented in Figure 4.1. A best-fit curve has been found for the raw PSD data by applying a non-linear regression analysis using the methodology presented in Chapter 3 Section 3.2.1. The parameters for the best-fit curve using the Fredlund et al. (2000) equation are also presented in Figure 4.1. A minimum particle size of 0.0001mm has been specified in the PSD equation as this ensures that the predicted SWRC using the Arya and Paris (1981) model tends towards a saturation of 0 at a maximum suction of 1 x 10^6 kPa. Note that selection of this parameter impacts the

Soil Property	Value	Unit
% Clay	27	%
% Silt	34	%
% Sand	39	%
Liquid Limit, LL	42	%
Plastic Limit, PL	20	%
Plasticity Index, PI	22	%
Dry Density, ρ_d	1.59	g/cm^3
Specific Gravity, G_s	2.66	g/cm^3
Saturated Volumetric Water Content, θ_s	0.401	-
Voids Ratio, e	0.669	-

Table 4.1: Soil Properties for the Durham Lower Boulder Clay.

position of the SWRC in the high suction range of the SWRC, however this has limited impact to the SWRC in the low suction range, which is of most interest for the application of this work in practice.

4.1.2 Step 2 - Determine if the soil is Cohesive or Granular

The soil must be classified as either cohesive or granular in order to determine the method of SWRC prediction and to calculate the correct confidence limits. This can be determined mathematically using the method proposed by Perera et al. (2005), which classifies the soil as cohesive if the weighted plasticity index (wPI) of the soil is greater than 1.0. This is calculated by multiplying the percentage passing the number 200 sieve, $P200$ (mesh size of 0.075mm), by the plasticity index, PI of the soil. For the Durham Lower Boulder Clay, $P200$ is 0.657 and the plasticity index, PI is 22.2%, therefore the wPI is calculated as 14.59, which indicates the soil is cohesive (plastic). Following the procedure outlined in Figure 3.20, we have determined that the soil is classified as cohesive, therefore the SWRC can be estimated using the Arya and Paris (1981) model and the confidence limits for cohesive soils can be used. As the plasticity index is available for this soil, the SWRC will also be estimated using both the Modified Kovács model (Aubertin et al., 2003) and the Perera et al. (2005) model, however no confidence limits can be calculated for these

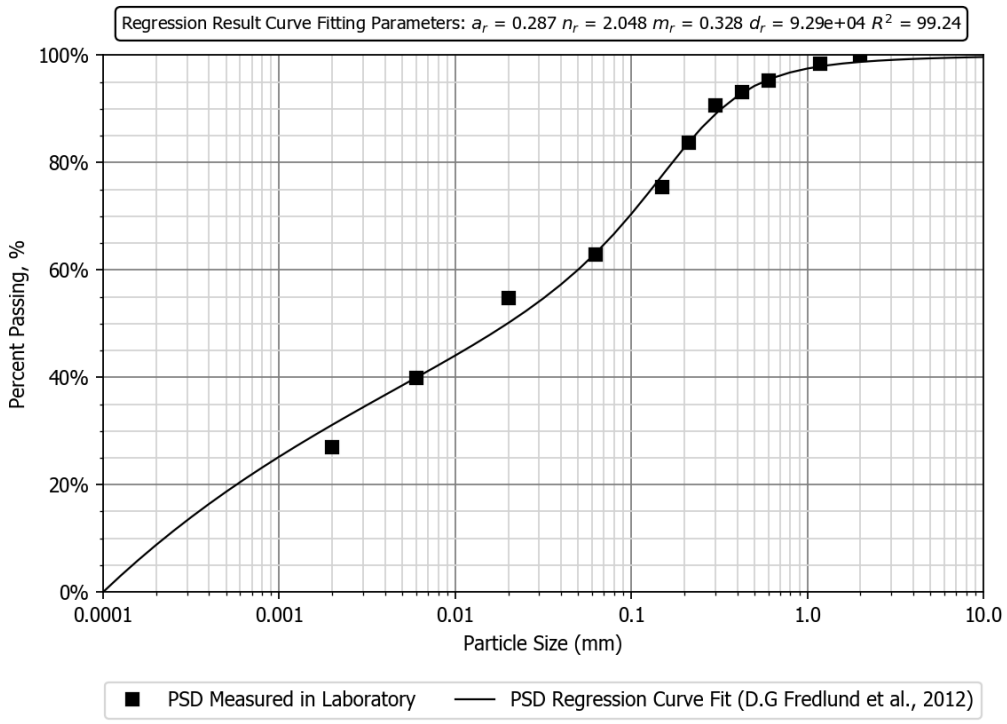

Figure 4.1: Particle size distribution for Durham Lower Boulder Clay (black points) with best-fit curve (black line).

SWRCs.

4.1.3 Step 3 - Estimate the SWRC

A SWRC is now estimated using the AP model, followed by the PM model and the MK model. For these models the PSD, void ratio, and dry density are required which are provided in Table 4.1. For the PM and MK models the Plasticity Index of the soil is also required. The predicted SWRC using each model, along with the measured SWRC, is plotted in Figure 4.2 as suction, ψ versus degree of saturation, S. The measured SWRC was determined using the Durham University high-capacity tensiometer in the low suction range (less than 700 kPa) and a WP4C Dewpoint Potentiameter over the high suction range (greater than 700 kPa) (Toll et al., 2016).

It can be seen from Figure 4.2 (a) that there is a significant offset between the predicted SWRC using the AP model and the measured SWRC, particularly in the degree of saturation range between 0.6 and 1.0. The large under prediction is similar to the

frequent under prediction of the Arya and Paris (1981) model observed during the data analysis of the cohesive soils in Chapter 3 Section 3.3.2, in particular the clay loam and sandy clay soils. Figure 4.2 (b) shows the predicted SWRC using the PM model. This SWRC prediction is a good fit to the measured data, especially within the high degree of saturation range between 0.8 and 1.0 and provides a significant improvement over the AP model. It also follows the shape of the measured SWRC closely. Figure 4.2 (c) shows the the predicted SWRC using the MK model, which provides a reasonable prediction of the SWRC. Of importance is the location of the air-entry value which is in the region of the measured SWRC air-entry value. However the shape of the SWRC causes the predicted SWRC to under predict suction at a given saturation value. The following stage shows how the confidence limits are calculated for the SWRC prediction based on the previous statistical analysis of the cohesive soils.

4.1.4 Step 4 - Calculate Confidence Limits

The final stage is to calculate the upper and lower confidence limits of suction for the predicted SWRC using the AP model. The confidence limits are based on the mean, 5^{th} and 95^{th} percentiles of suction error calculated during the analysis of the cohesive soils from the dataset (See Figure 3.16 and Table B.2). Based on the analysis of the cohesive soils, there is a 95% likelihood that the measured SWRC will lie within the confidence limits. The lower confidence limit (LCL) is given by the equation

$$LCL = 10^{(\log(\hat{\psi})-(\psi_{e_{95}}-\psi_{e_{50}}))} \tag{4.1.1}$$

and the upper confidence limit (UCL) is given by

$$UCL = 10^{(\log(\hat{\psi})+(\psi_{e_{50}}-\psi_{e_5}))} \tag{4.1.2}$$

where the lower and upper confidence limits are given in units of kPa, $\hat{\psi}$ is the predicted suction, $\psi_{e_{95}}$ is the 95^{th} percentile of suction error, $\psi_{e_{50}}$ is the mean or 50^{th} percentile of suction error and ψ_{e_5} is the 5^{th} percentile of suction error.

The calculated confidence limits for the AP model predicted SWRC are shown in Figure 4.2 (a) as the dashed blue lines. Despite the large offset between the predicted and measured suction, particularly in the high saturation range, the measured suction

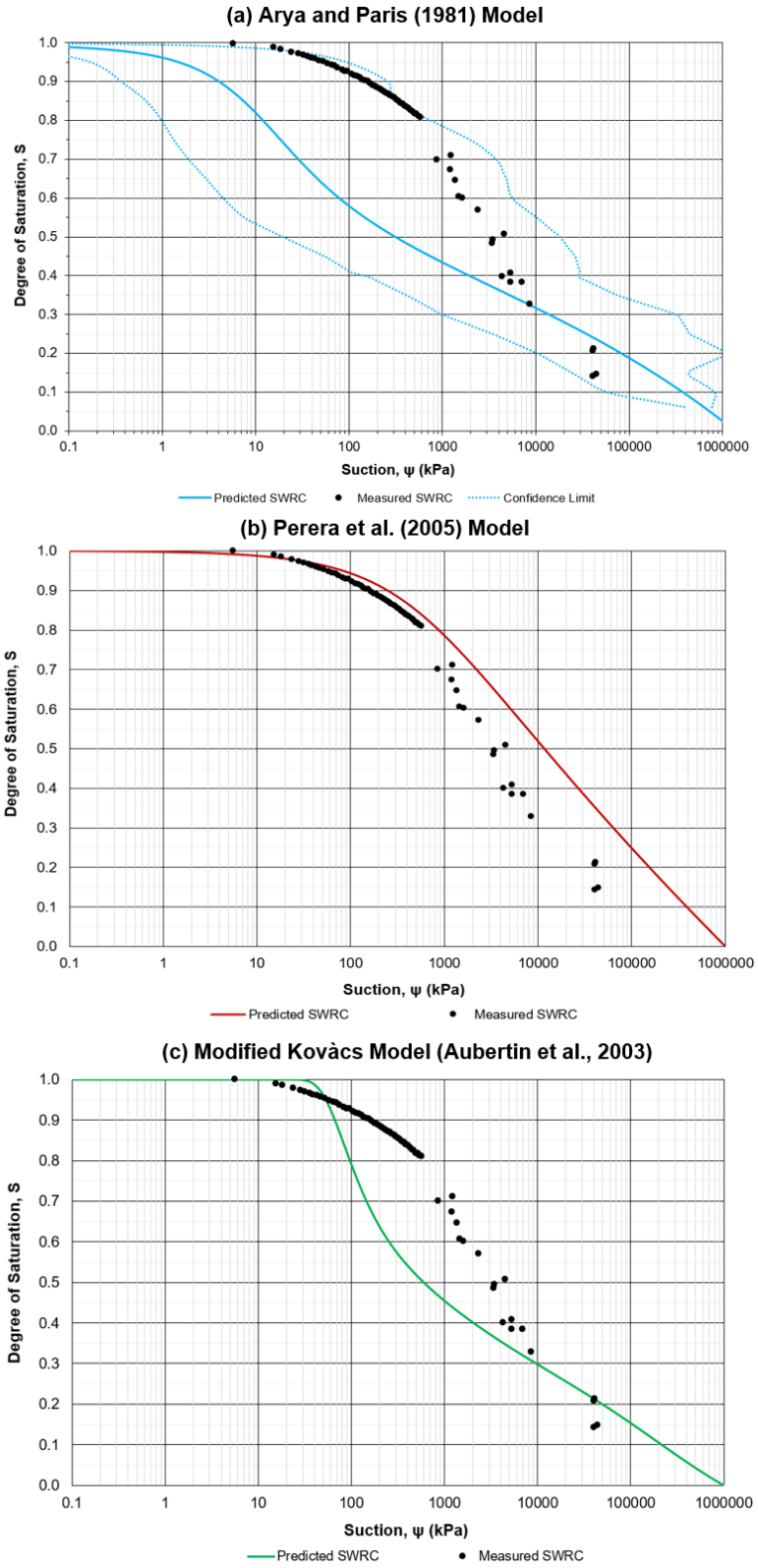

Figure 4.2: Measured SWRC (black circles) and predicted SWRC using (a) the AP model,(b) the PM model and (c) the MK model for the Durham Lower Boulder Clay. Calculated confidence limits for the AP model are shown as the blue dashed lines.

lies within the confidence limits. Between the degree of saturation values of 0.8 and 1.0, the measured suction lies just inside the upper confidence limit. As the saturation decreases, the confidence limits tighten towards the predicted curve, whilst the predicted curve converges towards the measured SWRC. This shows that predicted SWRC for the Durham Lower Boulder Clay has similar characteristics to the predicted SWRCs of the cohesive soils from the dataset, as the confidence limits are wide enough to accommodate the large error in the predicted SWRC by the Arya and Paris (1981). This shows that despite the poor performance of the Arya and Paris (1981) model at predicting the SWRC for this type of soil, the use of confidence limits can give a geotechnical engineer an idea of the likley range of suction that the SWRC of the soil may lie within. For the other SWRC predictive methods, confidence limits could not be calculated. However, if all three methods are used together, then they can be used to assess whether the SWRC is likely to lie within the AP model confidence limits. This shows how the confidence limits can be used for the SWRC estimation procedure for cohesive soils such as clay loams and sandy clay type soils. The following section will show how this procedure can be followed for sand soils, using the Vashon Advance Outwash Sand as an example.

4.2 Vashon Advance Outwash Sand

4.2.1 Step 1 - Collect Soil Data

The second soil sample is a clean sand soil from the Vashon Advance Outwash Sand formation collected from a coastal location near Edmonds, Washington State, USA (Likos et al., 2010). The U.S. Geological Survey collected these soil samples as a part of study on the hydrological response to rainfall in these soils.

The material is a clean sand which comprises 99% sand, 1% silt and 0% clay, which means that it classified within the sand textural class under the USDA soil classification system. The properties of this sand soil are presented in Table 4.2.

The particle size distribution for the sand is presented in Figure 4.3. A best-fit curve has been found for the raw PSD data by applying a non-linear regression analysis as shown in the previous example. The parameters for the best-fit curve using the Fredlund et al.

Soil Property	Value	Unit
% Clay	0	%
% Silt	1	%
% Sand	99	%
Dry Density, ρ_d	1.59	g/cm^3
Specific Gravity, G_s	2.65	g/cm^3
Saturated Volumetric Water Content, θ_s	0.40	-
Void Ratio, e	0.667	-

Table 4.2: Soil Properties for the Vashon Advance Outwash Sand (Likos et al., 2010).

(2000) equation are also presented in Figure 4.3. The curve is a good fit over the full range of particle sizes.

4.2.2 Step 2 - Determine if the soil is Cohesive or Granular

The soil must be classified as either cohesive or granular in order to determine the correct method of SWRC prediction. As this soil is a clean sand, there is no question that this a granular material. In the case where there is a larger proportion of fines within the sand, the method proposed by Perera et al. (2005) could be used if the plasticity index, PI is available for the soil. Following the procedure outlined in Figure 3.20, because the soil is granular, the SWRC can be predicted using the three models presented in this Thesis, the Arya and Paris (1981) model (AP), the Modified Kovács model (Aubertin et al., 2003) (MK) and the Perera et al. (2005) model (PM).

4.2.3 Step 3 - Estimate the SWRC

The SWRC can now be estimated using all three SWRC predictive methods. As outlined in Figure 3.20, as the soil is a poorly graded sand, the MK model should be considered first, followed by the AP model and the PM model. The predicted SWRC can then be compared to the measured SWRC for this soil, which was determined using a hanging water column apparatus which measures the outflow of water to determine water content (Likos et al., 2010).

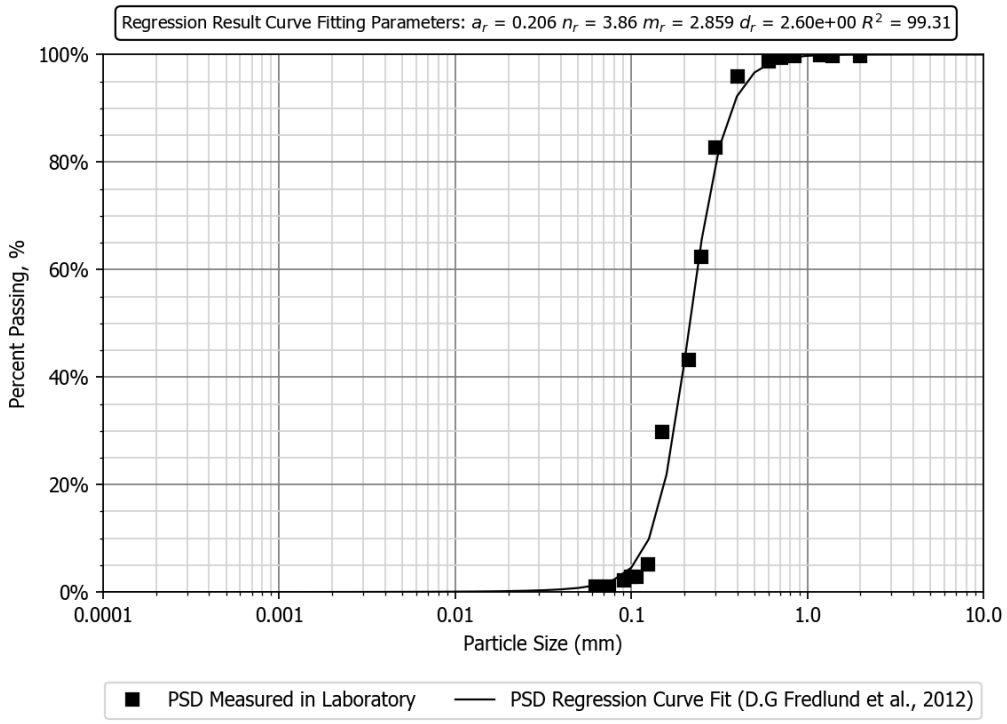

Figure 4.3: Particle size distribution for Vashon Advance Outwash Sand (black points) with best-fit curve (black line). Derived from (Likos et al., 2010).

The predicted SWRC using the MK model, AP model, and the PM model, along with the measured SWRC, is plotted in Figure 4.4 (a), (b) and (c) respectively. It can be seen from Figure 4.4 that all three methods predict a SWRC which is in close agreement to the measured SWRC. Both the MK and PM models give very good predictions, where the gradient of the curve and the offset of the curve on the suction axis are close to the measured. The AP model is slightly offset to the right on the suction axis, meaning it over estimates the suction at a given degree of saturation value. The next stage shows how the confidence limits can now be calculated for each SWRC prediction based on the previous statistical analysis of the dataset of soils.

4.2.4 Step 4 - Calculate Confidence Limits

The final stage is to calculate the upper and lower confidence limits of suction for each predicted SWRC. The confidence limits are based on the mean, 5^{th} and 95^{th} percentiles of suction error calculated during the analysis of the granular soils from the dataset (See Figures 3.15, 3.17 and 3.18 and Tables B.1, B.3 and B.4).

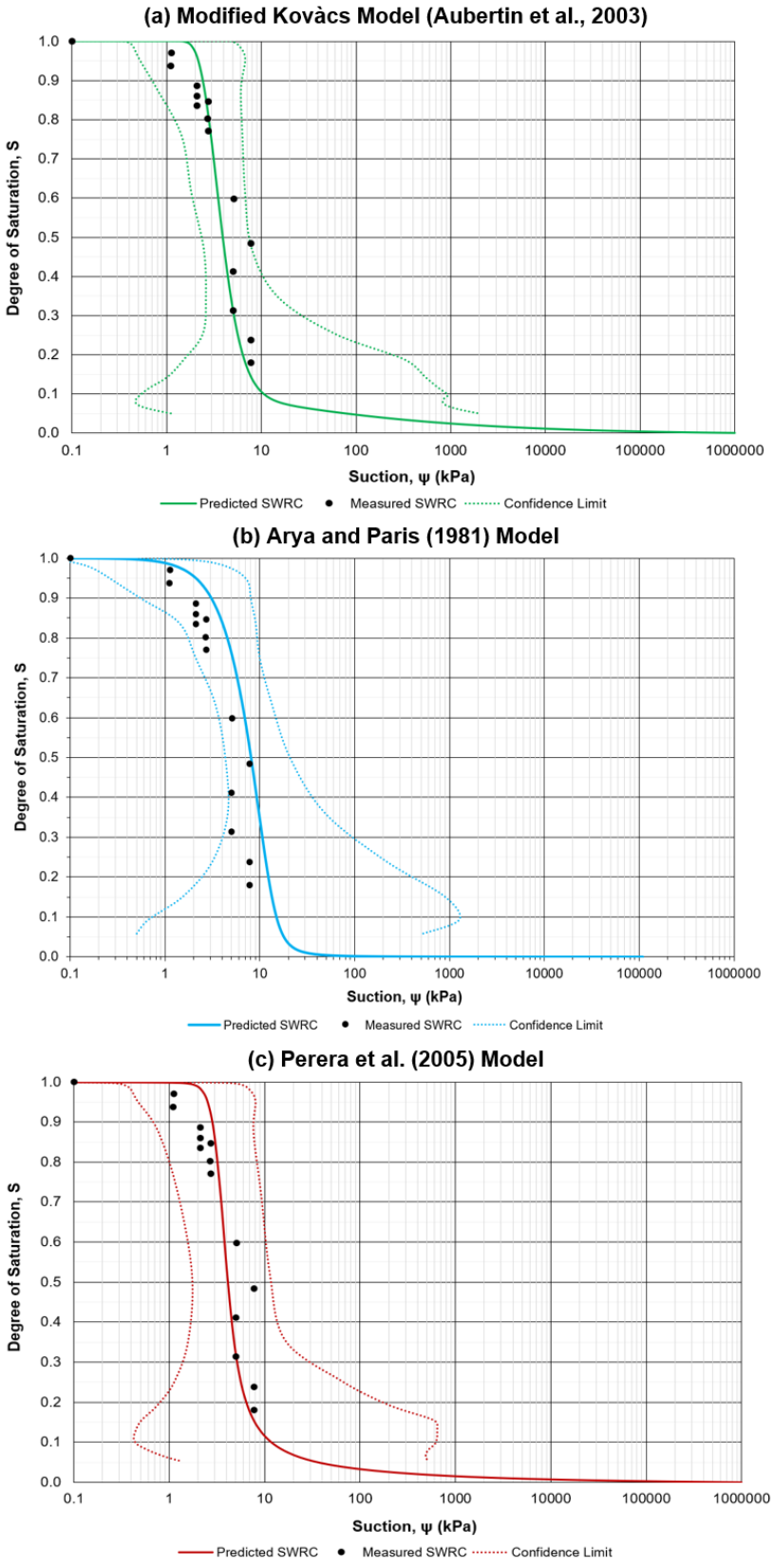

Figure 4.4: Predicted SWRC for the Vashon Advance Outwash Sand using (a) MK Model, (b) AP Model and (c) PM Model. For each case the measured SWRC, derived from Likos et al. (2010) is plotted using black circles. **May 5, 2021**

The calculated confidence limits for the Vashon Advance Outwash Sand are shown in Figure 4.4 (a), (b) and (c) respectively as the dashed lines. For each method, the measured SWRC lies within the confidence limits. This shows that the confidence limits, derived from the analysis of the granular soils (predominantly clean sands) of the UNSODA dataset, can be used to give confidence to the likely range of the true SWRC when predicting the SWRC using the methods shown here. It should be noted however that as the fines content of the sand soil increases i.e. if the sand is well graded, rather than poorly graded as presented here, the confidence limits may become less reliable. This is because the confidence limits were developed from analysis of mostly poorly graded sands from the UNSODA database. In the case of well graded sands, the gradient of the curve shallows towards residual conditions at higher values of saturation and over a larger suction range i.e. it follows a curve more closely resembling the shape of the upper confidence limit (Figure 4.4). Therefore if the confidence limits are being used for well graded sands, more weight should be given to the upper confidence limit side of the predicted curve. Secondly, of the three methods presented here, the Perera et al. (2005) model typically gives the best prediction in the low saturation range suggesting that this method should be preferred method for predicting the SWRC of well graded sands.

This section has shown how the confidence limits can be used to give the likely range of the true SWRC when using a predictive SWRC method. The next section will discuss some of the limitations of this method, and provide some recommendations for use in practice by a geotechnical engineer.

4.3 Limitations and Recommendations for Future Use

This section aims to outline some of the limitations of using the calculated confidence limits in practice, and provides some recommendations for geotechnical engineers when applying this method.

- When predicting the SWRC of sandy clay and clay loam soils with a large fraction of sand particles, the AP model typically under predicts the suction at high saturations. Based on engineering judgement, if the engineer considers this to be likely, then preference for the true SWRC can be given towards the upper confidence limit of

the predicted SWRC.

- When predicting the SWRC of cohesive soils, if the plasticity index for the soil is available, then the SWRC can be predicted using the MK model and the PM model. However, the calculated confidence limits from the AP model must not be used for these models, therefore care must be taken as there will be no indication of the likely error in the SWRC prediction. However, if both the MK and PM models are in good agreement, this can be used to give preference as to whether the AP model has under or over predicted the SWRC compared to the true SWRC.

- The confidence limits for granular soils were developed using soil samples of mostly poorly graded clean sands from the UNSODA database. Therefore, if the granular material contains a reasonable proportion of fines, the confidence limits may be unreliable. In this case care should be taken when using the confidence limits. The PM model typically models granular materials with high fines content with the closest fit, therefore this model should be given preference when predicting the SWRC of well graded sands.

- Only two silt soils were studied as part of the dataset analysis, therefore the granular confidence limits are unlikely to be reliable for silt soils and should not be used. Care should be taken if predicting the SWRC of a silts as the SWRC predictive methods can be unreliable for these types of soil. If the silt soil has a large proportion of fines, the soil may be classified as cohesive, in which case the cohesive confidence limits may be used.

- There are limitless possible SWRCs for a soil depending on the conditions that are placed upon the soil. For example the SWRC of a soil in-situ will be different to the SWRC determined in the laboratory. This is because there will be an overburden stress acting upon the soil depending on the weight of the soil above it. Increasing the overburden stress has the impact of reducing the porosity and void ratio of the soil, and increasing the density of the soil, which directly impacts the SWRC. Typically as the density increases, the SWRC shifts horizontally to the right on the suction axis. Therefore if predicting the SWRC of a soil in-situ, the density and void ratio of the soil should be measured from undisturbed samples at the depth of interest if possible.

- The SWRC predictive methods and associated confidence limits are based on drying conditions. Under wetting conditions, the SWRC will be offset to the left of the drying curve. The methods outlined here should not primarily be used to estimate the wetting SWRC however the user could use the lower confidence limit of the SWRC as guidance to the possible wetting SWRC.

- The AP model requires the selection of a value for the fitting parameter, α, which has the effect of shifting the SWRC horizontally along the suction axis. The confidence limits for the AP model were developed using the alpha value of 1.3, as this was the value suggested by Arya and Paris (1981). However this value can be adjusted depending on the soil being analysed if the geotechnical engineer takes the judgement that the predicted SWRC is likely to be largely offset from the true SWRC. This may be the case if the predicted SWRC using the AP model is considerably offset from both the MK model and the PM model. The alpha values for different soil types proposed by Arya and Paris (1981) are shown in Table 3.6 of Chapter 3.

This chapter has shown how the confidence limits calculated in Chapter 3 can be applied in practice by geotechnical engineers. The procedure has been validated by predicting the SWRC of a Durham Lower Boulder Clay and a sand sample from Vashon Advance Outwash Sand formation. In both cases the measured SWRC was within the confidence limits of the predicted SWRC. The next chapter will present a methodology for estimating the change in shear strength above the water table based on the predicted SWRC. The confidence limits presented here will be used to show the possible error in the shear strength due to the possible error in the predicted SWRC.

Chapter 5

Application of Unsaturated Shear Strength in Practice using Predicted SWRCs

The previous Chapter presented the validation of the SWRC estimation procedure using two soil samples available within the literature. The aim of this Chapter is to present a broad methodology for estimating the increase in shear strength of a soil due to an increase in soil suction as a consequence of lowering the groundwater table. To illustrate how these techniques can be applied in practice, a typical slope stability problem common within the construction industry has been set up and the Durham Lower Boulder Clay soil is used as an example. A predicted SWRC using each of the three predictive methods adopted in this Thesis will be used to estimate an unsaturated shear strength profile due to suction above the water table. The slope stability problem will then be simulated using the finite element software PLAXIS 2D (Bentley Systems, 2020) to determine the factor of safety for each profile. The variability in the calculated factor of safety will give an indication of the influence suction has on the stability of the slope.

5.1 Problem Definition

A typical geotechnical engineering problem will be used in this Chapter to illustrate how the shear strength of a soil may change due to a groundwater control operation. The problem of interest involves the construction of an 8.0m deep excavation surrounded by temporary battered slopes constructed at an angle of 45 degrees. A groundwater control system has been designed to lower the water table in the soil to enable construction of the 8.0m high batters. The water table must be reduced to the excavation level of 8.0m bgl (below ground level) from an initial water level of 1.0m bgl. Groundwater control wells will be located at the top of the batters at a distance of 1.0m from the crest. It has been assumed that the water table has first been lowered to excavation level using the external groundwater control wells before any excavation of the ground takes place. As excavation proceeds, any remaining water would drain out of the slope into the excavation and be pumped away using sump pumps. Figure 5.1 presents a schematic of the problem.

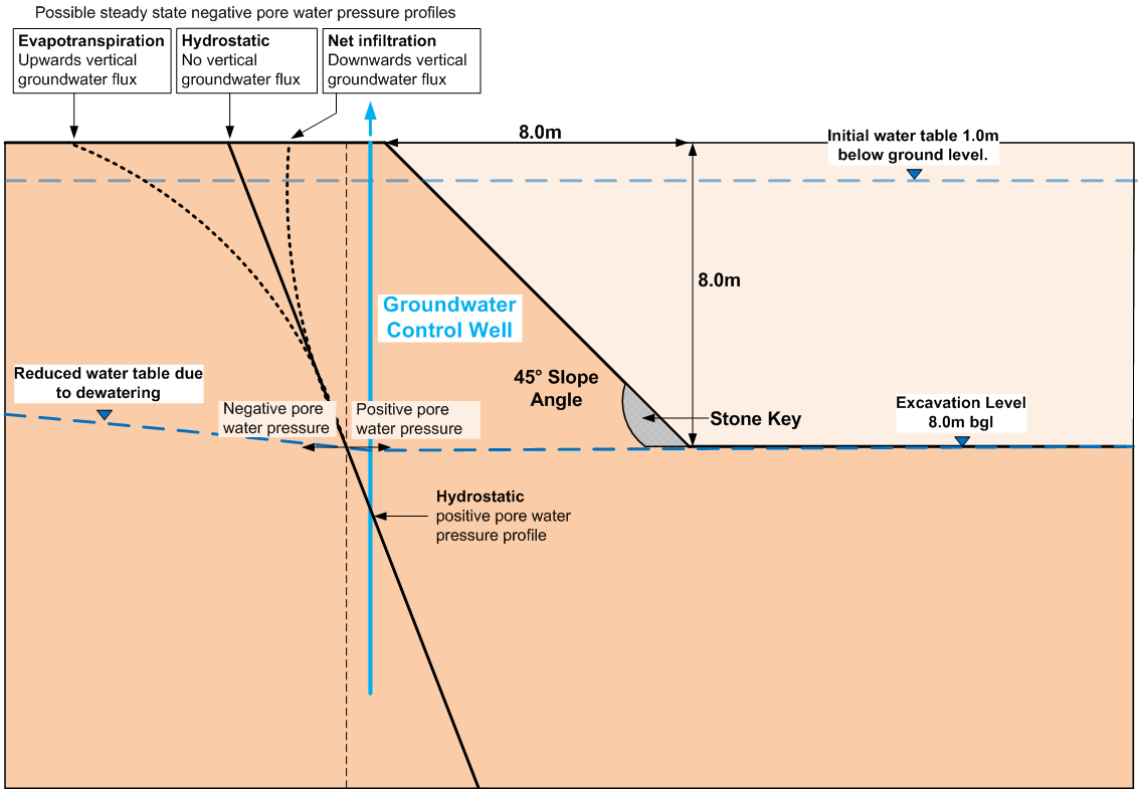

Figure 5.1: Conceptual model showing geometry of excavation with temporary battered slopes overlain with possible steady-state pore water pressure profiles after dewatering.

As the water table is lowered, a negative pore water pressure (suction) profile will

develop within the unsaturated zone above the water table. Once groundwater conditions have reached steady state and the water table has reached excavation level, a suction profile will exist in the unsaturated zone. This profile will follow the gradient of the hydrostatic pore water pressure profile if there is no net vertical flux of groundwater within the unsaturated zone i.e. infiltration (the process by which water on the ground surface enters the soil) and evapotranspiration (the process by which water is transferred from the land to the atmosphere by evaporation from the soil and by transpiration from plants) are in equilibrium, and assuming that pore water is continuous above the water table. If there is a net infiltration at steady state, the suction profile will be less than hydrostatic i.e. suction will be closer to zero in the unsaturated zone. If there is a net evapotranspiration at steady state, the suction profile will be greater than hydrostatic (shown by the dashed black lines in Figure 5.1).

The exact negative pore water pressure profile is difficult to calculate without undertaking field monitoring. This is because the profile is dependant on a number of variables including; precipitation, evaporation, transpiration, surface runoff, infiltration, the soil water retention curve of the soil, and the unsaturated hydraulic conductivity function of the soil. Due to these uncertainties, when applying unsaturated soil mechanics in practice it is recommended that a number of field tensiometers are installed within the ground at defined elevations to measure suction. The suction measurements can then be used to either estimate the steady state pore water pressure profile, or they can be used to calibrate a finite element model which can be used to generate the pore water pressure profile. If the installation of field tensiometers is not feasible, then several generalised pore pressure profiles should be used to assess the variability in the potential unsaturated shear strength profile of the soil. For example, if the site is located in a humid climate setting like in the UK, then there is likely to be net infiltration. In this case the hydrostatic suction profile above the water table could be multiplied by 0.5, as was demonstrated in the case study by Ng (1988) for a slope in Hong Kong. If the site is located in an arid climate setting, then there is likely to be net evapotranspiration. In this case the hydrostatic suction profile above the water table may be multiplied by 2.0. The United Kingdom typically has a humid climate with a lot of precipitation, therefore temporary battered slopes used during construction are typically covered with an impermeable material to prevent infiltration and surface erosion. This method of slope protection was demonstrated

by Thomas et al. (2020) during the stabilisation of steep temporary batters required for the construction of a storm water water tank in Oldham, Greater Manchester. Given the complexities in determining the suction profile above water table, for the purpose of the remaining research and analysis, the suction profile will be taken as hydrostatic. The following section will demonstrate how the unsaturated shear strength of the soil can be calculated using a hydrostatic suction profile, however this technique can be used regardless of how the suction profile above the water is determined or calculated.

5.2 Calculation of Unsaturated Shear Strength

The unsaturated shear strength of the soil can be estimated using a modified version of the Extended Mohr-Coulomb equation originally proposed by Fredlund et al. (1978). The model has been adopted here because it offers the simplest approach of integrating unsaturated soil mechanics into geotechnical engineering practice. Numerous equations have been proposed within the literature for estimating the unsaturated shear strength of the soil using the SWRC, as discussed in depth in the Literature Review (see Chapter 2, Section 2.3.3). The literature review also presented some comparisons between the estimated shear strength and the measured shear strength determined from mechanical shear strength testing. It was found that the modified Extended Mohr-Coulomb equations by Vanapalli et al. (1996) and Fredlund et al. (1996) provided the most reliable shear strength predictions, particularly in the low suction range ($\leq$1,000kPa). Therefore, both of these equations will be used as part of this study to estimate the unsaturated shear strength profile of the soil for the example problem outlined above.

Fredlund et al. (1996) proposed the non-linear form of the Extended Mohr-Coulomb failure criteria

$$\tau = c' + (\sigma - u_a)\tan\phi' + (u_a - u_w)S^{\kappa}\tan\phi'. \tag{5.2.1}$$

This equation can be split into two components, the first of which, $c' + (\sigma - u_a)\tan\phi'$, describes that saturated shear strength of the soil in terms of net total stress. The second component describes the additional shear strength due to suction and requires the use of a fitting parameter κ and the SWRC in terms of degree of saturation, S. Garven and Vanapalli (2006) provided an empirical relationship between the fitting parameter κ and

the Plasticity Index, PI, of the soil

$$\kappa = -0.0016(PI)^2 + 0.0975(PI) + 1 \tag{5.2.2}$$

however this equation is only applicable for soils with Plasticity Index great than 0, which is typically cohesive soils such as sandy clays.

Vanapalli et al. (1996) proposed an equation where the SWRC is normalised between saturated and residual saturation conditions

$$\tau = c' + (\sigma - u_a)\tan\phi' + (u_a - u_w)\Big(\frac{S - S_r}{1 - S_r}\Big)\tan\phi' \tag{5.2.3}$$

where S_r is the residual degree of saturation. In order to use the Vanapalli et al. (1996) equation, a value for the residual degree of saturation must be determined. Vanapalli et al. (1998) presents a computational procedure for determining the residual water content from the SWRC. This involves drawing tangents along sections of the curve and using the intercept points to calculate the residual degree of saturation. The following section presents calculations of additional shear strength due to suction using a suction profile behind the crest of the slope for the example problem outlined above, assuming the slope is constructed from Durham Lower Boulder Clay.

5.3 Calculation of Suction and Shear Strength Profiles

A vertical section is taken half a metre behind the crest of the slope. The pore water pressure profile is calculated using a weight density of water of 10.0 kN/m^3. The net total stress profile is calculated using the weight density of soil, which is be a function of soil saturation, and can be calculated using the dry density of the soil, ρ_d, weight density of water, γ_w, the particle density of the soil, G_s, the void ratio, e and the degree of saturation, S (using the predicted SWRC using the AP model) (See Table 5.1). The calculated net total stress profile is shown in Figure 5.2. Note that compression is presented as positive values of stress.

The assumed saturated shear strength properties of Durham Lower Boulder Clay are given in Table 5.1. These shear strength properties are derived from mechanical shear strength testing of the soil using a triaxial cell apparatus at the Durham University

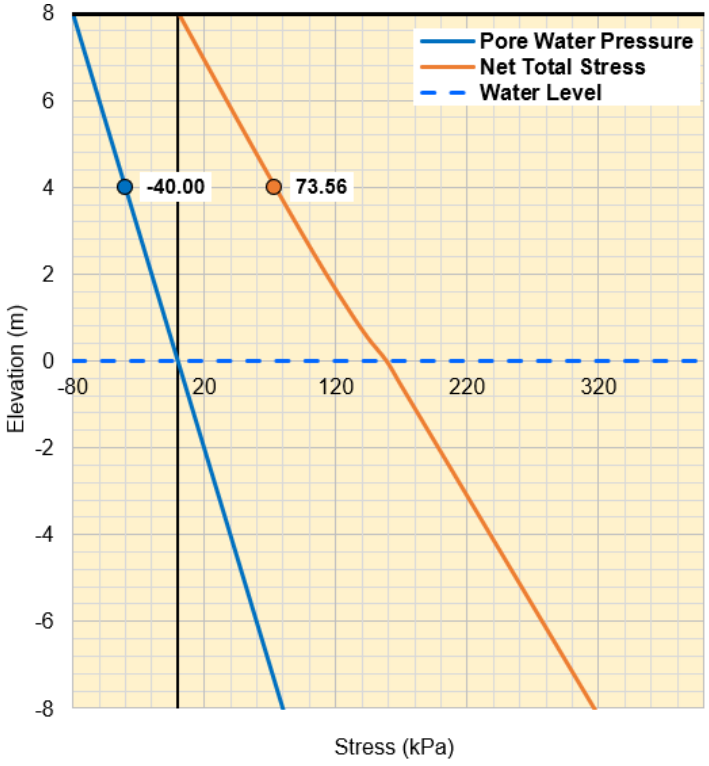

Figure 5.2: Pore water pressure profile and net total stress profile for vertical section taken behind the crest of the slope using properties given in Table 5.1.

Soil Property	Symbol	Value	Unit
Dry Density	ρ_d	1.59	g/cm^3
Particle Density	G_s	2.66	g/cm^3
Void Ratio	e	0.70	-
Effective Cohesion	c'	10.0	kPa
Angle of Internal Friction	ϕ'	25.5	$^\circ$

Table 5.1: Soil properties for the Durham Lower Boulder Clay. The shear strength properties have been derived from triaxial testing of the soil by Mendes and Toll (2016).

Laboratory (Mendes and Toll, 2016). The saturated shear strength component is first calculated using the net total stress $(\sigma - u_a)$, effective cohesion, c' and the angle of internal friction, ϕ'. The saturated shear shear strength component increases from 10 kPa at the crest of the slope surface to 85 kPa at the excavation level.

The increase in shear strength due to suction can be estimated using the equations by Fredlund et al. (1996) (Eq. 5.2.1) or Vanapalli et al. (1996) (Eq. 5.2.3). Both equations

require a SWRC to calculate the shear strength. The results presented here show the calculated additional shear strength for both equations using each of the predicted SWRCs using the Arya and Paris (1981) Model (AP), the Modified Kovaćs Model (MK) (Aubertin et al., 2003) and the Perera et al. (2005) (PM) model respectively, along with the measured SWRC (M) for comparison. In addition the confidence limits for the AP model, i.e. AP (UCL) and AP (LCL), are used to assess the sensitivity of the error in the SWRC to the shear strength estimation. Because confidence limits could not be calculated for the MK and PM model SWRCs, the estimated additional shear strength using these models are used to assess whether the prediction of the AP model is reasonable.

The Fredlund et al. (1996) equation (Eq. 5.2.1) requires that the fitting parameter κ is first calculated using the Plasticity Index, PI of the soil (Equation 5.2.2), which is calculated to be 1.0214 for a PI of 22%. The Vanapalli et al. (1996) equation (Eq. 5.2.3) requires the SWRC to be normalised between saturated and residual water content conditions meaning the residual degree of saturation, S_r must be specified. Vanapalli et al. (1998) presents a method for determining this value, however this procedure can be difficult for soils with a high proportion of fines, which could lead to significant errors. For each SWRC predictive method, the residual degree of saturation has been calculated as 0.42, 0.45 and 0.5 for the AP, MK and PM models respectively.

Figure 5.3 (a) shows the calculated increase in shear strength profile above the water table using the Fredlund et al. (1996) equation (Eq. 5.2.1). The blue solid line is calculated using the AP model predicted SWRC, the green solid line by the MK model predicted SWRC and the red solid line by the PM model predicted SWRC. The purple line is calculated using the measured SWRC. Using the AP model predicted SWRC, the additional shear strength due to suction increases from 0 kPa at the water table to approximately 22 kPa at the ground surface. At the midway point at an elevation of 4.0m, highlighted by the annotated points in Figure 5.3, the calculated additional shear strength due to suction is 12.57 kPa. The additional shear strength due to suction can also be calculated using the lower and upper confidence limits of the AP model predicted SWRC. These are shown by the dashed light blue lines Figure 5.3 (a). At an elevation of 4.0m, the calculated additional shear strength due to suction ranges from 8.74 kPa to 18.53 kPa, a difference of 9.79 kPa. This shows that despite the potentially large range in suction between the SWRC confidence limits for the AP model, this does not translate into a significantly large

difference in shear strength over the suction profile. Table 5.2 summarises these results at elevations of 4.0m and 8.0m.

Elevation (m)	Additional Shear Strength due to Suction (kPa)					
	AP	AP (LCL)	AP (UPL)	MK	PM	M
4.0	12.57	8.74	18.53	18.83	18.46	18.34
8.0	22.60	16.00	36.44	32.60	36.22	35.83

Table 5.2: Calculated additional shear strength due to suction above the water table at defined elevations using the Fredlund et al. (1996) equation (Eq. 5.2.1).

Figure 5.3 (b) shows the calculated increase in shear strength above the water table using the Vanapalli et al. (1996) equation (Eq. 5.2.3). The additional shear strength due to suction calculated using the AP model SWRC is lower than when calculated using the Fredlund et al. (1996) equation (Eq. 5.2.1). At an elevation of 4.0m, the calculated additional shear strength due to suction is 8.05 kPa (4.62kPa (38%) less than the Fredlund et al. (1996) equation (Eq. 5.2.1)). The difference between the two equations becomes greater as the elevation increase above the water table towards the ground surface, where the additional shear strength due to suction is 11.7 kPa (10.9 kPa (48%) less than the Fredlund et al. (1996) equation (Eq. 5.2.1)). It is well reported in the literature that the Vanapalli et al. (1996) equation (Eq. 5.2.3) is quite sensitive to the residual degree of saturation value, particularly for the case of fine grain size cohesive soils (Vanapalli and Fredlund, 2000), which may account for some of the discrepancy between the two predictive equations. It is also apparent that there is a larger spread between the upper and lower confidence limits when using the Vanapalli et al. (1996) equation (Eq. 5.2.3). This again may be due to the selection of a residual degree of saturation value, which is particularly difficult to determine for the SWRC confidence limits as they may not necessarily follow the shape of a SWRC. The results from using the Vanapalli et al. (1996) equation (Eq. 5.2.3) are documented in Table 5.3.

The additional shear strength due to suction has been calculated for both shear strength equations using the MK and PM predicted SWRCs, shown by the green and red lines respectively in Figure 5.3. Interestingly, both shear strength equations give very similar results. For example at an elevation of 4.0m, using the Fredlund et al. (1996) model (Eq. 5.2.1), the calculated additional shear strength due to suction is 18.83 kPa for

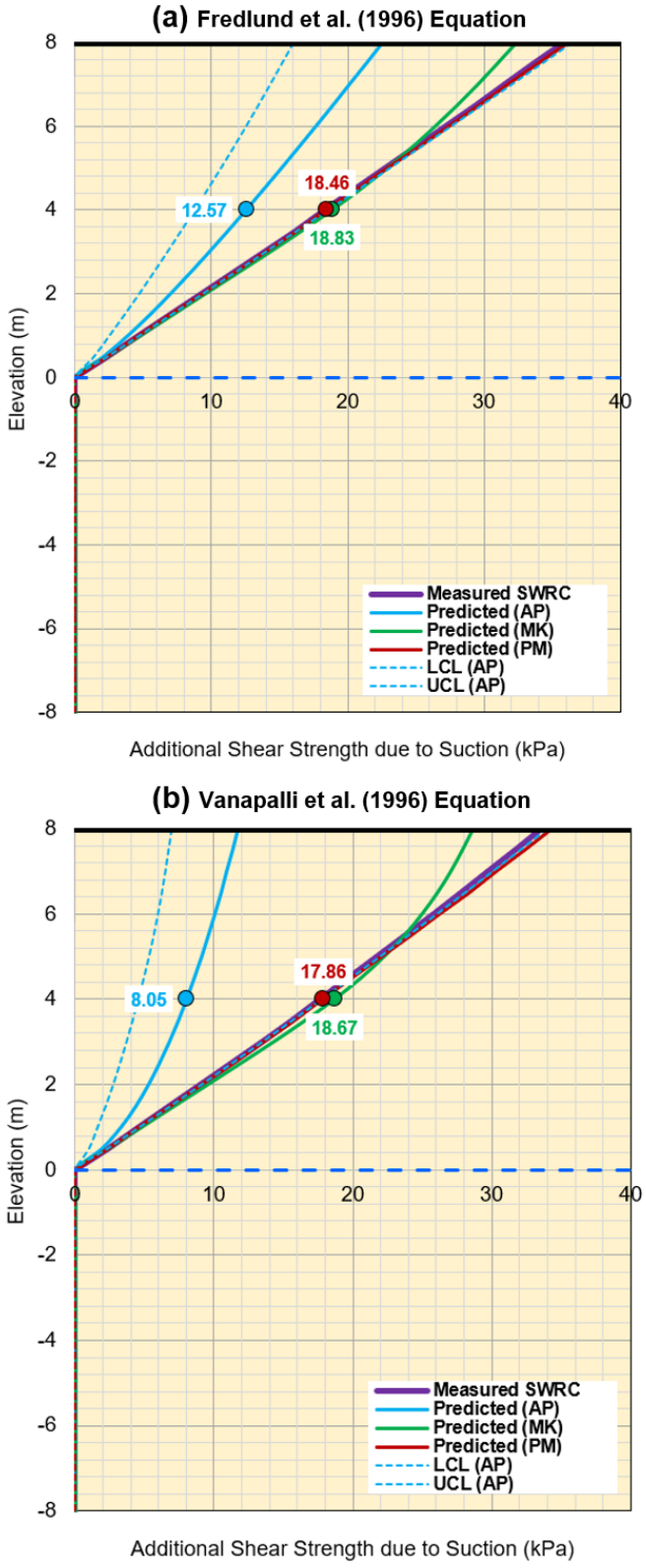

Figure 5.3: Plots showing the calculated additional shear strength profiles due to suction above the water table using (a) the Fredlund et al. (1996) equation (Eq. 5.2.1) and (b) the Vanapalli et al. (1996) equation (Eq. 5.2.3).

Elevation (m)	Additional Shear Strength due to Suction (kPa)					
	AP	AP (LCL)	AP (UPL)	MK	PM	M
4.0	8.05	4.51	17.74	18.67	17.86	17.63
8.0	11.77	6.92	33.96	28.68	34.36	33.60

Table 5.3: Calculated additional shear strength due to suction above the water table at defined elevations using the Vanapalli et al. (1996) equation (Eq. 5.2.3).

the MK model and 18.46 kPa for the PM model. When using the Vanapalli et al. (1996) equation (Eq. 5.2.3), the calculated additional shear strength due to suction is 18.67 kPa for the MK model and 17.86 kPa for the PM model. These results are all within a 1 kPa range. Of further significance is that the calculated additional shear strength for the AP model UCL is also very close to these values (18.53 kPa for the Fredlund et al. (1996) equation (Eq. 5.2.1) and 17.74 kPa for the Vanapalli et al. (1996) equation (Eq. 5.2.3).) Because all of these results are in close agreement, we can have greater confidence that the most likely additional shear strength profile for the soil is likely to be within the range of these profiles, which demonstrates the value of using all three SWRCs to generate the shear strength profile.

The additional shear strength profile has then been plotted as the purple line when using the measured drying SWRC. This profile plots within the same range as the MK and PM models, which means that both the PM and MK SWRCs result in very similar shear strength profiles to the profile estimated using the measured SWRC. These models seem to be in good agreement because they quite accurately model the SWRC in the low suction range, in particular the location of the air-entry value is in good agreement. As has been noted previously, the AP model often under predicts the suction for cohesive soils with a significant proportion of granular material, such as sandy clay type soils. The analysis presented here demonstrates that despite the large error in the AP model SWRC prediction, by utilising all three SWRC predictive models in conjunction we can gain a reasonable prediction of the likely increase in shear strength profile due to suction.

This analysis has shown that by excavating and lowering the water table by 7.0m, suctions of up to 80 kPa can develop in the soil at the crest of the slope for a hydrostatic pore water pressure profile. The development of suctions within the soil matrix will lead to an increase in soil shear strength. The analysis has shown that for a sandy clay type

soil, the shear strength could increase in the order of 18 kPa at 4.0m above the water table and 33 kPa at the top of the soil batter. Clearly the composition of the soil will have a great impact on the potential increase in shear strength, with the fine grained soils resulting in the greatest increase in shear strength. An increase in shear strength due to suction in the soil may lead to a significant increase in the stability of a temporary battered slope, resulting in an increased factor of safety value. The following section will present some analysis undertaken using the geotechnical finite element model PLAXIS 2D (Bentley Systems, 2020) to assess how suction may increase the factor of safety of a slope.

5.4 PLAXIS 2D Slope Stability Analysis

The purpose of this analysis is to assess how the factor of safety of the slope changes as a consequence of accounting for the influence of suction on shear strength. This analysis is also presented to demonstrate how these techniques can be applied in practice by a geotechnical engineer who uses finite element software on a regular basis.

PLAXIS 2D is a finite element package designed for the two-dimensional analysis of soil deformation and stability in geotechnical engineering. It is equipped with features to deal with various aspects of geotechnical and construction processes using robust and theoretically sound computational procedures. PLAXIS divides the domain into several finite elements and these are typically connected by nodes to form a finite element mesh. The model result is calculated at each node, therefore the higher the concentration of elements and nodes, the greater the accuracy of the model result. Figure 5.4 shows the model geometry for the example problem with the finite element mesh overlain.

There are two approaches to modelling the unsaturated shear strength behaviour of the soil in PLAXIS 2D. The first is to ignore suction and specify an increase in the effective cohesion, c', of the soil over a number of horizontal layers above the water table, as demonstrated by Ng (1988) during a project in Hong Kong. PLAXIS 2D then simulates the soil using standard soil mechanics theory for saturated soils using the Mohr-Coulomb model. The second approach is to use the built in tools in PLAXIS to simulate the unsaturated behaviour of the soil, which requires the specification of the SWRC using van Genuchten SWRC parameters (van Genuchten, 1980). This method calculates the

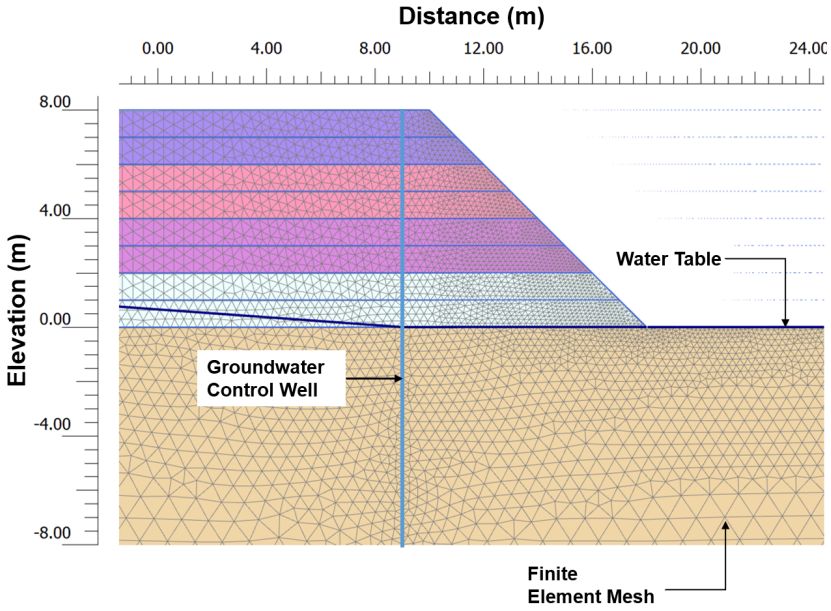

Figure 5.4: PLAXIS 2D model geometry and finite element mesh.

unsaturated effective stress i.e. Bishop stress, where χ is equal to the effective saturation $S_{eff} = (S - S_r)/(S_s - S_r)$. PLAXIS however does not enable χ to be specified using another form of the Extended Mohr-Coulomb equation, such as the equation by Fredlund et al. (1996), where $\chi = S^{\kappa}$. For this a user defined soil model would need to be developed for PLAXIS. Development of a user defined soil model would be time consuming and is therefore not within the scope of this MScR. Therefore the first approach has been undertaken for the following analysis in this section.

The soil above the water table (a level of 0.0m) is split into four 2.0m thick horizontal layers (Figure 5.4). The average increase in shear strength is calculated for each soil layer based on the additional shear strength profiles shown in Figure 5.3. This has been done for each additional shear strength profile (i.e. for each SWRC) and for both shear strength equations, which results in a total of 10 simulations in PLAXIS 2D, i.e. 5 for each shear strength equation. The additional shear strength is added to the effective cohesion, c' value of 10 kPa in each soil layer. The calculated average increase in shear strength for each case is shown in Table 5.4 for the Fredlund et al. (1996) equation and Table 5.5 for the Vanapalli et al. (1996) equation.

To determine the factor of safety, a 'Safety' analysis is undertaken in PLAXIS 2D. This method of analysis progressively reduces the strength properties (effective cohesion,

Layer	Average Additional Shear Strength due to Suction (kPa)				
	AP	AP (LCL)	AP (UPL)	MK	PM
0-2m	3.71	2.44	4.69	4.77	4.69
2-4m	9.84	6.74	13.95	14.24	13.91
4-6m	15.15	10.65	23.05	22.74	22.94
6-8m	20.16	14.27	32.01	29.45	31.82

Table 5.4: Calculated average additional shear strength due to suction for each 2.0m layer above the water table using the Fredlund et al. (1996) equation.

Layer	Average Additional Shear Strength due to Suction (kPa)				
	AP	AP (LCL)	AP (UPL)	MK	PM
0-2m	2.98	1.50	4.58	4.77	4.61
2-4m	6.73	3.64	13.44	14.19	13.53
4-6m	9.10	5.25	21.90	22.04	22.08
6-8m	10.95	6.44	30.01	26.95	30.32

Table 5.5: Calculated average additional shear strength due to suction for each 2.0m layer above the water table using the Vanapalli et al. (1996) equation.

Shear Strength Equation	Calculated Factor of Safety for Slope Stability Analysis				
	AP	AP (LCL)	AP (UPL)	MK	PM
Fredlund et al. (1996)	1.436	1.370	1.503	1.510	1.504
Vanapalli et al. (1996)	1.376	1.293	1.497	1.502	1.498

Table 5.6: Calculated factor of safety by PLAXIS 2D for the slope stability analysis. Results are presented for each additional shear strength profile derived from the predicted SWRCs.

c' and friction angle, ϕ') of the soil until failure occurs. The factor of safety is then derived from the strength reduction of the soil properties. The slope stability analysis was first undertaken using the standard soil mechanics approach where suction and additional shear strength due to suction are ignored. This results in a calculated factor of safety of 1.138, meaning the slope is stable for the simulated conditions and soil properties. The simulated displacement contours at failure produced by PLAXIS 2D (shown in Figure 5.5) show the likely method of slope failure, which in this case is a circular slip failure. Following this, the slope stability analysis was undertaken for all 10 cases, with the factor of safety results

given in Table 5.6.

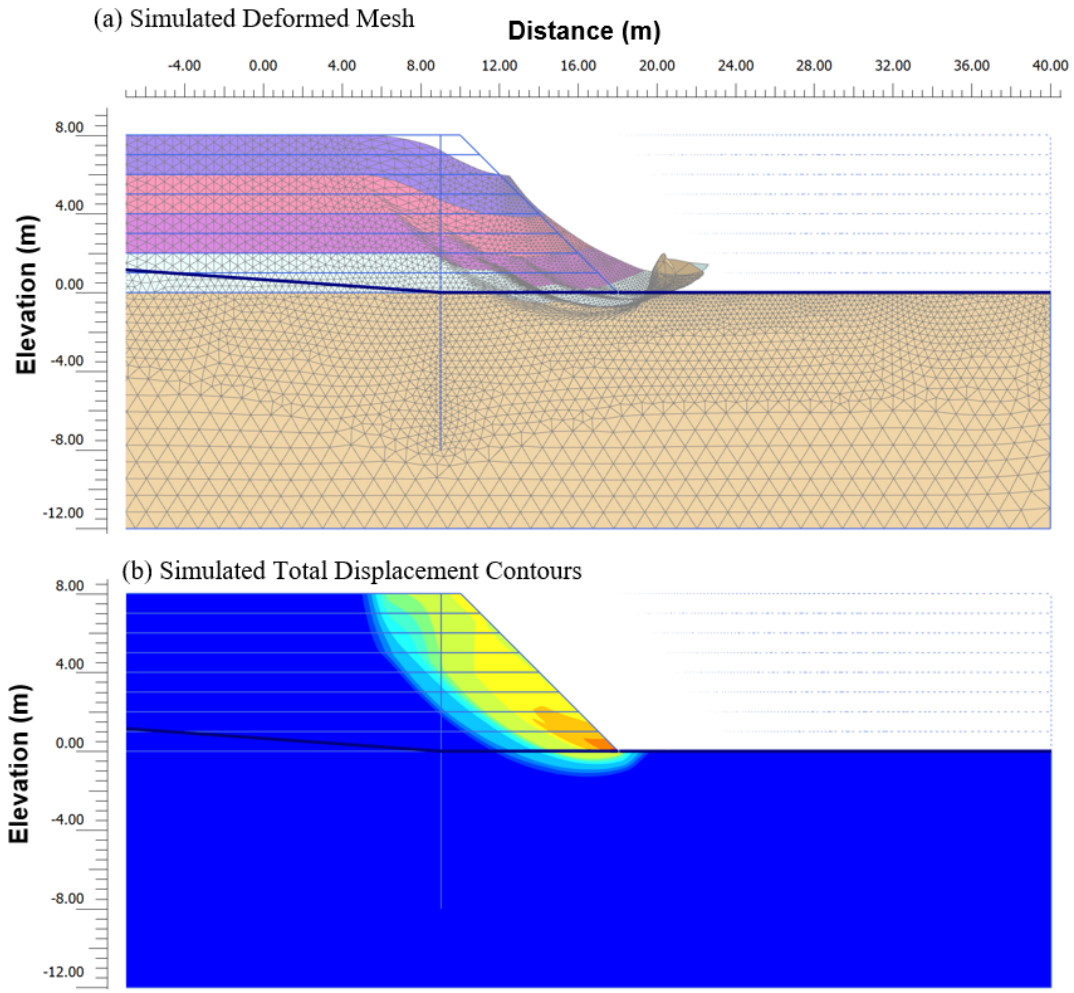

Figure 5.5: PLAXIS 2D output from a safety analysis showing (a) the deformed mesh at failure (b) simulated displacement contours at failure.

The results show that there is a significant increase in factor of safety for all cases when the unsaturated shear strength of the ground is taken into account. For the AP model predicted SWRC, which significantly under predicts the suction, the factor of safety increased from 1.138 to 1.436 when using the Fredlund et al. (1996) shear strength equation (Eq. 5.2.1). As expected, when using the additional shear strength profiles derived from the MK and PM model SWRCs, the calculated factor of safety for both is 1.510 and 1.504 respectively. Of most significance however is the difference in factor of safety between the AP (LCL) and AP (UCL) simulations. The difference in suction between the two confidence limits is significant, often 3 orders of magnitude at a given degree of saturation value. At the centre of the slope the degree of saturation for the AP (UCL)

is 0.97 and for the AP (LCL) it is 0.66, however this only translates to a difference in factor of safety of 0.133. Even for the worst case SWRC, the AP (LCL) case, there is a significant improvement in factor of safety of 0.232 over the scenario where suction is ignored. Where the Vanapalli et al. (1996) equation is used instead of the Fredlund et al. (1996) equation, the AP (LCL) case yields an increase in factor of safety of 0.155. This analysis demonstrates that despite a potentially large error in the SWRC prediction, this may not translate in to a large difference in the factor of safety of a slope, particularly if the soil is fine grained. It also demonstrates that by simply taking into consideration the unsaturated shear strength of the soil, there could be a significant impact on the calculated factor of safety of a slope when compared to the standard approach which ignores suction. It must be noted that this analysis is based on a sandy clay soil, and these results may not hold true across the entire grain size spectrum of soils. In particular clean sands (poorly graded) may only see a minor increase in shear strength as they typically desaturate a much lower suctions in the order of 1-10kPa, which may result in only a minimal change in calculated factor of safety. It is recommended for future work that a similar analysis is undertaken for a range of soil types to assess how the SWRC may influence the factor of safety of a slope.

To assess whether it is appropriate to split the soil into 2.0m thick horizontal layers, some additional analysis has been undertaken where the soil has been split into eight 1.0m thick layers and two 4.0m thick layers. Figure 5.6 shows how the finite element mesh and material layers have been set up in PLAXIS 2D for each modelling scenario. The modelling has been undertaken using the shear strength profiles calculated using the Fredlund et al. (1996) equation (Eq. 5.2.1). The calculated factors of safety for each scenario are given in Table 5.7 and Figure 5.7.

Layer Thickness	Calculated Factor of Safety for Slope Stability Analysis				
	AP	AP (LCL)	AP (UPL)	MK	PM
1.0m (8 layers)	1.431	1.359	1.500	1.500	1.501
2.0m (4 layers)	1.436	1.370	1.503	1.510	1.504
4.0m (2 layers)	1.460	1.385	1.533	1.535	1.535

Table 5.7: Calculated factor of safety from PLAXIS 2D slope stability analysis for 8, 4 and 2 horizontal layers above the water table for each shear strength profile derived from the predicted SWRCs when using the Fredlund et al. (1996) equation (Eq. 5.2.1).

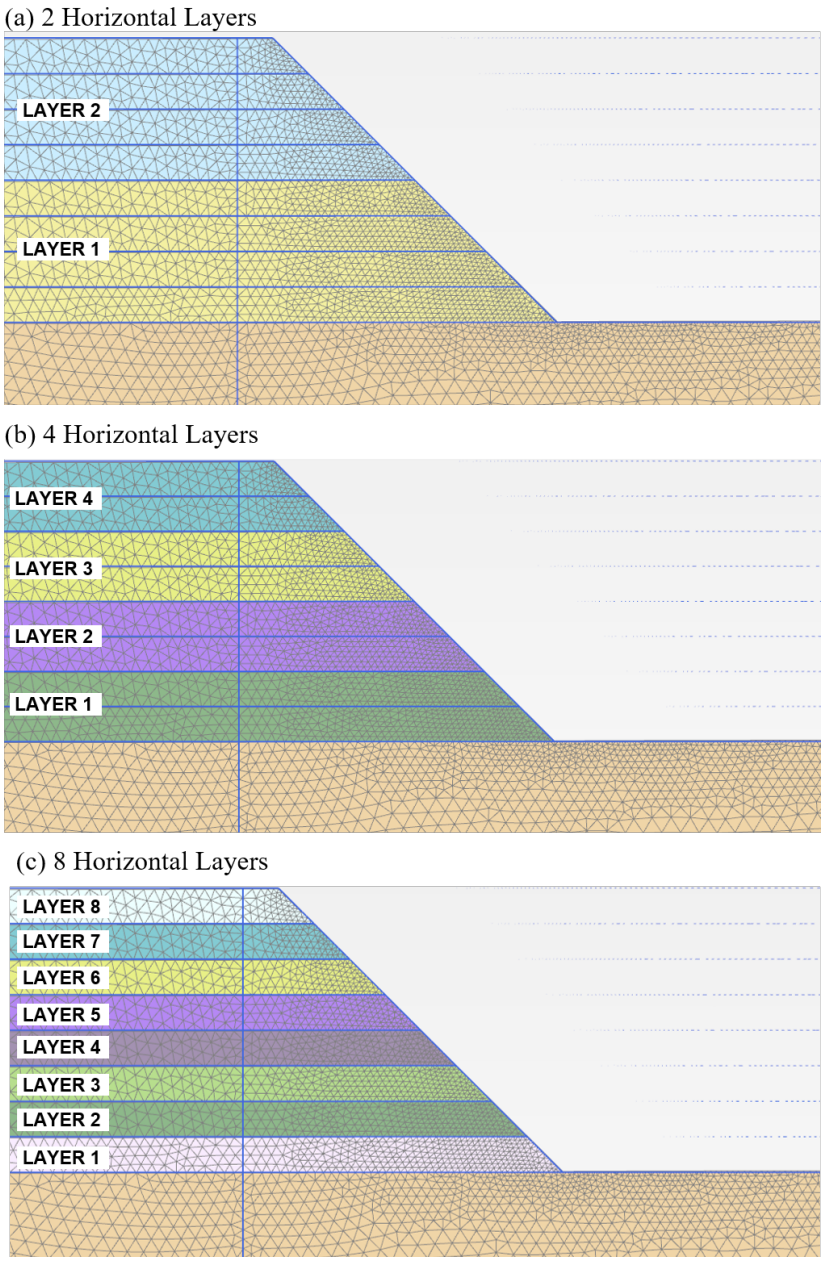

Figure 5.6: Finite element mesh for the following modelling scenarios (a) 2 horizontal layers (b) 4 horizontal layers and (c) 8 horizontal layers.

The calculated factors of safety using 8 horizontal layers is only marginally different when compared with the results calculated using 4 layers. The largest difference between the 8 and 4 layer simulations occurs for the AP (LCL) shear strength profile where there is a 0.8% percentage difference between the two. For both the MK and PM models the percentage difference is less than 0.4%, indicating that the results are very similar. Because the difference in calculated factor of safety between the 4 and 8 layer simulations is less

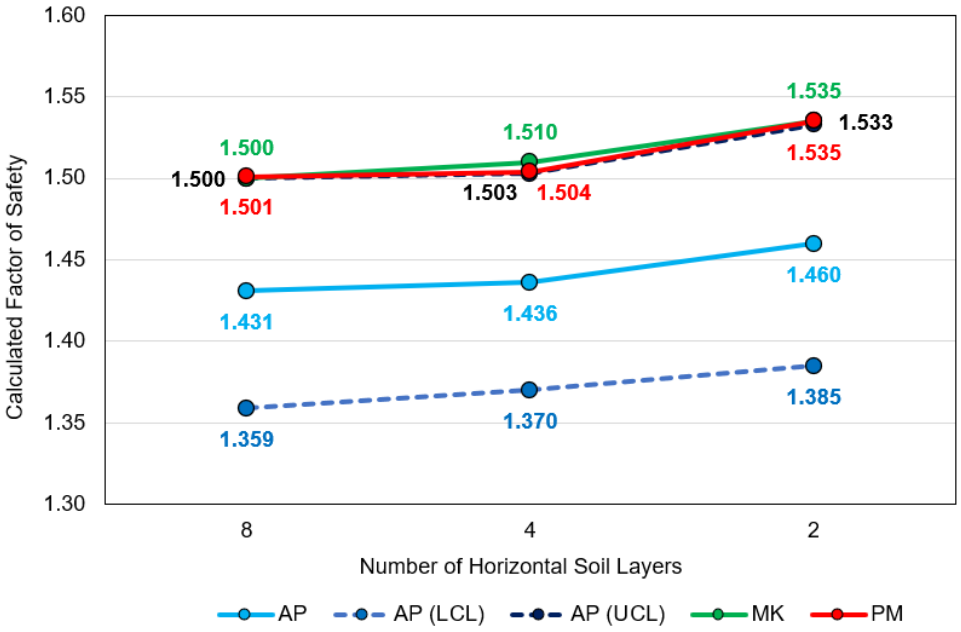

Figure 5.7: Calculated factor of safety from PLAXIS 2D slope stability analysis for 8, 4 and 2 horizontal layers above the water table for each shear strength profile derived from the predicted SWRCs when using the Fredlund et al. (1996) equation (Eq. 5.2.1).

than 1%, we can conclude that for this model example, it is appropriate to use 2.0m thick horizontal layers instead of 1.0m thick layers. When using 2 horizontal layers which are 4.0m thick however, the difference in the calculated factor of safety between the results using 8 layers is more significant than when using 4 layers. For every shear strength profile, the percentage difference between the 2 and 8 layer models is within the range of 1.9% and 2.3%. It is clear from these results that the use of 4.0m thick horizontal layers is insufficient to accurately model the shear strength profile. It is important that a sufficient number of horizontal layers is used so that the shear strength at the toe of the slope is not overestimated, as this is critical to the stability of the slope. The results shown here demonstrate this fact, as the factor of safety was overestimated by 2%. Therefore we can conclude that use of 2.0m thick horizontal layers is an appropriate approximation in this example, however careful thought should be taken by the geotechnical engineer to ensure that the average shear strength profile used in the model is sufficient to model the slope conditions accurately.

The following section will look at some of the limitations and benefits of the methods presented here, and give some recommendations for geotechnical engineers who aim to use

these concepts and procedures presented in this Chapter in practice.

5.5 Limitations, Benefits and Recommendations for Future Use

This section aims to outline some of the limitations of using the predicted SWRC to calculate an increase in shear strength due to suction, and provides some recommendations for geotechnical engineers when applying this method in practice.

- The methods for estimating the unsaturated shear strength due to suction presented in this Chapter should be used with caution during the design stage of a construction project as there could be significant errors in the calculation. The upper and lower confidence limits give a range of possible shear strength due to the possible error in the SWRC prediction. However, they do not give the possible error in shear strength due to the error in the unsaturated shear strength equations by Fredlund et al. (1996) (Eq. 5.2.1) and Vanapalli et al. (1996) (Eq. 5.2.3). Further work would be required to assess what the likely error in these equations is for a range of soil types. It is therefore recommended that the geotechnical engineer apply these concepts with caution, and assess stability problems with a range of parameter values and suction profiles. If possible, gathering of field measurements including suction, water content and shear strength would greatly reduce the possible error in these calculations as they could be used to calibrate a finite element model.

- The two unsaturated shear strength equations proposed by Fredlund et al. (1996) (Eq. 5.2.1) and Vanapalli et al. (1996) (Eq. 5.2.3) both have strengths and weaknesses when used in practice. The Vanapalli et al. (1996) equation (Eq. 5.2.3) requires that the SWRC is normalised between fully saturated and residual degree of saturation, however determining the residual degree of saturation can be difficult for fine grained cohesive soils such as clays, which could lead to a significant error in the estimated shear strength. Therefore the Fredlund et al. (1996) equation (Eq. 5.2.1) is likely to be the preferred equation as this requires the Plasticity Index of the soil which is normally available for fine grained cohesive soils in standard site investigation reports. If the soil is granular however, where PI=0, then the Fredlund et al. (1996)

equation is not applicable. In this case the Vanapalli et al. (1996) equation (Eq. 5.2.3) should be used instead.

- The accuracy of the unsaturated shear strength profile is dependent of the quality of the SWRC prediction, therefore it is recommended to use all three methods of SWRC prediction and apply these to the shear strength calculations. As was shown for the Durham Lower Boulder Clay, both the MK and PM models produced similar shear strength profiles whilst the AP model was significantly lower. If only the AP model was used, this could lead to a significant under prediction of the shear strength profile. By applying all three SWRC predictions, it became clear that the AP model was likely under predicting the increase in shear strength due to suction.

- Calculating a reasonable prediction of unsaturated shear strength is also dependant on the suction profile within the soil. The calculations presented here are based on a hydrostatic pore water pressure profile, i.e. there is no net infiltration or evapotranspiration, however this is unlikely to be the case in practice. Therefore, it is recommended that the suction profile is determined using a series of field tensiometers installed in the ground or by using an unsaturated groundwater flow model. This requires the careful selection of net infiltration or evapotranspiration at the ground surface, along with a hydraulic conductivity function which describes how hydraulic conductivity changes with suction. To determine the hydraulic conductivity function, either laboratory testing would be required or it could be estimated from the PSD and SWRC using methods presented in the literature (Vereecken, 1995). Researching these estimation procedures was outside the original scope of this Thesis project, however this could form an area of future research that could expand the work presented here and improve the prediction of suction profiles above the water table. If undertaking a finite element simulation is not possible due to a lack of quality input parameters, then a series of suction profiles could be calculated which are either reduced from hydrostatic by a factor to represent net infiltration or increased from hydrostatic by a factor to represent net evapotranspiration. Alternatively a moisture content profile could be determined, and suctions calculated using the SWRC.

- If applying the additional shear strength due to suction in a finite element model using the approach taken here i.e. adding shear strength to the effective cohesion

parameter, care should be taken to model the layers parallel to the water table. If the water table is highly non-linear, then this method should not be used and the second approach which requires a user defined soil model should be developed. The second approach will provide much greater accuracy as it will model the position of the water table and the resulting suction profile above the water table.

- This analysis presented within the Chapter has demonstrated that by using the developed procedure for estimating the SWRC, the unsaturated shear strength of the soil can also be reasonably estimated. The main benefit of this is that geotechnical design using unsaturated soil parameters can be achieved without expensive and time consuming unsaturated soil testing, which opens up the possibilities of using unsaturated soil mechanics on live construction projects. In addition, the estimated unsaturated shear strength of the soil can be validated in the field using conventional shear strength test methods such as the hand shear vane test or the standard penetration test. In the future, with the advancement of tensiometer techniques, it is hoped that SWRC measurement will become available at UK laboratories and regularly used during construction project site investigation.

This chapter has shown that lowering of the groundwater table due to dewatering can lead to an increase in the shear strength of the soil. It was shown how the unsaturated shear strength of the soil can be predicted in practice using an estimated SWRC derived from standard laboratory tests. By modelling the measured SWRC, it was shown that all three SWRCs can be used together to give the likely range in shear strength for a given suction profile with reasonable confidence. The SWRC confidence limits were used to provide a range of shear strength values due to the possible error in the SWRC prediction, however it was noticed that the shear strength profile was not highly sensitive to the large difference in suction between the two SWRC confidence limits. The PLAXIS 2D analysis demonstrated how the methods and techniques presented in this Thesis can be integrated into finite element modelling of a slope stability problem which is typical in the construction industry. The results demonstrated how significant the increase in the factor of safety of a slope can be as a result of applying unsaturated soil mechanics to slope stability problems. The following chapter concludes the findings from this Thesis.

Chapter 6

Conclusions

As a soil dries out it becomes harder and stronger. When it gets wet it becomes softer and weaker. People from across the globe, from construction workers, agricultural workers and geotechnical engineers, to walkers and cyclists, have regularly experienced this phenomenon. It is of particular significance to the construction industry however, where the soil on construction sites is often churned up by machinery and difficult to work on. During construction projects where a groundwater control system is required to lower the water table, the soil dries out and becomes more workable. Despite this regular occurrence, the mechanics and theory that govern this phenomenon are not well understood or utilised by geotechnical engineers working within the construction industry. There has been a significant effort by the research community to understand, formulate and apply this understanding, however the regular use and application of this theory has not transferred down to geotechnical engineers working within industry. There may be several reasons for this, such as a lack of understanding and knowledge in the subject area, unsaturated soil testing required may be too costly or time consuming for the project, engineers may be more comfortable taking the more conservative approach, or there is a lack of tools and procedures that help engineers apply these concepts in practice. The aim of this Masters by Research project has been to investigate the relationship between water content, soil suction and shear strength and the apply these concept to typical engineering problems within the construction industry by developing a set of set of tools which can be used by a geotechnical engineer in practice. This aim is summarised by the following key objectives:

- To present a scientific foundation that describes the mechanics and theories of unsaturated soil behaviour, with a focus on understanding how the shear strength of a soil increases as the water content decreases.
- To develop a procedure that can be used by geotechnical engineers in practice to estimate the soil water retention curve (SWRC) of a soil using standard site investigation test data such as a particle size distribution and dry density, and then quantify the possible error in the SWRC prediction.
- To develop a procedure that can be used by geotechnical engineers in practice to estimate the increase in shear strength due to suction using a predicted SWRC, and quantify the possible variability in shear strength due to the possible error on the SWRC prediction.

The following paragraphs present the key findings of this research project within the context of the overall research objectives. The Literature Review in Chapter 2 presents an in depth review of the published science that links soil testing, soil suction, water content and shear strength, and provides the foundation to the research work presented in Chapters 3 to 5. The literature review aims to fulfil the first research objective. If a geotechnical engineer aims to apply in practice the procedure developed during this research project, they should first familiarise themselves with the content of Chapter 2.

The second aim of this research project was to develop a procedure for estimating the SWRC of a soil using only standard site investigation laboratory tests. The SWRC describes the fundamental behaviour of how a soil desaturates with respect to soil suction (i.e negative pore-water pressure) and is therefore critical to the relationship between shear strength and soil suction. The laboratory tests used to determine a SWRC are time consuming and expensive and are rarely included within a site investigation study for a construction project, therefore estimating the SWRC from standard laboratory test results is usually the only feasible option. Chapter 3 presents the methodology undertaken to develop this procedure, which estimates the SWRC of a soil using the particle size distribution, dry density and Atterberg limit test results using three well documented SWRC prediction methods presented within the literature (the Arya and Paris (1981) Model (AP), the Modified Kovács Model (MK) (Aubertin et al., 2003) and the Perera et al. (2005) Model (PM)). The novel aspect of this procedure is the calculation of 5% and

95% confidence limits for the SWRC which give the likely range in error of the SWRC prediction. The confidence limits for a SWRC prediction can be calculated using the 5^{th} and 95^{th} percentiles of suction error (given in Tables B.1 to B.4 of Appendix B) which were calculated as a result of undertaking statistical analysis on a dataset of 102 soils from the UNSODA database (Nemes et al., 2001). For each soil in the dataset, the SWRC was predicted using the available soil data and predictive methods and then compared to the measured SWRC from the laboratory. This was presented on plots of suction error (logarithmic error between the predicted and measured suction) vs degree of saturation. By reviewing the plots of suction error vs degree of saturation, some key findings became apparent:

- All three SWRC predictive methods provide reasonable estimates for the drying SWRC when the soil is granular and does not contain a large spread of particle sizes (i.e. clean sands). When the soil contains a larger proportion of fines, the SWRC prediction may become less reliable in the low saturation range.
- The MK model was shown to be most effective at predicting the SWRC for poorly graded sands, with the PM model most effective for well graded sands.
- For cohesive soils, only the Arya and Paris (1981) model could be studied due to plasticity index being omitted from the UNSODA database. For purely clay soils, the Arya and Paris (1981) performs reasonably well.
- Significant errors in the predicted SWRC arise when then soil contains a significant portion of granular and fine particles, as is the case for sandy clay and clay loam type soils. The Arya and Paris (1981) model performs poorly when this is the case, with the spread in the suction error percentiles for cohesive soils highlighting this fact.

Understanding the possible error in material properties and functions is crucial if new concepts and techniques are to be adopted and applied in practice. The development of the confidence limits together with the three SWRC predictive methods results in a procedure which geotechnical engineers can use effectively in practice as a design tool. To improve this tool further, confidence limits could be calculated fo each soil type of the USCS or USDA classification system, however this would require analysis a large dataset

of soils across the entire soil particle size spectrum.

The aim of Chapter 4 was to present a validation of the procedure presented in Chapter 3. For this validation two soil sample were used, the first is a sandy clay soil from the Durham Lower Boulder Clay, UK (Toll et al., 2012) and the second is a clean sand from the Vashon Advance Outwash Sand from Washington State, USA (Likos et al., 2010). The chapter guides the reader through the procedure by applying it to these soil datasets. The SWRC was predicted using all three SWRC methods as Plasticity Index was available for the soil, however the confidence limits could only be calculated using the Arya and Paris (1981) model. It was shown that the SWRC predicted by the AP model was significantly offset from the measured SWRC, however it did remain within the calculated confidence limits. Both the PM and MK models resulted in better predictions for the SWRC, with the PM model giving the most accurate SWRC. Despite the poor prediction by the AP model, it was shown that the confidence limits were effective at giving the likely range of error of the AP model, and should be used during design to assess the sensitivity of the SWRC to changes in shear strength. This analysis also demonstrated the value of predicting the SWRC using all three methods despite the fact that the confidence limits could not be calculated using the MK and PM models. If two of the predicted SWRCs are in good agreement, and within the AP model confidence limits, this increases the likelihood that the SWRC will lie within that range and reduces the risk of using an inaccurate SWRC in practice. The analysis of the Vashon Advance Outwash Sand demonstrated that the procedure is valid for clean sand soils, as the measured SWRC lies within the calculated confidence limits for each of the three SWRC predictive models. Further analysis of a greater range of sand type soils would be required to determine if the procedure is valid for all sand soils. The validation of the procedure using two soils from within the literature has demonstrated that this procedure can be used successfully by geotechnical engineers who aim to use the SWRC in practice but do not have access to expensive and time consuming laboratory testing.

The aim of Chapter 5 was to build on the procedure outlined in Chapter 3 and 4 such that the final part of the research objected can be fulfilled. Using the predicted SWRC, Chapter 5 showed how the shear strength of a soil may increase as a consequence of decreasing water content and increasing soil suction. This has been demonstrated by applying the unsaturated Extended Mohr-Coulomb Equation (Fredlund et al., 1996;

Vanapalli et al., 1996) to an example problem which commonly occurs within the construction industry. The example problem involves the construction of an excavation with temporary battered slopes, groundwater control wells located around the perimeter to lower the water table and a surface covering to protect against erosion and prevent infiltration. All these measures therefore result in a hydrostatic negative pore-water pressure profile above the water table. Using the predicted SWRCs the additional shear strength due to suction was calculated. Taking a vertical section behind the crest of the slope, and using the Durham Lower Boulder Clay as an example, it was shown that the shear strength could be increased between 8 and 18 kPa at 4.0m above the water table for each of the SWRCs. It became apparent that the large range in suction between the AP model upper and lower confidence limits resulted in a difference in shear strength of only 14kPa at 4.0m above the water table. This shows that the change in shear strength due to suction may not be highly sensitive to the SWRC, however further analysis would be required to understand this relationship is greater detail, particularly for other soil types. Typically, it is common practice for a geotechnical engineer to undertake a finite element model to assess the stability of any engineered structure and check that it conforms to design standards such as Eurocode 7. Chapter 5 showed how it is possible to implement the increase in shear strength due to suction into a finite element model using PLAXIS 2D. The increase in shear strength due to suction was modelled by simulating several layers above the water table and specifying an additional effective cohesion value in each layer. It was shown that by modelling the unsaturated shear strength using any of the predicted SWRCs, the factor of safety on the slope stability was significantly improved. Using the AP model to estimate the SWRC, which often under predicts the suction on the SWRC, there was a reasonable improvement in factor of safety of 0.238 when using the Vanapalli et al. (1996) version of the Extended Mohr-Coulomb equation. The SWRCs generated using the MK, PM and AP (UCL) models were all in reasonable agreement, so when using the shear strength profiles for each SWRCs, the calculated factors of safety were remarkably similar ranging from 1.497 to 1.502. This may be in part due to the fact that for the suction range observed in the example case (0 to 80kPa), the predicted degree of saturation did not become less than 98% for each model. This is still significant however as for most construction site projects, 0kPa to 100kPa is likely to be the typical range of suction within the unsaturated zone. Given there can still be a reasonable improvement in factor of safety when using the lower confidence limit of the SWRC, it is recommended that a SWRC is taken on the

conservative side of the predicted SWRC when used to estimate change in shear strength due to suction for geotechnical designs such as temporary slopes. If there is doubt in the quality of the prediction, the lower confidence limit of the SWRC should be adopted. This is because the lower confidence limit side of the SWRC is still likley to result in a favourable improvement in factor of safety over the alternative approach of ignoring suction completely. It is the skill and responsibility of the geotechnical engineer to assess the quality of the SWRC prediction and determine if the result is reasonable from the soil information available. Where the predicted SWRC cannot be relied upon, then the SWRC should be determined from laboratory testing if feasible.

The conclusion of Chapter 5 showed that the factor of safety of an engineered slope can be significantly increased if the unsaturated shear strength of the soil is taken into consideration. An important question to ask is why the effect of suction is so often ignored by geotechnical engineers working across the globe. The combination of ignoring suction effects and the application of partial factors on material properties required by the Eurocode design standard can lead to significantly over-conservative and over-engineered slope stabilisation designs, often at the expense of the end client. Clearly there are benefits to ignoring the effects of suction, such as reducing the risk of slope failure, along with requiring less knowledge of unsaturated soil mechanics to undertake the slope design. There is clearly a balance to be made however, and the procedure developed during this Masters by Research project aim to go some way to achieving that balance. By developing a set of tools, which will later be developed in a simple set of Excel spreadsheets that are free to use, understanding and applying the topic becomes more achievable. The calculation of SWRC confidence limits enables the likely range in error of the SWRC to be assessed and the effect this may have on slope stability can be reviewed. The procedure also only requires standard laboratory soil tests, such as the particle size distribution and triaxial shear strength testing, meaning no expensive laboratory tests are required. Clearly if these tests can be undertaken they should, but this should not be a barrier to developing these concepts into the tool set of a geotechnical engineer. The engineering community has aimed to make unsaturated soil mechanics more accessible within the industry, with the works by Fredlund et al. (2012) providing the most comprehensive study on the subject. Continually advancing software packages such as PLAXIS and Soil Vision (Bentley Systems, 2020) make this area more accessible every day, but these can come at

considerable cost and may not be regularly used by engineering companies to justify the expense. The procedures and tools developed during this research project are not perfect and will require further development, however they can add a small but valuable set of tools to a geotechnical engineer working within the construction industry who wishes to apply the concepts of unsaturated soil mechanics to the design of geotechnical structures.

References

G. D. Aitchison. Relationships of moisture stress and effective stress functions in unsaturated soils. In *Pore pressure and suction in soils: conference organised by the British National Society of the International Society of Soil Mechanics and Foundation Engineering*, pages 47–52. Butterworths, London, 1961.

H. Akaike. A New Look at the Statistical Model Identification. *IEEE Transactions on Automatic Control*, 19(6):716–723, 1974.

E. E. Alonso, A. Gens, and A. Josa. A constitutive model for partially saturated soils. *Géotechnique*, 40(3):405–430, 1990.

L. M. Arya and J. F. Paris. A Physicoempirical Model to Predict the Soil Moisture Characteristic from Particle-Size Distribution and Bulk Density Data. *Soil Science Society of America Journal*, 45(6):1023–1030, 1981.

L. M. Arya, J. C. Richter, and S. A. Davidson. A Comparison of Soil Moisture Characteristics Predicted By The Arya-Paris Model with Laboratory-Measured Data. Technical report, A Joint Program for Agriculture and Resources Inventory Surveys through Aerospace Remote Sensing, 1982.

ASTM International. Standard Practice for Classification of Soils for Engineering Purposes (Unified Soil Classification System). Technical report, 2006.

M. Aubertin, J.-F. Ricard, and R. P. Chapuis. A predictive model for the water retention curve: application to tailings from hard-rock mines. *Canadian Geotechnical Journal*, 35 (1):55–69, 1998.

M. Aubertin, M. Mbonimpa, B. Bussière, and R. P. Chapuis. A model to predict the water

retention curve from basic geotechnical properties. *Canadian Geotechnical Journal*, 40 (6):1104–1122, 2003.

C. H. Benson, I. Chiang, T. Chalermyanont, and A. Sawangsuriya. Estimating van Genuchten parameters α and n for clean sands from particle size distribution data. In *From Soil Behavior Fundamentals to Innovations in Geotechnical Engineering*, number 233, pages 410–427. 2014. ISBN 9780784413265.

Bentley Systems. SVSOILS - Knowledge-Based Saturated/Unsaturated Soil Property Database, 2020.

A. W. Bishop. The principle of effective stress. *Teknisk Ukeblad (Norwegian Geotechnical Institute)*, 106(39):859–863, 1959.

A. W. Bishop and G. E. Blight. Some Aspects of Effective Stress in Saturated and Partly Saturated Soils. *Géotechnique*, 13(3):177–197, 1963.

R. H. Brooks and A. T. Corey. Hydraulic Propertities of Porous Media. Technical report, Colorado State University, Fort Collins, Colorado, 1964.

P. G. Bruch. *Laboratory study of evaporative fluxes in homogeneous and layered soils.* Thesis of the degree of master science, University of Saskatchewan, 1993.

BSI. BS EN 1997-1:2004+A1:2013 Eurocode 7: Geotechnical design. General rules. Technical report, British Standards Institution, 2004.

BSI. BS 5930:2015+A1:2020 Code of practice for ground investigations. Technical report, British Standard Institution, 2015.

E. Buckingham. Studies on the movement of soil moisture. Technical report, U. S. Department of Agriculture Beureau of Soils, Washington, 1907.

R. Bulut. A Re-Evaluation of the Filter Paper Method of Measuring Soil Suction . Technical report, Texas Tech University, 1996.

R. Cardoso, E. Romero, A. Lima, and A. Ferrari. A Comparative Study of Soil Suction Measurement Using Two Different High-Range Psychrometers. In *Experimental Unsaturated Soil Mechanics*, pages 79–93. Springer Berlin Heidelberg, 2007.

J. Chai and P. Khaimook. Prediction of soil-water characteristic curves using basic soil properties. *Transportation Geotechnics*, 22:100295, 2020.

R. Ching, D. Sweeney, and D. Fredlund. Increase in factor of safety due to soil suction for two Hong Kong slopes. In *Fourth International Symposium on Landslides*, pages 617–623, 1984.

D. Croney, J. D. Coleman, and W. P. Black. Movement and Distribution of Water in Soil in Relation to Highwat Design and Performance. Technical Report 40, Highway Research Board, 1958.

M. R. Cunningham, A. M. Ridley, K. Dineen, and J. B. Burland. The mechanical behaviour of a reconstituted unsaturated silty clay. *Géotechnique*, 53(2):183–194, 2003.

V. Escario and J. F. T. Jucá. Strength and Deformation of Partially Saturated Soils. In *Proceedings of the 12th International Conference on Soil Mechanics and Foundation Engineering*, volume 02, pages 43–46, Rio de Janeiro, 1989.

D. G. Fredlund and N. R. Morgenstern. Stress State Variables for Unsaturated Soils. *ASCE J Geotech Eng Div*, 103(5):447–466, 1977.

D. G. Fredlund and A. Xing. Equations for the soil-water characteristic curve. *Canadian Geotechnical Journal*, 31(4):521–532, 1994.

D. G. Fredlund, N. R. Morgenstern, and R. A. Widger. Shear Strength of Unsaturated Soils. *Canadian Geotechnical Journal*, 15(3):313–321, 1978.

D. G. Fredlund, A. Xing, M. D. Fredlund, and S. L. Barbour. The relationship of the unsaturated soil shear strength to the soil-water characteristic curve. *Canadian Geotechnical Journal*, 33(3):440–448, 1996.

D. G. Fredlund, H. Rahardjo, and M. D. Fredlund. *Unsaturated Soil Mechanics in Engineering Practice*. John Wiley & Sons, Inc., 2012.

M. D. Fredlund, D. G. Fredlund, and G. W. Wilson. An equation to represent grain-size distribution. *Canadian Geotechnical Journal*, 37(4):817–827, 2000.

M. D. Fredlund, G. W. Wilson, and D. G. Fredlund. Use of the grain-size distribution for estimation of the soil-water characteristic curve. *Canadian Geotechnical Journal*, 39(5): 1103–1117, 2002.

J. K. M. Gan, D. G. Fredlund, and H. Rahardjo. Determination of the shear strength parameters of an unsaturated soil using the direct shear test. *Canadian Geotechnical Journal*, 25(3):500–510, 1988.

R. A. García-Gaines and S. Frankenstein. USCS and the USDA Soil Classification System, Development of a Mapping Scheme. Technical Report March, Cold Regions Research and Engineering Laboratory, 2015.

W. R. Gardner. Some steady-state solutions of the unsaturated moisture flow equation with application to evaporation from a water table. *Soil Science*, 85(4):228–232, 1958.

E. A. Garven and S. K. Vanapalli. Evaluation of Empirical Procedures for Predicting the Shear Strength of Unsaturated Soils. In *Unsaturated Soils 2006*, number 147, pages 2570–2592, Reston, VA, 2006. American Society of Civil Engineers.

S. C. Gupta and R. P. Ewing. Modelling water retention characteristics and surface roughness of tilled soils. In M. T. van Genuchten, F. J. Leij, and L. J. Lund, editors, *Indirect Methods for Estimating the Hydraulic Properties of Unsaturated Soils*, pages 379–388. Department of Enviornmental Sciences, University of California, Riverside, California, 1992.

S. C. Gupta and W. E. Larson. Estimating soil water retention characteristics from particle size distribution, organic matter percent, and bulk density. *Water Resources Research*, 15(6):1633–1635, 1979.

R. M. Hen-Jones, P. N. Hughes, R. A. Stirling, S. Glendinning, J. E. Chambers, D. A. Gunn, and Y. J. Cui. Seasonal effects on geophysical - geotechnical relationships and their implications for electrical resistivity tomography monitoring of slopes. *Acta Geotechnica*, 12(5):1159–1173, 2017.

J. W. Hilf. *An Investigation of Pore Water Pressure in Compacted Cohesive Soils*. PhD thesis, United State Department of the Interior Bureau of Reclamation, Denver, Colorado, 1956.

P. N. Hughes, S. Glendinning, J. Mendes, G. Parkin, D. G. Toll, D. Gallipoli, and P. E. Miller. Full-scale testing to assess climate effects on embankments. *Proceedings of the Institution of Civil Engineers - Engineering Sustainability*, 162(2):67–79, 2009.

J. E. Jennings. A revised effective stress law for use in the prediction of the behaviour of unsaturated soils. In *Proceedings of Conference on Pore Pressure and Suction in Soils*, pages 26–30, London, 1961. Butterworths.

H. Jin, Y. Wang, Q. Zheng, H. Liu, and E. Chadwick. Experimental study and modelling of the thermal conductivity of sandy soils of different porosities and water contents. *Applied Sciences (Switzerland)*, 7(2), 2017.

C. Jommi. Remarks on the constitutive modelling of unsaturated soils. In A. Tarantino and C. Mancuso, editors, *Experimental evidence and theoretical approaches in unsaturated soils*, pages 139–153, Rotterdam: Balkema, 2000.

N. Khalili and M. H. Khabbaz. A unique relationship for χ for the determination of the shear strength of unsaturated soils. *Géotechnique*, 48(5):681–687, 1998.

G. Kovacs. *Seepage hydraulics*, volume 10. Elsevier Scientific Pub. Co., 1 edition, 1981.

J. Krahn and D. G. Fredlund. On total, matric and osmotic suction. *Soil Science*, 114(5): 339–348, 1972.

R. H. Latief and A. K. E. Zainal. Effects of water table level on slope stability and construction cost of highway embankment. *Engineering Journal*, 23(5):1–12, 2019.

E. C. Leong. Stress State Variables for Unsaturated SoilsConsensus and Controversy. In K. Ilamparuthi and R. Robinson, editors, *Indian Geotechnical Conference IGC2016*, pages 79–89, Madras, 2016. Springer, Singapore.

E. C. Leong and H. Rahardjo. Review of Soil-Water Characteristic Curve Equations. *Journal of Geotechnical and Geoenvironmental Engineering*, 123(12):1106–1117, 1997.

E. C. Leong, S. Tripathy, and H. Rahardjo. Total suction measurement of unsaturated soils with a device using the chilled-mirror dew-point technique. *Géotechnique*, 53(2): 173–182, 2003a.

E. C. Leong, S. Tripathy, and H. Rahardjo. Total suction measurement of unsaturated soils with a device using the chilled-mirror dew-point technique. *Géotechnique*, 53(2): 173–182, 2003b.

W. J. Likos, A. Wayllace, J. Godt, and N. Lu. Modified direct shear apparatus for unsaturated sands at low suction and stress. *Geotechnical Testing Journal*, 33(4), 2010.

A. Lilly, J. Wösten, A. Nemes, and C. L. Bas. The development and use of the HYPRES database in Europe. In M. T. van Genuchten, F. J. Leij, and L. Wu, editors, *Characterization and measurement of the hydraulic properties of unsaturated porous media*, pages 1283–1294. 1999.

S. D. Lourenço, D. Gallipoli, D. G. Toll, C. E. Augarde, and F. D. Evans. A new procedure for the determination of soilwater retention curves by continuous drying using high-suction tensiometers. *Canadian Geotechnical Journal*, 48(2):327–335, 2011.

S. D. N. Lourenço. *Suction Measurements and Water retention in Unsaturated Soils*. PhD thesis, Durham University, 2008.

F. A. Marinho, W. A. Take, and A. Tarantino. Measurement of matric suction using tensiometric and axis translation techniques. *Geotechnical and Geological Engineering*, 26(6):615–631, 2008.

J. Mendes and D. G. Toll. Influence of Initial Water Content on the Mechanical Behavior of Unsaturated Sandy Clay Soil. *International Journal of Geomechanics*, 16(6):D4016005, 2016.

N. R. Morgenstern. Properties of compacted soils. In *Panamerican Conference on Soil Mechanics and Foundation*, 1979.

Y. Mualem. A conceptual model of hysteresis. *Water Resources Research*, 10(3):514–520, 1974.

A. Nemes, M. G. Schaap, F. J. Leij, and J. H. Wösten. Description of the unsaturated soil hydraulic database UNSODA version 2.0. *Journal of Hydrology*, 251(3-4):151–162, 2001.

T. N. Ng. *The effect of negative pore-water pressures on slope stability analysis*. Msc, University of Saskatchewan, Saskatoon, SK., 1988.

J. R. Nimmo. Modeling Structural Influences on Soil Water Retention. *Soil Science Society of America Journal*, 61(3):712–719, 1997.

A. Oberg and G. Sallfors. Determination of Shear Strength Parameters of Unsaturated Silts and Sands Based on the Water Retention Curve. *Geotechnical Testing Journal*, 20 (1):40, 1997.

O. M. Oliveira and F. A. Marinho. Suction equilibration time for a high capacity tensiometer. *Geotechnical Testing Journal*, 31(1):101–105, 2008.

Y. Ostovari, K. Asgari, and W. Cornelis. Performance Evaluation of Pedotransfer Functions to Predict Field Capacity and Permanent Wilting Point Using UNSODA and HYPRES Datasets. *Arid Land Research and Management*, 29(4):383–398, 2015.

Y. Y. Perera, C. E. Zapata, W. N. Houston, and S. L. Houston. Prediction of the soil-water characteristic curve based on grain-size-distribution and index properties. *Geotechnical Special Publication*, 40776(130-142):49–60, 2005.

N. Peroni and A. Tarantino. Measurement of osmotic suction using the squeezing technique. In *Unsaturated Soils: Experimental Studies*, pages 159–168. Springer-Verlag, 2006.

H. Q. Pham and D. G. Fredlund. Equations for the entire soil-water characteristic curve of a volume change soil. *Canadian Geotechnical Journal*, 45(4):443–453, apr 2008.

J. P. Powers, A. B. Corwin, P. C. Schmall, and W. E. Kaeck. *Construction Dewatering and Groundwater Control*. John Wiley & Sons, Inc., Hoboken, NJ, USA, 2007.

W. Rawls and D. Brakensiek. Prediction of soil water properties for hydrologic modeling. In *Watershed management in the eighties*. ASCE, 1985.

W. J. Rawls, D. L. Brakensiek, and K. E. Saxtonn. Estimation of Soil Water Properties. *Transactions of the ASAE*, 25(5):1316–1320, 1982.

B. G. Richards. The significance of moisture flow and equilibria in unsaturated soils in relation to the design of engineering structures built on shallow foundations in. In *Symposium On Permeability and Capillary, American Society Testing Materials*, Atlantic City, New Jersey, 1966.

A. M. Ridley and J. B. Burland. A new instrument for the measurement of soil moisture suction. *Géotechnique*, 43(2):321–324, 1993.

M. G. Schaap and F. J. Leij. Using neural networks to predict soil water retention and soil hydraulic conductivity. *Soil and Tillage Research*, 47(1-2):37–42, 1998.

M. G. Schaap, F. J. Leij, and M. T. van Genuchten. Neural Network Analysis for Hierarchical Prediction of Soil Hydraulic Properties. *Soil Science Society of America Journal*, 62(4):847–855, 1998.

A. C. Scheinost, W. Sinowski, and K. Auerswald. Regionalization of soil water retention curves in a highly variable soilscape, I. Developing a new pedotransfer function. *Geoderma*, 78(3-4):129–143, 1997.

SciPy.org. SciPy SciPy v1.4.1 Reference Guide, 2019.

D. Sheng, D. G. Fredlund, and A. Gens. A new modelling approach for unsaturated soils using independent stress variables. *Canadian Geotechnical Journal*, 45(4):511–534, 2008.

D. Sheng, A. Zhou, and D. G. Fredlund. Shear Strength Criteria for Unsaturated Soils. *Geotechnical and Geological Engineering*, 29(2):145–159, 2011.

W. Sillers. *The mathematical representation of the soil-water characteristic curve.* Msc, University of Saskatchewan, Saskatoon, SK, 1997.

D. Stannard. Tensiometers: Theory, Construction, and Use. *Geotechnical Testing Journal*, 15(1):48, 1992.

R. A. Stirling, D. G. Toll, S. Glendinning, P. R. Helm, A. Yildiz, P. N. Hughes, and J. D. Asquith. Weather-driven deterioration processes affecting the performance of embankment slopes. *Géotechnique*, pages 1–43, 2020.

D. A. Sun, H. Matsuoka, Y.-P. Yao, and W. Ichihara. An Elasto-Plastic Model for Unsaturated Soil in Three-Dimensional Stresses. *Soils and Foundations*, 40(3):17–28, 2000.

A. M. Tang, P. N. Hughes, T. A. Dijkstra, A. Askarinejad, M. Brenčič, Y. J. Cui, J. J. Diez, T. Firgi, B. Gajewska, F. Gentile, G. Grossi, C. Jommi, F. Kehagia, E. Koda, H. W. TerMaat, S. Lenart, S. Lourenco, M. Oliveira, P. Osinski, S. M. Springman, R. Stirling, D. G. Toll, and V. Van Beek. Atmosphere-vegetation-soil interactions in a climate change context; Impact of changing conditions on engineered transport infrastructure slopes in Europe. *Quarterly Journal of Engineering Geology and Hydrogeology*, 51(2): 156–168, 2018.

K. Terzaghi. Erdbaumechanik auf bodenphysikalischer grundlage. Technical report, F. Deuticke, 1925.

K. Terzaghi. The shearing resistance of saturated soils and the angle between the planes of shear. In *First international conference on soil Mechanics*, volume 1, pages 54–59, 1936.

K. Terzaghi. *Theoretical Soil Mechanics*. John Wiley & Sons, Inc., 1943.

S. Thomas, G. French, and M. Thomas. Designing Steep Stable and Sustainable Retaining Embankments in Weak Saturated Ground Using the Stable-EarthTM Technique. In J. Monteiro, J. António, A. Mortal, J. Aníbal, M. M. da Silva, M. Oliveira, and S. Nelson, editors, *INCREaSE 2019 Proceedings of the 2nd International Congress on Engineering and Sustainability in the XXI Century*, pages 1102–1116. Springer International Publishing, 2020.

T. M. Thu, H. Rahardjo, and E.-C. Leong. Shear Strength and Pore-Water Pressure Characteristics during Constant Water Content Triaxial Tests. *Journal of Geotechnical and Geoenvironmental Engineering*, 132(3):411–419, 2006.

D. G. Toll. A framework for unsaturated soil behaviour. *Géotechnique*, 40(1):31–44, 1990.

D. G. Toll and B. H. Ong. Critical-state parameters for an unsaturated residual sandy clay. *Géotechnique*, 53(1):93–103, 2003.

D. G. Toll, J. Mendes, D. Gallipoli, S. Glendinning, and P. N. Hughes. Investigating the impacts of climate change on slopes: Field measurements. *Geological Society Engineering Geology Special Publication*, 26(1):151–161, 2012.

D. G. Toll, S. D. Lourenço, and J. Mendes. Advances in suction measurements using high suction tensiometers. *Engineering Geology*, 165:29–37, 2013.

D. G. Toll, J. D. Asquith, A. Fraser, A. A. Hassan, G. Liu, S. D. Lourenço, J. Mendes, T. Noguchi, P. Osinski, and R. Stirling. Tensiometer techniques for determining soil water retention curves. *Unsaturated Soil Mechanics from Theory to Practice - Proceedings of the 6th Asia-Pacific Conference on Unsaturated Soils*, pages 15–22, 2015.

D. G. Toll, J. D. Asquith, P. N. Hughes, and P. Osinski. Soil Water Retention Behaviour of a Sandy Clay Fill Material. *Procedia Engineering*, 143:308–314, 2016.

S. W. Tyler and S. W. Wheatcraft. Application of Fractal Mathematics to Soil Water Retention Estimation. *Soil Science Society of America Journal*, 53(4):987–996, 1989.

M. T. van Genuchten. A Closed-form Equation for Predicting the Hydraulic Conductivity of Unsaturated Soils. *Soil Science Society of America Journal*, 44(5):892–898, 1980.

S. K. Vanapalli and D. G. Fredlund. Comparison of Different Procedures to Predict Unsaturated Soil Shear Strength. *Advances in Unsaturated Geotechnics*, 40510(July 2000):195–209, 2000.

S. K. Vanapalli, D. G. Fredlund, D. E. Pufahl, and A. W. Clifton. Model for the prediction of shear strength with respect to soil suction. *Canadian Geotechnical Journal*, 33(3): 379–392, 1996.

S. K. Vanapalli, W. S. Sillers, and M. D. Fredlund. The meaning and relevance of residual state to unsaturated soils. *Proceedings of the 51st Canadian Geotechnical Conference*, (October 1998):1–8, 1998.

S. K. Vanapalli, D. G. Fredlund, and D. E. Pufahl. The influence of soil structure and stress history on the soil-water characteristics of a compacted till. *Géotechnique*, 49(2): 143–159, 1999.

S. K. Vanapalli, M. V. Nicotera, and R. S. Sharma. Axis translation and negative water column techniques for suction control. *Geotechnical and Geological Engineering*, 26(6): 645–660, 2008.

C. M. P. Vaz, M. de Freitas Iossi, J. de Mendonça Naime, Á. Macedo, J. M. Reichert, D. J. Reinert, and M. Cooper. Validation of the Arya and Paris Water Retention Model for Brazilian Soils. *Soil Science Society of America Journal*, 69(3):577–583, 2005.

H. Vereecken. Estimating the unsaturated hydraulic conductivity from theoretical models using simple soil properties. *Geoderma*, 65(1-2):81–92, 1995.

H. Vereecken, J. Maes, J. Feyen, and P. Darius. Estimating the soil moisture retention characteristic from texture, bulk density, and carbon content. *Soil Science*, pages 389–403, 1989.

S. J. Wheeler and V. Sivakumar. An elasto-plastic critical state framework for unsaturated soil. *Géotechnique*, 45(1):35–53, 1995.

J. H. Wösten, A. Lilly, A. Nemes, and C. Le Bas. Development and use of a database of hydraulic properties of European soils. *Geoderma*, 90(3-4):169–185, 1999.

C. E. Zapata, W. N. Houston, S. L. Houston, and K. D. Walsh. Soil-water characteristic curve variability. In *Proceedings of Sessions of Geo-Denver 2000 - Advances in Unsaturated Geotechnics, GSP 99*, volume 287, pages 84–124, 2000.

Appendix A

Regression Analysis Results Data Tables

A.1 PSD Curve Fit Equation

Equation from Fredlund et al. (2000). See Chapter 3 for description of equation parameters.

$$P_p(d) = \frac{1}{\left\{ \ln \left[e + (a/d)^n \right] \right\}^m} \times \left\{ 1 - \left[\frac{\ln(1 + d_r/d)}{\ln(1 + d_r/d_m)} \right]^7 \right\} \qquad \text{(A.1.1)}$$

A.2 PSD Regression Analysis Results

Soil Code	USDA Textural Class	a	n	m	d_r	R^2
1014	Sand	0.23	3.26	1.29	5.68E+06	99.90
1020	Sand	1.02	25.85	0.53	4.49E-04	99.85
1021	Sand	0.96	13.07	0.57	4.31E-05	99.61
1022	Sand	1.00	19.16	0.53	1.53E+05	99.80
1041	Sand	0.22	4.53	1.37	3.20E+07	99.89
1042	Sand	0.21	4.65	1.61	1.20E+09	99.89
1043	Sand	0.23	4.65	1.36	7.74E+03	99.82
1050	Sand	0.62	4.87	1.03	6.22E-01	100.00
1052	Sand	0.76	4.80	0.98	1.52E-07	99.86
1053	Sand	0.74	4.46	1.34	2.69E-07	99.90
1054	Sand	0.73	4.23	1.71	5.20E-08	99.93
1060	Sand	0.44	3.01	1.50	1.59E-07	99.89
1061	Sand	0.49	3.16	1.27	3.28E-09	99.87
1063	Sand	0.50	2.64	1.57	2.11E-06	99.80
1070	Sand	0.53	2.16	1.57	1.06E-11	99.63
1071	Sand	0.70	2.56	1.28	2.51E-08	99.65
1072	Sand	0.79	2.41	1.29	8.94E-09	99.26
1073	Sand	0.89	2.71	1.45	3.91E-07	99.25
1074	Sand	0.83	2.76	1.58	2.09E-07	99.51
1075	Sand	0.78	3.54	1.24	1.12E-07	99.79
1110	Sand	0.30	3.09	1.42	5.24E+04	99.76
1123	Clay Loam	0.20	1.62	0.50	2.15E+03	99.22
1134	Sandy Clay	0.52	3.11	0.33	2.87E-05	99.71
1135	Sandy Clay	0.58	2.93	0.34	1.29E-05	99.12
1140	Sand	0.26	2.58	1.91	7.01E+03	99.81
1141	Sand	0.27	2.76	1.60	4.12E+05	99.80
1142	Sand	0.29	2.74	1.35	5.03E+05	99.81
1162	Clay	1.05	3.39	0.20	6.52E+02	99.94
1163	Clay	1.05	3.05	0.23	1.47E+02	99.97
1172	Clay Loam	0.19	3.84	0.33	8.79E-03	100.00

1173	Clay Loam	0.23	2.27	0.38	2.42E+01	100.00
1180	Clay Loam	0.17	3.52	0.35	1.31E-04	100.00
1301	Clay Loam	0.12	3.16	0.45	2.46E-03	100.00
1400	Clay	0.02	1.38	0.38	4.61E+01	99.44
1460	Sand	0.64	10.57	1.15	2.12E-07	99.99
1462	Sand	0.33	5.73	1.48	4.43E+04	99.97
1463	Sand	0.32	8.29	1.26	8.94E-07	99.99
1464	Sand	0.21	49.26	0.65	9.76E-05	99.97
1465	Sand	0.13	3.69	1.33	2.85E+05	99.95
1466	Sand	0.11	6.99	1.60	2.37E+04	99.99
1467	Sand	0.54	3.46	1.05	6.18E-07	99.87
2220	Sand	0.02	0.94	10.00	2.06E+06	99.13
2221	Sand	0.13	0.87	4.19	7.50E+03	98.45
2310	Sand	0.29	3.83	2.31	4.54E-03	99.97
2360	Clay	0.10	1.15	0.46	9.93E+02	99.73
2361	Clay	0.02	1.32	0.45	3.04E+01	99.58
2362	Clay	0.01	1.25	0.43	7.70E+03	99.90
2390	Clay Loam	0.14	3.11	0.45	2.53E-03	100.00
2391	Clay Loam	0.11	3.10	0.44	1.03E-03	100.00
2392	Clay Loam	0.07	2.68	0.47	4.21E-03	100.00
2393	Clay Loam	0.11	5.32	0.41	1.27E+00	100.00
2430	Clay Loam	0.08	4.58	0.41	1.20E-05	100.00
2431	Clay Loam	0.07	2.79	0.47	1.35E-03	100.00
2433	Clay Loam	0.10	2.88	0.45	2.70E-03	100.00
2740	Clay Loam	0.09	2.95	0.50	7.69E-04	100.00
2743	Clay Loam	0.07	4.46	0.42	4.43E-05	100.00
3031	Clay Loam	0.03	0.67	1.24	1.39E-07	98.10
3032	Clay Loam	0.12	0.41	1.39	2.33E-10	95.51
3033	Clay Loam	0.01	0.32	2.23	5.67E+01	96.41
3070	Sand	0.15	5.37	3.24	7.64E-01	100.00
3132	Sand	0.27	4.75	1.07	1.17E-06	99.99
3141	Sand	0.28	5.01	1.09	3.29E+03	99.99

3142	Sand	0.26	4.35	1.26	1.20E-05	99.98
3143	Sand	0.27	5.35	1.17	9.33E-09	99.98
3144	Sand	0.27	5.60	1.26	3.13E+01	99.99
3153	Sand	0.28	4.47	1.03	2.21E+02	99.99
3154	Sand	0.27	4.87	1.05	5.94E-07	99.99
3155	Sand	0.30	5.04	1.10	4.17E+03	99.99
3162	Sand	0.17	2.78	1.53	3.49E+03	99.91
3163	Sand	0.16	3.42	1.46	3.42E+04	99.80
3164	Sand	0.15	2.88	1.89	2.13E+04	99.94
3165	Sand	0.23	2.22	1.67	1.88E-05	99.87
3172	Sand	0.17	3.93	1.36	1.34E+04	99.90
3173	Sand	0.18	4.29	1.30	6.85E-06	99.90
3174	Sand	0.30	3.47	1.29	4.51E+02	99.86
3175	Sand	0.36	7.89	1.37	3.09E+03	99.99
3181	Sand	0.20	3.22	1.29	2.11E-05	99.83
3182	Sand	0.26	19.94	0.75	3.15E-04	99.98
3183	Sand	0.27	10.12	0.98	1.70E-04	99.99
3206	Sand	0.52	6.55	1.08	3.35E+01	99.99
3214	Silt	0.02	20.45	0.53	2.69E+03	100.00
3340	Sand	0.29	2.82	2.11	2.11E+05	99.77
4001	Sand	0.18	6.51	1.48	3.57E+03	100.00
4440	Sand	0.27	7.60	1.42	3.51E+06	99.96
4441	Sand	0.24	8.06	1.61	1.59E+07	99.94
4442	Sand	0.30	3.85	2.29	7.27E+00	99.96
4443	Sand	0.25	5.09	4.88	1.92E+02	100.00
4444	Sand	0.36	4.08	1.71	1.51E+01	99.93
4445	Sand	0.28	4.55	1.52	2.99E-04	99.62
4520	Sand	0.17	2.72	4.77	4.78E+03	99.98
4521	Sand	0.17	2.72	4.77	4.78E+03	99.98
4522	Sand	0.17	2.72	4.77	4.78E+03	99.98
4523	Sand	0.17	2.72	4.77	4.78E+03	99.98
4650	Sand	0.44	4.21	1.26	5.50E+03	99.97

4651	Sand	0.41	3.03	1.64	3.09E-02	99.99
4660	Sand	0.45	4.86	1.01	5.94E-06	99.99
4661	Sand	0.45	5.49	1.04	1.88E-09	100.00
4670	Silt	0.03	5.28	0.91	3.16E+03	99.99
4680	Clay	0.06	1.54	0.43	2.35E+01	99.97
4681	Clay	0.04	1.10	0.50	8.92E-06	99.68
4810	Sand	0.60	6.32	1.27	4.11E+01	99.88
4941	Sand	0.70	5.38	0.64	8.92E+03	99.84

Table A.1: Best-fit curve parameters for PSD equation (Fredlund et al., 2000) determined by regression analysis of raw PSD data.

A.3 SWRC Cure Fit Equation

Equation from Fredlund and Xing (1994). See Chapter 3 for description of equation parameters.

$$\theta(\psi) = C(\psi)\frac{\theta_s}{\left\{\ln\left[e + (\psi/a)^n\right]\right\}^m} \tag{A.3.2}$$

where

$$C(\psi) = \frac{\ln(1 + \psi/\psi_r)}{\ln[1 + (10^6/\psi_r)]} \tag{A.3.3}$$

A.4 SWRC Regression Analysis Results

Soil Code	USDA Textural Class	θ_s	a	n	m	ψ_r	R^2
1014	Sand	0.36	2.71	3.62	0.94	1.44E+02	99.93
1020	Sand	0.75	2.04	15.62	0.25	1.00E+04	99.90
1021	Sand	0.37	0.77	2.40	0.56	1.58E+01	99.58
1022	Sand	0.37	0.75	2.19	0.71	1.67E+01	99.63
1041	Sand	0.32	3.23	5.85	0.67	1.00E+04	99.84
1042	Sand	0.33	3.30	5.77	0.77	1.00E+04	99.87
1043	Sand	0.31	3.76	6.59	0.84	1.00E+04	99.88
1050	Sand	0.36	1.87	5.82	0.61	1.00E+04	99.54
1052	Sand	0.35	1.13	5.84	0.63	1.00E+04	99.49
1053	Sand	0.34	1.15	5.08	0.87	1.00E+04	98.92
1054	Sand	0.35	1.10	6.52	0.91	1.00E+04	99.44
1060	Sand	0.35	2.00	5.89	0.63	1.00E+04	99.85
1061	Sand	0.33	1.84	7.35	0.65	1.00E+04	99.70
1063	Sand	0.35	1.70	5.79	0.78	1.00E+04	99.47
1070	Sand	0.45	1.38	3.09	0.80	1.00E+04	99.74
1071	Sand	0.30	1.71	5.76	0.59	1.00E+04	99.66
1072	Sand	0.32	1.31	3.41	0.80	1.00E+04	99.61

1073	Sand	0.31	1.30	3.65	1.00	1.00E+04	99.61
1074	Sand	0.35	1.03	2.59	1.29	1.00E+04	99.79
1075	Sand	0.35	0.97	3.05	0.88	1.00E+04	99.16
1110	Sand	0.30	3.48	7.61	0.39	1.00E+04	98.43
1123	Clay Loam	0.37	43.29	0.48	0.37	1.00E+04	99.34
1134	Sandy Clay	0.37	65.86	2.75	0.14	1.00E+04	96.85
1135	Sandy Clay	0.41	63.39	3.54	0.18	1.00E+04	98.23
1140	Sand	0.37	3.05	7.01	0.60	1.00E+04	99.89
1141	Sand	0.29	3.55	7.32	0.45	1.00E+04	99.59
1142	Sand	0.24	4.17	11.09	0.22	2.58E+00	99.87
1162	Clay	0.41	2.29	1.89	0.10	3.15E+03	87.81
1163	Clay	0.40	1.77	1.81	0.10	2.24E+03	96.10
1172	Clay Loam	0.54	0.10	0.95	0.17	8.70E+02	99.27
1173	Clay Loam	0.48	2.16	0.90	0.15	1.00E+04	99.37
1180	Clay Loam	0.52	0.10	1.82	0.20	5.60E+02	99.80
1301	Clay Loam	0.37	3.66	2.12	0.17	1.91E+01	96.72
1400	Clay	0.46	67.55	0.59	0.49	1.00E+04	99.91
1460	Sand	0.49	3.44	50.00	0.56	7.82E+02	73.69
1462	Sand	0.51	2.53	7.99	0.74	8.22E+03	99.99
1463	Sand	0.38	3.59	50.00	0.47	3.81E+01	100.00
1464	Sand	0.36	3.74	20.80	0.47	6.04E+00	99.91
1465	Sand	0.32	4.89	1.68	1.10	1.05E+03	99.95
1466	Sand	0.38	5.79	8.46	0.83	1.00E+04	99.87
1467	Sand	0.48	1.32	0.52	1.88	2.13E+01	99.82
2220	Sand	0.32	7.36	10.04	0.46	2.90E+00	99.06
2221	Sand	0.31	5.36	6.25	0.62	1.99E+00	99.11
2310	Sand	0.36	3.65	15.06	0.96	1.00E+04	99.91
2360	Clay	0.50	5.03	0.94	0.20	1.65E+03	99.72
2361	Clay	0.56	4.86	1.05	0.10	4.44E+02	99.93
2362	Clay	0.56	133.07	0.98	0.28	1.00E+04	99.70
2390	Clay Loam	0.44	5.53	2.06	0.33	7.67E+01	99.94
2391	Clay Loam	0.43	3.26	1.48	0.35	1.75E+01	99.92

2392	Clay Loam	0.43	2.93	1.26	0.36	1.57E+01	99.84
2393	Clay Loam	0.35	4.99	4.16	0.53	7.29E+00	99.95
2430	Clay Loam	0.44	3.64	1.88	0.27	2.36E+01	99.95
2431	Clay Loam	0.43	2.75	1.95	0.22	1.36E+01	99.62
2433	Clay Loam	0.36	2.92	1.20	0.40	1.00E+04	99.91
2740	Clay Loam	0.70	1.33	1.18	0.43	1.01E+02	99.70
2743	Clay Loam	0.70	1.35	1.42	0.37	1.03E+02	99.96
3031	Clay Loam	0.54	1.07	0.72	0.29	1.00E+04	99.80
3032	Clay Loam	0.55	3.29	0.81	0.40	1.00E+04	99.76
3033	Clay Loam	0.57	2.92	1.94	0.34	1.00E+04	99.65
3070	Sand	0.31	4.04	5.39	6.79	1.00E+04	98.63
3132	Sand	0.30	2.81	5.16	0.57	1.00E+04	99.84
3141	Sand	0.34	3.01	3.34	0.59	1.30E+02	99.80
3142	Sand	0.36	2.65	4.94	0.57	1.01E+02	99.88
3143	Sand	0.34	3.02	7.22	0.61	1.00E+04	99.86
3144	Sand	0.34	3.11	7.49	0.55	1.00E+04	99.82
3153	Sand	0.40	2.62	4.64	0.62	1.00E+04	99.92
3154	Sand	0.40	2.95	3.96	0.72	1.00E+04	99.96
3155	Sand	0.37	2.78	7.07	0.59	1.00E+04	99.85
3162	Sand	0.40	4.08	6.62	0.54	1.00E+04	99.84
3163	Sand	0.40	4.52	5.43	0.65	1.00E+04	99.35
3164	Sand	0.38	4.84	7.40	0.58	1.00E+04	99.22
3165	Sand	0.39	3.67	4.90	0.59	1.00E+04	99.71
3172	Sand	0.36	4.54	6.15	0.56	1.00E+04	99.70
3173	Sand	0.34	4.96	4.40	0.50	1.00E+04	99.80
3174	Sand	0.37	4.71	3.52	0.46	1.00E+04	99.75
3175	Sand	0.32	2.91	50.00	0.47	1.00E+04	99.94
3181	Sand	0.41	4.75	8.55	0.55	1.00E+04	99.57
3182	Sand	0.38	3.07	9.48	0.44	1.20E+06	99.64
3183	Sand	0.37	3.68	61.43	0.31	7.20E+07	99.98
3206	Sand	0.33	3.47	7.65	0.17	5.00E+00	99.34
3214	Silt	0.61	3.08	3.25	0.06	8.80E+01	99.69

3340	Sand	0.31	1.99	4.92	0.75	4.28E+03	99.27
4001	Sand	0.34	5.09	2.08	1.11	1.00E+04	99.88
4440	Sand	0.39	4.32	11.71	0.48	3.14E-01	99.58
4441	Sand	0.33	4.25	4.14	2.05	1.00E+04	98.39
4442	Sand	0.33	3.97	10.71	0.53	1.00E-01	94.93
4443	Sand	0.31	2.04	9.32	1.08	4.05E+00	99.69
4444	Sand	0.29	3.75	6.53	0.82	1.00E+04	99.47
4445	Sand	0.30	5.23	5.28	1.16	1.00E+04	99.14
4520	Sand	0.35	3.99	7.80	0.95	1.00E+04	99.73
4521	Sand	0.35	3.99	7.80	0.95	1.00E+04	99.73
4522	Sand	0.35	4.66	37.84	0.56	8.83E+03	99.57
4523	Sand	0.35	4.66	37.84	0.56	8.79E+03	99.57
4650	Sand	0.38	2.10	4.76	0.62	7.71E-01	99.93
4651	Sand	0.35	1.63	2.63	0.72	1.00E+04	99.03
4660	Sand	0.45	0.79	1.09	1.01	1.00E+04	98.94
4661	Sand	0.41	0.98	1.65	1.08	1.00E+04	99.57
4670	Silt	0.47	73.07	6.83	0.33	5.79E-01	99.60
4680	Clay	0.55	31.85	0.78	0.45	6.21E+03	99.91
4681	Clay	0.58	677.52	0.53	1.22	3.61E+03	99.80
4810	Sand	0.41	2.04	11.31	0.71	1.00E+04	99.86
4941	Sand	0.37	4.96	3.13	9.36	1.00E-01	99.70

Table A.2: Best-fit curve parameters for SWRC equation (Fredlund and Xing, 1994) determined by regression analysis of raw SWRC data.

Appendix B

Confidence Limit Suction Error Tables

B.1 Calculated Suction Error Percentiles for the Arya and Paris (1981) Model - Granular Soils

Saturation, S	5^{th} Percentile	Mean Suction Error	95^{th} Percentile
0.95	-0.54	0.00	0.92
0.90	-0.34	0.08	0.82
0.85	-0.26	0.10	0.57
0.80	-0.20	0.13	0.52
0.75	-0.15	0.13	0.52
0.70	-0.18	0.15	0.46
0.65	-0.15	0.15	0.44
0.60	-0.20	0.15	0.43
0.55	-0.24	0.15	0.44
0.50	-0.28	0.14	0.41
0.45	-0.34	0.11	0.41
0.40	-0.52	0.08	0.40
0.35	-0.68	0.03	0.36
0.30	-0.96	-0.04	0.38
0.25	-1.35	-0.16	0.37
0.20	-1.97	-0.35	0.34
0.15	-2.48	-0.65	0.30
0.10	-3.14	-1.15	0.18
0.05	-2.86	-1.48	0.10

Table B.1: Calculated mean suction error and 5^{th} and 95^{th} percentiles for the analysis of the 75 No. granular soils using the Arya and Paris (1981) model

B.2 Calculated Suction Error Percentiles for the Arya and Paris (1981) Model - Cohesive Soils

Saturation, S	5^{th} Percentile	Mean Suction Error	95^{th} Percentile
0.95	-1.57	0.22	1.17
0.90	-1.80	0.00	1.06
0.85	-1.64	-0.06	0.99
0.80	-1.96	-0.17	0.92
0.75	-2.34	-0.30	0.85
0.70	-2.54	-0.40	0.77
0.65	-2.51	-0.48	0.71
0.60	-2.38	-0.54	0.71
0.55	-2.38	-0.53	0.77
0.50	-2.24	-0.47	0.73
0.45	-1.91	-0.36	0.77
0.40	-1.36	-0.16	1.04
0.35	-0.97	0.18	1.28
0.30	-0.76	0.61	1.76
0.25	0.15	1.26	2.26
0.20	0.58	1.72	2.62
0.15	1.54	1.88	2.75
0.10	1.29	1.65	2.50
0.05	1.91	1.91	1.91

Table B.2: Calculated mean suction error and 5^{th} and 95^{th} percentiles for the analysis of the 27 No. cohesive soils using the Arya and Paris (1981) model

B.3 Calculated Suction Error Percentiles for the Modified Kovács model (Aubertin et al., 2003) - Granular Soils

Saturation, S	5^{th} Percentile	Mean Suction Error	95^{th} Percentile
0.95	-0.28	0.22	0.84
0.90	-0.24	0.17	0.71
0.85	-0.21	0.14	0.61
0.80	-0.21	0.12	0.51
0.75	-0.22	0.11	0.41
0.70	-0.21	0.10	0.39
0.65	-0.19	0.09	0.38
0.60	-0.21	0.08	0.36
0.55	-0.22	0.07	0.28
0.50	-0.24	0.05	0.27
0.45	-0.26	0.02	0.24
0.40	-0.34	-0.01	0.22
0.35	-0.54	-0.06	0.21
0.30	-0.82	-0.13	0.17
0.25	-1.30	-0.24	0.13
0.20	-2.08	-0.43	0.15
0.15	-2.52	-0.70	0.13
0.10	-3.04	-1.09	0.21
0.05	-2.60	-1.16	0.65

Table B.3: Calculated mean suction error and 5^{th} and 95^{th} percentiles for the analysis of the 75 No. granular soils using the MK model (Aubertin et al., 2003).

B.4 Calculated Suction Error Percentiles for the Perera Model (Perera et al., 2005) - Granular Soils

Saturation, S	5^{th} Percentile	Mean Suction Error	95^{th} Percentile
0.95	-0.29	0.22	0.95
0.90	-0.26	0.18	0.78
0.85	-0.24	0.15	0.71
0.80	-0.22	0.14	0.66
0.75	-0.25	0.12	0.60
0.70	-0.34	0.11	0.54
0.65	-0.38	0.10	0.49
0.60	-0.38	0.09	0.46
0.55	-0.38	0.08	0.44
0.50	-0.37	0.07	0.44
0.45	-0.41	0.06	0.45
0.40	-0.44	0.04	0.46
0.35	-0.52	0.02	0.50
0.30	-0.69	-0.01	0.56
0.25	-1.14	-0.06	0.64
0.20	-1.55	-0.14	0.75
0.15	-2.21	-0.28	0.92
0.10	-2.29	-0.54	0.90
0.05	-1.90	-0.72	0.66

Table B.4: Calculated mean suction error and 5^{th} and 95^{th} percentiles for the analysis of the 75 No. granular soils using the Perera model

Appendix C

Digital Appendix: PSD and SWRC Graphs

Figures C1 to C301 can seen by following the web link below.

http://www.ogi.co.uk/wp-content/uploads/2020/12/GF-MScR-Appendix-C-Digital-1.pdf